https://doi.org/10.15388/vu.thesis.964
https://orcid.org/0009-0004-6233-509X

VILNIUS UNIVERSITY

Anastasiia Shelest

Functionality of Voltage-Gated Ion Channels: Influence of Cytokines and Genetic Variation

DOCTORAL DISSERTATION

Natural Sciences
Biophysics (N 011)

VILNIUS 2026

The dissertation was prepared between 2020 and 2026 at Vilnius University. The research was supported by the Research Council of Lithuania.

The doctoral studies were financed from the EU structural funds.

Academic supervisor:
Prof. Dr. Aidas Alaburda (Vilnius University, Natural Sciences, Biophysics – N 011).

This doctoral dissertation will be defended in a public/closed meeting of the Dissertation Defence Panel:

Chairman – **Prof. Dr. Vilma Kisnierienė** (Vilnius University, Natural Sciences, Biophysics– N 011);

Members:
Assoc. Prof. Dr. Rokas Buišas (Vilnius University, Natural Sciences, Biophysics– N 011);
Prof. Dr. Vitalijus Karabanovas (National Cancer Institute, Natural Sciences, Biophysics – N 011);
Prof. Dr. Vitalii Kostenko (Poltava State Medical University, Ukraine, Medical and Health Sciences, Medicine – M 001);
Prof. Dr. Saulius Šatkauskas (Vytautas Magnus University, Natural Sciences, Biophysics – N 011).

The dissertation shall be defended at a public meeting of the Dissertation Defence Panel at 11:00 hour on 4th of September 2026. in room R401 of the VU Life Sciences Center. Adress: Saulėtekio av. 7, R401, Vilnius, Lithuania.

https://doi.org/10.15388/vu.thesis.964
https://orcid.org/0009-0004-6233-509X

VILNIAUS UNIVERSITETAS

Anastasiia Shelest

Potencialo valdomų joninių kanalų funkcionalumas: citokinų ir genetinės variacijos įtaka

DAKTARO DISERTACIJA

Gamtos mokslai,
Biofizika (N 011)

VILNIUS 2026

Disertacija rengta 2020–2026 metais Vilniaus universitete. Mokslinius tyrimus rėmė Lietuvos mokslo taryba.

Doktorantūra buvo finansuojama ES struktūrinių fondų lėšomis.

Mokslinis vadovas:
Prof. dr. Aidas Alaburda (Vilniaus universitetas, gamtos mokslai, biofizika – N011).

Gynimo taryba:
Pirmininkė – prof. dr. Vilma Kisnierienė (Vilniaus universitetas, gamtos mokslai, biofizika – N 011);
Nariai:
doc. dr. Rokas Buišas (Vilniaus universitetas, gamtos mokslai, biofizika – N 011);
prof. dr. Vitalijus Karabanovas (Nacionalinis vėžio institutas, gamtos mokslai, biofizika – N 011);
prof. dr. Vitalii Kostenko (Poltavos valstybinis medicinos universitetas, Ukraina, medicinos ir sveikatos mokslai, medicina – M 001);
prof. dr. Saulius Šatkauskas (Vytauto Didžiojo universitetas, gamtos mokslai, biofizika – N 011).

Disertacija ginama viešame Gynimo tarybos posėdyje 2026 m. rugsėjo mėn. 4 d. 11 val. Vilniaus universiteto Gyvybės mokslų centro R-401 auditorijoje. Adresas: Saulėtekio al. 7, R-401, Vilnius, Lietuva.

COPYRIGHT

CONTENT

ABBREVIATIONS

A371P – *KCNQ1* variant c.1111G>C [p.(Ala371Pro)]
ATP2A2 – gene encoding sarco/endoplasmic reticulum Ca^{2+}-ATPase 2
BM-MSCs – bone marrow–derived mesenchymal stem cells
Ca^{2+} – calcium
CACNA1C – gene encoding the α1C subunit of the voltage-gated calcium channel
CaMKII – Ca^{2+}/calmodulin-dependent protein kinase II
Ct – threshold cycle
CyOFP1 – cyan-excitable orange fluorescent protein 1
DMEM – Dulbecco's modified Eagle medium
ΔI – change in current
ΔV – change in membrane potential
ECF – extracellular fluid
ECG – electrocardiogram
ECM – extracellular matrix
EGFP – enhanced green fluorescent protein
EGTA – ethylene glycol-bis(2-aminoethyl ether)-N,N,N′,N′-tetraacetic acid
ER – endoplasmic reticulum
EST – exercise stress test
FBS – fetal bovine serum
GAG – glycosaminoglycan
G_{max} – maximum conductance
G_{min} – minimal conductance
G-V – conductance–voltage
HEK293 – human embryonic kidney 293 cells
HEPES – 4-(2-hydroxyethyl)-1-piperazineethanesulfonic acid
$I_{Ca,L}$ – L-type calcium current
ICF – intracellular fluid
I_{Ks} – late-repolarizing potassium current
IL-1β – interleukin-1 beta
I_{LSN} – leak-subtracted and normalized to the leak current
IMC – Innovative Medicine Center
iCa^{2+} – intracellular calcium concentration
KCNE1 – gene encoding potassium voltage-gated channel subfamily E member 1
KCNQ1 – gene encoding potassium voltage-gated channel subfamily Q member 1
$Kv_{7.1}$ (KvLQT1) – potassium voltage-gated channel subfamily q member 1

L-VGCCs – L-type voltage-gated calcium channels
LOF – loss-of-function
LQTS – long QT syndrome
MMP13 – matrix metallopeptidases-13
MSCs – mesenchymal stem cells
NCX – sodium–calcium exchanger
NF-κB – nuclear factor of κB
OA – osteoarthritis
PD – pore domain
PMCA – plasma membrane Ca^{2+}-ATPase
PS – penicillin–streptomycin
QTc – corrected QT interval
SD – standard deviation
SEM – standard error of the mean
SERCA – sarco/endoplasmic reticulum Ca^{2+}-ATPase
Sox9 – gene encoding SRY-box transcription factor 9
TβRI – type I receptor
TβRII – type II receptor
TGF-β – transforming growth factor beta
TRPA1 – transient receptor potential ankyrin 1
$V_{1/2}$ – midpoint of voltage-dependent activation
VGCCs – voltage-gated calcium channels
VSD – voltage-sensing domain
WT – wild type

INTRODUCTION

Ion channels are fundamental for cellular signaling and play a critical role in regulating cell function across a wide range of cell types. In excitable cells, such as neurons and muscle, ion channels are essential for the generation of electrical signals (Kawai, 2024; Varró et al., 2021). However, many ion channels are also expressed in non-excitable cells, where they perform a wide range of functions through cellular signaling, including maintaining homeostasis, regulating proliferation, differentiation, controlling hormone secretion, and regulating cell volume (Bijlenga et al., 2000; Jahn et al., 2021; Pérez-García et al., 2018; Thompson & Satin, 2021). Proper ion channel function is therefore critical for maintaining physiological functions in both excitable and non-excitable cells.

Among non-excitable cells, chondrocytes represent a specialized cell type in which ion channel-mediated signaling plays a key regulatory role (Matta et al., 2015). Consequently, Ca^{2+} signaling is considered a central regulator of chondrocyte biological functions, including apoptosis (Nakatani et al., 2025), migration (Shen et al., 2021), proliferation (Mancilla et al., 2007) and chondrogenic differentiation (Atsuta et al., 2019; Wu & Chen, 2000).

Alterations in intracellular Ca^{2+} levels (iCa^{2+}) are considered among the earliest cellular responses of chondrocytes to physical stimuli, including compression (Pingguan-Murphy et al., 2005), mechanical loading (Lv et al., 2017), fluid flow (Degala et al., 2012), hydrostatic pressure (Browning et al., 2004), and osmotic stress (W. Li et al., 2022). iCa^{2+} fluctuations act as intracellular second messenger signals that activate multiple downstream signaling pathways involving Ca^{2+}-dependent mediators, including Ca^{2+}/calmodulin-dependent kinase II (CaMKII) (Wei et al., 2018), calcineurin, and the transcription factor NFAT (Yoo et al., 2007), thereby regulating gene expression (Park et al., 2020).

The regulation of iCa^{2+} in chondrocytes depends on Ca^{2+} influx through channels located on the plasma membrane or on Ca^{2+} release from internal stores (Mobasheri et al., 2019). Previous studies indicated a wide diversity of Ca^{2+} channel expression in chondrocytes, such as voltage-gated Ca^{2+} channels (VGCC) (Shao et al., 2005), transient receptor potential (TRP) channels (Gavenis et al., 2009; Phan et al., 2009), and store-operated Ca^{2+} (SOC) channels (Inayama et al., 2015).

Potential mediators for iCa^{2+} regulation in chondrocytes are L-type voltage-operated calcium channels (L-VOCCs). These channels have been identified in both developing (Shao et al., 2005) and mature chondrocytes (Atsuta et al., 2019; Matta et al., 2015; Uzieliene, Bironaite, Miksiunas, et al.,

2023). L-VGCCs have been identified as important regulators of chondrocyte proliferation and growth, as pharmacological inhibition of these channels significantly suppressed proliferation (Uzieliene et al., 2019; Q. Wu & Chen, 2000) and impaired growth (Mancilla et al., 2007). In addition, L-VGCCs appear to contribute to the maintenance of the biomechanical properties, as inhibition of these channels with nifedipine reduced sGAG synthesis in mechanically stimulated chondrocytes (Mouw et al., 2007).

Furthermore, Ca^{2+} influx through L-VGCCs has been shown to be essential for cartilage formation, as inhibition of these channels reduces expression of key chondrogenic markers, including *Sox9, Col2a1,* and *Agc*, thereby impairing normal cartilage development (Atsuta et al., 2019). However, conflicting findings have also been reported, with some studies showing that inhibition of L-VGCCs enhances chondrogenic marker expression, such as *Col2a1* and *Agc* (Takamatsu et al., 2014; Uzieliene et al., 2019), while also reducing the expression of osteoarthritis-related genes, including *AXIN2* and *MMP3,* in chondrocytes (Takamatsu et al., 2014; Yao et al., 2020).

Overall, these findings highlight the important role of L-VGCCs in determining chondrocyte fate, although it remains unclear whether the observed effects result directly from L-VGCC inhibition or from additional pharmacological effects of the inhibitors themselves. Further direct investigations of L-VGCC activity are needed to clarify their role in cartilage physiology and pathology.

During OA, chondrocytes experience a marked increase in interleukin-1β (IL-1β) production (Daheshia & Yao, 2008; Jenei-Lanzl et al., 2019). Elevated IL-1β further amplifies inflammatory responses and stimulates the synthesis of nitric oxide (NO) and matrix-degrading enzymes, including MMP-1 and MMP-3, in chondrocytes (Yoo et al., 2007). These catabolic factors drive extracellular matrix degradation and contribute to cartilage breakdown. Therefore, IL-1β is also widely used to induce OA in experimental models (Marrero - Berrios et al., 2024; Choi et al., 2013; Henderson & Pettipher, 1988; Pettipher et al., 1986; Kurata et al., 2026).

IL-1β has been observed to increase iCa^{2+} levels in pig (Pritchard & Guilak, 2006) and mouse (Kurata et al., 2026) chondrocytes. In mouse chondrocytes, this mediated through L-VGCCs. Furthermore, IL-1β-induced Ca^{2+} influx through these channels may cause mouse chondrocyte apoptosis by disrupting mitochondrial function (Kurata et al., 2026). In addition, IL-1β treatment was reported to significantly upregulate the expression of the L-VGCCs in bovine chondrocytes (Lv et al., 2019). A treatment with IL-1β

significantly increases L-VGCCs expression localized at the plasma membrane in mouse chondrocytes (Kurata et al., 2026). However, how IL-1β affects Ca^{2+} homeostasis in human chondrocytes remains poorly understood.

Bone marrow-derived mesenchymal stem cells (BM-MSCs) can differentiate into several cell types, including chondrocytes, osteoblasts, and adipocytes (L. Hu et al., 2018; Mardones et al., 2020). In vitro, transforming growth factor beta (TGF-β), particularly TGF-β3, is commonly utilized to promote chondrogenic differentiation by activating cartilage-specific gene expression (Xia et al., 2017; Y. T. Lu et al., 2018; Uzieliene et al., 2019; Wee et al., 2022; Uzieliene, Bironaite, Miksiunas, et al., 2023). Therefore, BM-MSC cultivated with TGF-β3, have attracted considerable attention for their chondrogenic potential and are widely used in cell-based therapies for OA management (Le et al., 2020; Xia et al., 2017; Lu et al., 2018; Uzieliene et al., 2019; Wee et al., 2022; Uzieliene et al., 2023).

TGF-β3 is capable of altering iCa^{2+} dynamics in many cell types through multiple signaling pathways, thereby influencing cellular fate (Alevizopoulos et al., 1997; Cailotto et al., 2011; Ishiyama et al., 1996; LUO et al., 1997; McGowan et al., 2002; Mukherjee et al., 2012; Yin et al., 2018). For example, in fibroblasts, TGF-β causes an increase in iCa^{2+} levels by promoting both Ca^{2+} influx and Ca^{2+} release from the endoplasmic reticulum (ER) (Alevizopoulos et al., 1997; Mukherjee et al., 2012).

TGF-β-mediated increase in iCa^{2+} may depend on Ca^{2+} entry through L-VGCCs, as demonstrated in insulinoma cells (Ishiyama et al., 1996; Lv et al., 2019). In rat chondrocytes, TGF-β stimulation significantly increased iCa^{2+} via T- and L-VGCCs (Cailotto et al., 2011). It was shown that TGF-β3 resulted in a tendency to increase L-VGCCs expression at the gene level in MenSCs, BMMSCs, and chondrocytes (Uzieliene, Bironaite, Miksiunas, et al., 2023). Nevertheless, the precise mechanisms by which TGF-β affects Ca^{2+} signaling during human BM-MSCs chondrogenesis remain unclear. Addressing this knowledge gap may advance regenerative strategies for cartilage repair.

Extracellular regulatory influences on ion channels are often temporal and reversible, subsiding upon removal of the external stimulus (Plata-Salamán & ffrench-Mullen, 1993). In contrast, alterations in ion channel structure and function, such as those caused by genetic variants, tend to exert persistent effects on channel activity. In excitable tissues such as the heart, *KCNQ1* encodes the voltage-gated potassium channel $Kv_{7.1}$, which underlies the cardiac I_{Ks} current, and genetic mutations in this gene can lead to severe pathological outcomes. For instance, *KCNQ1* variants may either increase or decrease ionic currents (Brewer et al., 2025), and such functional deviations

can disrupt the finely tuned balance required for normal cardiac electrophysiology. One of the most well-characterized clinical conditions arising from such ion channel dysfunction is Long QT Syndrome (LQTS). This cardiac disorder is characterized by delayed repolarization of the myocardium, electrocardiographic QT prolongation, and heightened risk of syncope and sudden cardiac death due to polymorphic ventricular tachycardia known as Torsades de Pointes (Liang & Callans, 2017).

Pathogenic variants in *KCNQ1*, *KCNH2*, and *SCN5A* are the most common genetic causes of LQTS. Among the identified genetic causes, KCNQ1-related LQTS accounts for approximately 45% of all cases and represents the most prevalent genetic subgroup of the disorder (Morgat et al., 2024). Recently, a rare *KCNQ1* variant c.1111G>C [p.(Ala371Pro)], has been identified in several unrelated Lithuanian families. However, there is still a limited understanding of how this pathogenic variant alters channel function. Electrophysiological characterization of ion channel alterations has emerged as a decisive approach for establishing the pathogenicity of DNA variants by directly linking genetic changes to their functional impact on channel activity and clinical relevance.

Aim and Objectives

The study aimed to evaluate the effects of cytokines on Ca^{2+} homeostasis with a focus on L-VGCCs encoded by *CACNA1C*, and to assess the functional consequences of the rare *KCNQ1* variant c.1111G>C [p.(Ala371Pro)] on the biophysical properties of the $Kv_{7.1}$ channel.

The objectives were as follows:

- To assess the effects of TGF-β3 and IL-1β on Ca^{2+} homeostasis in bone marrow-derived mesenchymal stem cells (hBM-MSCs).
- To assess the effects of TGF-β3 and IL-1β on Ca^{2+} homeostasis in osteoarthritic chondrocytes.
- To analyze the impact of the *KCNQ1* p.(Ala371Pro) variant on late-repolarizing potassium current (I_{Ks}).

Scientific Novelty

This study for the first time provides:

- Direct electrophysiological evidence that TGF-β3 functionally upregulates L-VGCCs activity in hBM-MSCs, linking cytokine to increased Ca^{2+} influx through VGCCs.
- Evidence that TGF-β3 elevates iCa^{2+} in osteoarthritic chondrocytes without concomitant activation of L-VGCCs.
- The demonstration of distinct mechanisms underlying TGF-β3–induced iCa^{2+} elevation in BM-MSCs and osteoarthritic chondrocytes.
- Electrophysiological evidence demonstrates that the *KCNQ1* p.(Ala371Pro) variant leads to a significant reduction of the I_{Ks}.
- The demonstration that the *KCNQ1* p.(Ala371Pro) reduces channel conductance without affecting the voltage dependence of activation.

Practical Implication

- Insights into cytokine-dependent regulation of L-VGCCs in BM-MSCs may inform the optimization of chondrogenic differentiation protocols for cartilage tissue engineering.
- Identification of cell-type–specific differences in Ca^{2+} channel regulation may guide the development of more targeted therapeutic strategies for osteoarthritis.
- Functional assessment of the *KCNQ1* p.(Ala371Pro) variant provides clinically relevant evidence that supports its pathogenic classification in diagnostics of LQTS.

Thesis Statements

- TGF-β3 induces a functional increase in L-VGCCs activity in hBM-MSCs, resulting in enhanced Ca^{2+} influx, whereas this mechanism is absent in osteoarthritic chondrocytes.
- In chondrocytes, TGF-β3–induced elevation of intracellular Ca^{2+} occurs independently of L-VGCCs activation, indicating the involvement of alternative Ca^{2+} signaling pathways.
- IL-1β does not functionally modulate L-VGCCs activity in either hBM-MSCs or osteoarthritic chondrocytes under the experimental conditions applied.
- The *KCNQ1* p.(Ala371Pro) variant causes partial loss of I_{Ks} function by reducing channel conductance without affecting voltage-dependent

activation, providing direct electrophysiological evidence of its pathogenicity in LQTS.

Research structure

The thesis consists of 2 studies, both published in peer-reviewed journals. In Study I, we investigated the effects of TGF-β3 and IL-1β on L-VGCCs and Ca^{2+} homeostasis in OA chondrocytes and hBM-MSCs during chondrogenesis. Considering the established role of Ca^{2+} signaling in chondrogenesis and OA pathophysiology, we hypothesized that TGF-β3- and IL-1β-mediated modulation of L-VGCCs contributes to altered iCa^{2+} homeostasis and thereby regulates chondrogenic and inflammatory responses. In Study II, we investigated the functional consequences of the *KCNQ1* c.1111G>C [p.(Ala371Pro)] variant associated with Long QT Syndrome. We hypothesized that this pathogenic variant alters $Kv_{7.1}$ channel function and disrupts cardiac electrophysiological properties contributing to arrhythmogenic risk (Figure 1).

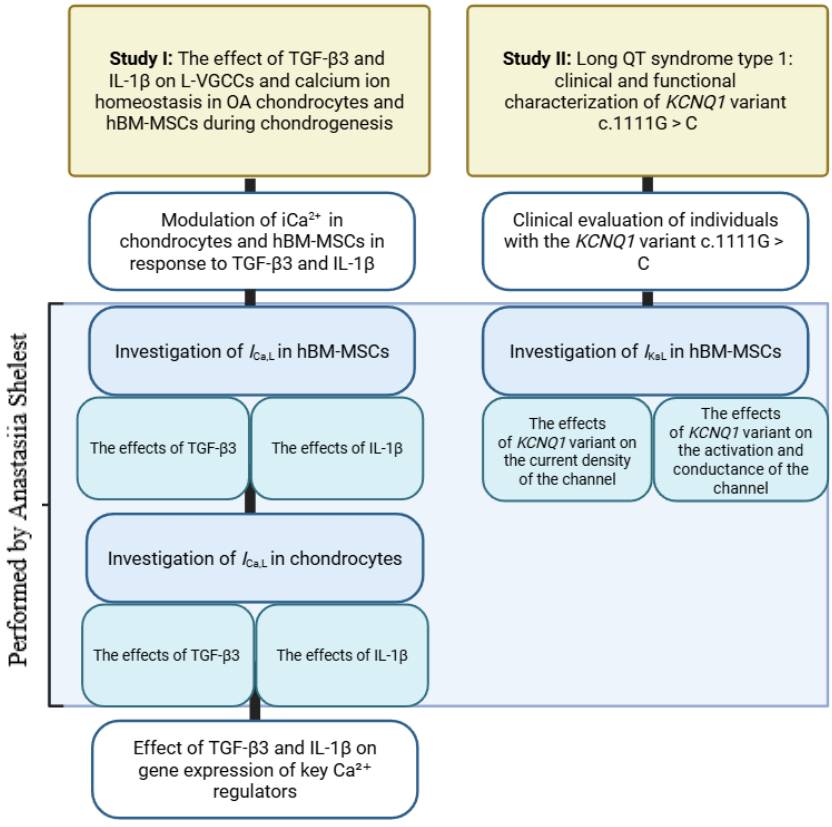

Figure 1. Scheme of studies included in the thesis. The image was created with BioRender.com (www.biorender.com, accessed on 25 May 2026).

LITERATURE REVIEW

1.1 Limited Repair Capacity of Cartilage

Cartilage is a specialized, smooth, and elastic connective tissue that plays a crucial role in distributing mechanical loads and minimizing friction within joints. Typically measuring 2–4 mm in thickness, it is composed of a dense ECM sparsely populated by highly specialized cells called chondrocytes (Abula et al., 2015). Notably, cartilage is avascular, aneural, and lacks lymphatic vessels, yet it endures substantial mechanical stress throughout life (Hunziker et al., 2002; Sophia Fox et al., 2009). These structural characteristics severely limit its regenerative capacity, as the absence of vascularization creates a poor nutritive environment for tissue repair (X. Guo et al., 2023). In addition, chondrocytes exhibit inherently low proliferative and differentiation potential (Simsa-Maziel & Monsonego-Ornan, 2012). Moreover, the cell density and *in vitro* proliferative capacity of articular chondrocytes decrease with age, with a notably lower level observed after 30 years (Barbero et al., 2004). As a result, even minor cartilage injuries can become clinically significant.

Such limitations in cartilage self-repair contribute directly to the development of joint diseases, particularly OA, which is a widespread degenerative condition affecting millions of people worldwide. It is characterized by the gradual breakdown of cartilage, leading to joint pain, stiffness, and loss of mobility (Tong et al., 2022). Although there is currently no cure for OA, various therapeutic approaches aim to manage symptoms and potentially slow disease progression (T. Chen et al., 2021).

1.2 Permanent and Transient Cartilage

The chondrocyte population in healthy cartilage consists of resting and differentiated cells responsible for maintaining a dynamic balance between the anabolism and catabolism of ECM compounds (Alford & Cole, 2005; Sophia Fox et al., 2009).

Cartilage can be classified into two types: permanent and transient. Healthy articular cartilage is referred to as permanent cartilage and consists of resting chondrocytes found in joints. Under normal physiological conditions, permanent cartilage exhibits a low proliferation rate and does not undergo terminal differentiation or endochondral ossification (Van der Kraan & van den Berg, 2012). Instead, transient cartilage is initially formed as cartilage but eventually undergoes endochondral ossification, resulting in bone formation.

In this case, differentiation of chondroprogenitor cells into the chondrocyte lineage typically does not give rise to permanent cartilage but instead promotes progression of hypertrophy and bone development (Van der Kraan & van den Berg, 2012).

1.3 Chondrocytes and Hypertrophy

In vivo, chondrocytes arise from pluripotent mesenchymal stem cells (MSCs) through a tightly regulated sequence of differentiation. This process is crucial for both embryonic development of the skeleton and for cartilage repair in adults. In the early stages of chondrogenesis, MSCs form aggregates and give rise to chondroprogenitor cells, which then mature into fully functional chondrocytes. Over time, these cells may enter a hypertrophic state, marking the transition toward terminal differentiation. Hypertrophic chondrocytes are cells that normally found between two different types of tissues, such as non-mineralized cartilage and ossified bone, at cartilage growth plate (Fernández-Iglesias et al., 2021).

Hypertrophy in chondrocytes refers not only to an increase in cell size, which distinguishes them from resting or proliferative chondrocytes, but also to a shift in gene expression. In this state, the expression of cartilage-specific markers such as aggrecan, collagen type II, and SRY-box 9 (*Sox9*) is decreased. In contrast, hypertrophic chondrocytes exhibit upregulation of genes associated with terminal differentiation, including collagen type X (Eyre, 1991; Zheng et al., 2003), runt-related transcription factor 2 (D. Chen et al., 2020), alkaline phosphatase (H.-M. Park et al., 2020), and matrix metallopeptidases-13 (MMP13) (Q. Hu & Ecker, 2021) all of which are recognized hypertrophic markers (Dreier, 2010; Zheng et al., 2003). As the surrounding cartilage matrix begins to calcify, hypertrophic chondrocytes undergo apoptosis and are progressively replaced by osteoblasts through the mechanism of endochondral ossification. Although this process is natural and essential for normal skeletal development where chondrocytes enlarge and mature, it can also be reactivated in damaged cartilage, leading to unwanted calcification and hastening the onset of degenerative conditions such as OA (Rim et al., 2020). These hypertrophic markers are recognized as hallmarks of OA progression when expressed in inappropriate locations such as articular cartilage, where they are not normally present (N. Chen et al., 2023; S. Park et al., 2021; Van der Kraan & van den Berg, 2012). This tendency toward hypertrophic differentiation is also a well-recognized challenge in regenerative medicine, where chondroprogenitor or stem-cell–derived chondrocytes frequently deviate from the stable chondrocyte phenotype and

progress toward hypertrophy (S. Chen et al., 2015). It is therefore crucial to find optimal strategies to stimulate chondroprogenitor cells to differentiate into chondrocytes and prevent them from hypertrophy and mineralization.

1.4 BM-MSCs and Chondrogenic Differentiation

MSCs are multipotent progenitor cells isolated from various tissues and organs (Colombini et al., 2019), such as adipose tissue (Fülber et al., 2021; Tsuji et al., 2014; Vidal et al., 2008; Zuk et al., 2002), menstrual blood (Faramarzi et al., 2016), umbilical cord (Chin et al., 2025; H.-S. Wang et al., 2004), placenta (Moonshi et al., 2022), synovium (Fülber et al., 2021; Lee et al., 2009) and bone marrow (Bhat et al., 2021; Fülber et al., 2021; Vidal et al., 2008). Among mesenchymal stem cell sources, BM-MSCs have been reported to possess a strong chondrogenic differentiation potential (Johnstone et al., 1998; Vidal et al., 2008). Their ability to differentiate into chondrocytes makes them particularly valuable for the treatment of OA and other joint disorders. Moreover, BM-MSCs are easily isolated and rarely cause immune reactions (Baghaei et al., 2017) (Figure 2). BM-MSCs can be applied in cell-based therapies, often in combination with biomaterials such as scaffolds, to replace or repair damaged cartilage in both human and veterinary medicine (Browe et al., 2022; Goldberg et al., 2017; Le et al., 2020; Peng et al., 2023; Yamagata et al., 2018). Ongoing research aims to elucidate the mechanisms underlying their chondrogenic differentiation in order to enhance therapeutic outcomes and to establish reliable *in vitro* models for studying disease processes and testing potential drugs (Gale et al., 2019; He et al., 2022; Neybecker et al., 2020; Uzieliene, Popov, Lisyte, et al., 2023). This approach also reduces the reliance on animal experimentation, offering a more ethical and humanistic alternative – cultivating and differentiating a cell line rather than using live animals.

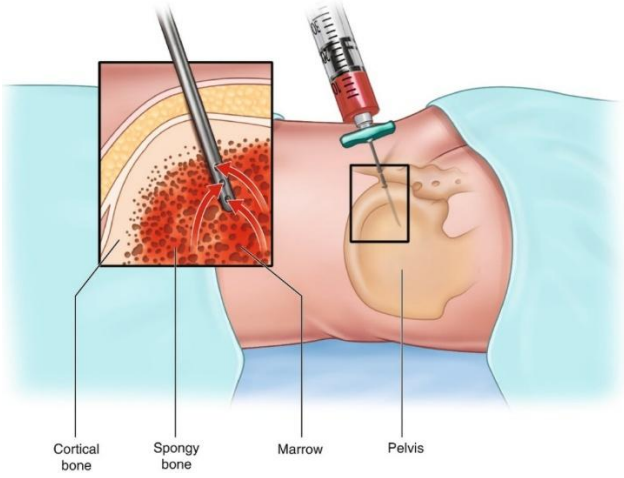

Figure 2. Bone marrow isolation from the iliac crest (R. R. Liu & Danesh, 2023).

BM-MSCs are multipotent and can differentiate into a variety of cell types, including osteoblasts (Hanna et al., 2018; Meesuk et al., 2022), chondrocytes (Johnstone et al., 1998; Nakagawa et al., 2016), adipocytes (Krawczenko & Klimczak, 2022), cardiomyocytes (J. Kim et al., 2015; Shi et al., 2016), hepatocytes (Lange et al., 2005), neurons (Qi et al., 2010) and nerve-like cells (Q. Liu et al., 2015). Each of these differentiation directions can be guided *in vitro* by applying specific culture conditions. BM-MSCs are generally maintained in Dulbecco's modified Eagle's medium (DMEM) supplemented with essential nutrients, hormones, growth factors, and other bioactive molecules that support lineage-specific differentiation (Futrega et al., 2021; Mauck et al., 2006; Solchaga et al., 2011; Uzieliene, Bironaite, Bagdonas, et al., 2023). For adipogenic differentiation, a medium contains components such as dexamethasone, indomethacin, 1-methyl-3-isobutylxanthine, and insulin (Pittenger et al., 1999). Osteogenic differentiation is typically promoted by culturing BM-MSCs in a medium enriched with dexamethasone, ascorbate-2-phosphate, and β-glycerophosphate (Jaiswal et al., 1997). Finally, chondrogenic differentiation can be triggered by BM-MSCs cultivation in medium containing dexamethasone, ascorbate-2-phosphate, insulin, transferrin-selenium, high glucose, L-proline, penicillin-streptomycin and TGF-β (Solchaga et al., 2011; Uzieliene, Bironaite, Bagdonas, et al., 2023). While several components are common in differentiation media, the presence of some distinct inductive factors defines differential direction. For chondrogenic differentiation, TGF-β acts as the main driving cytokine guiding BM-MSCs toward chondrogenic

differentiation (Uzieliene et al., 2019; Wee et al., 2022; Xia et al., 2017). However, in the joint environment, TGF-β is not the only cytokine influencing cells fate. Other cytokines present in inflamed cartilage can exert opposing effects. Among them, IL-1β has been shown to antagonize TGF-β–induced chondrogenesis (Wehling et al., 2009) and to promote catabolic activity within the cartilage microenvironment (Kobayashi et al., 2005). Therefore, understanding how both anabolic and catabolic cytokines influence BM-MSCs function is essential for optimizing cell-based cartilage repair strategies and for developing *in vitro* models that reflect the pathological environment of osteoarthritic joints.

1.5 Cytokines: General Features and Signaling Pathways in Chondrogenesis

Cytokines are small polypeptide signaling molecules that regulate a wide range of cellular processes in all tissues. They play dual roles in chondrogenesis, the process responsible for cartilage formation. TGF-β acts as a key anabolic cytokine that promotes chondrogenesis by stimulating chondrocyte differentiation and the synthesis of the ECM (H.-J. Kim et al., 2008; Mauck et al., 2006). In contrast, proinflammatory cytokines, such as IL-1β exert catabolic effects, inhibiting chondrogenic differentiation and promoting cartilage matrix degradation (Kobayashi et al., 2005). The balance between these opposing cytokine actions is essential for maintaining cartilage homeostasis and ensuring proper tissue development and repair.

1.5.1 Transforming Growth Factor-Beta

TGF-β is a pleiotropic cytokine belonging to the transforming growth factor superfamily that includes three different mammalian isoforms (TGF-β1, TGF-β2, and TGF-β3). It is now known that their sequences are 71–80% identical, and they activate signaling through the same receptors (T. Huang et al., 2014).

TGF-β was first identified in 1978 during studies on “sarcoma growth factors,” where it was found to stimulate cell proliferation and colony formation (de Larco & Todaro, 1978). Interestingly, TGF-β plays a dual role in tumorigenesis: while it suppresses tumor growth in early stages, its overexpression at later stages promotes cell proliferation, invasion, and metastasis (Haque & Morris, 2017). Although initially associated with tumor-related processes, TGF-β is now recognized as a cytokine widely produced by a wide range of normal tissues, including the muscles, kidneys, liver, heart,

brain, developing embryos and joints (Baugé et al., 2013; Derynck et al., 1985; J. Kim & Lee, 2017; Roberts et al., 1981).

TGF-β demonstrated therapeutic potential in various clinical contexts, including the treatment of venous stasis ulcers (Robson et al., 1995), prevention or alleviation of chemotherapy-induced oral mucositis in patients with lymphomas or solid tumors (Foncuberta et al., 2001), and protection against severe cardiac injury (Lefer et al., 1990). The widespread expression of TGF-β in healthy tissues highlights its essential and diverse roles in physiological processes, such as proliferation (Battegay et al., 1990; Sorensen & van Berlo, 2020), differentiation (M.-K. Wang et al., 2012), apoptosis (Ramesh et al., 2009), embryonic development (Heine et al., 1987; M. Y. Wu & Hill, 2009), immune regulation (Kehrl et al., 1986; Lebman & Edmiston, 1999) and tumor development (Derynck et al., 2021; Furler et al., 2018). All these processes primarily mediated through the activation of intracellular signaling cascades by TGF-β.

TGF-β initiates signaling cascades by binding to a receptor complex located on the plasma membrane, which consists of two serine/threonine kinase receptors: the type II receptor (TβRII) and the type I receptor (TβRI) (X.-H. Feng & Derynck, 2005). When TGF-β binds directly to TβRII, it triggers a conformational change that allows TβRII to recruit and phosphorylate TβRI, forming a receptor heterocomplex. Phosphorylation process activates TβRI, which in turn can initiate distinct signaling events, particularly canonical (Smad-dependent) and non-canonical (Smad-independent) signaling pathways (Figure 3) (Du et al., 2023). Non-canonical pathways are signaling cascades that function independently of Smad proteins and activate a variety of downstream cascades, including activation of extracellular signal-regulated kinase, nuclear factor of κB (NF-κB), c-Jun NH2-terminal kinase, and p38 mitogen-activated protein kinase (Figure 3B) (C. Li et al., 2023; N. G. M. Thielen et al., 2019).

In canonical pathways (Figure 3A), activated TβRI phosphorylates the Smad proteins, thereby transmitting signals through either the Smad1/5/8 or Smad2/3 signaling pathways (Du et al., 2023; N. G. M. Thielen et al., 2019). Then, phosphorylated Smads bind to Smad4, forming a complex that translocates to the nucleus. Once in the nucleus, Smad2/3-Smad4 or Smad1/5/8-Smad4 interacts with DNA and other transcription factors to regulate gene expression (X. Chen & Xu, 2011; X.-H. Feng & Derynck, 2005; Massagué et al., 2005; F. Xu et al., 2016). These target genes vary depending on the cell type. For instance, in stem cells, TGF-β signaling induces the

expression of genes involved in chondrogenic differentiation, such as *Sox9*, *Col2a1*, and *ACAN* (H.-J. Kim et al., 2008; Mauck et al., 2006).

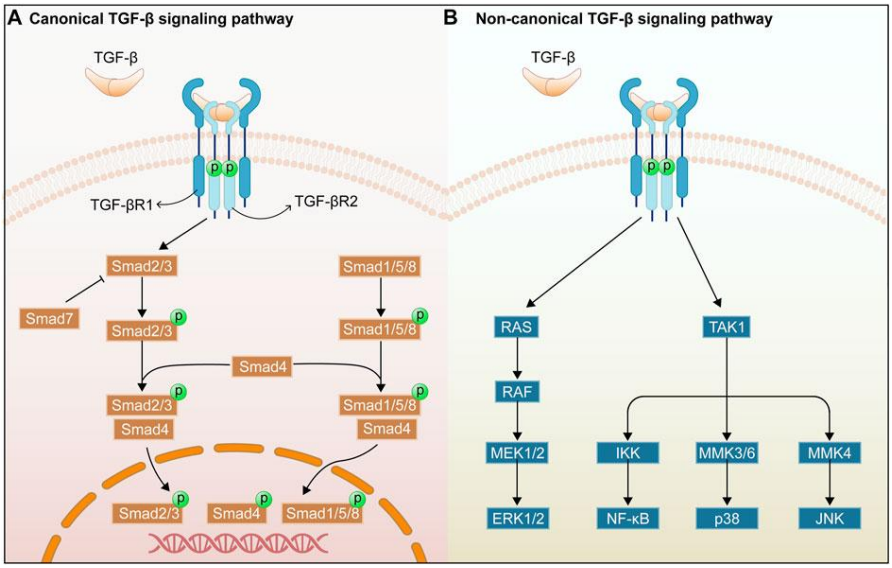

Figure 3. TGF-β signaling pathways. A) Canonical (Smad-dependent) TGF-β signaling pathway. B) Non-canonical (Smad-independent) TGF-β signaling pathway (C. Li et al., 2023).

Currently, TGF-β is widely used for inducing chondrogenesis in human BM-MSCs (Uzieliene et al., 2019; Wee et al., 2022; Xia et al., 2017). However, some studies have reported that TGF-β may also contribute to chondrocyte hypertrophy under certain conditions (N. G. M. Thielen et al., 2022). The involvement of TGF-β in cartilage physiology or pathology depends particularly on canonical signaling pathways (Du et al., 2023; N. G. M. Thielen et al., 2019). Activation of the Smad2/3 pathway is generally associated with healthy cartilage maintenance and chondrogenesis (Remst et al., 2014; X. Yang et al., 2001), while signaling through Smad1/5/8 has been linked to pathological changes, such as chondrocyte hypertrophy and cartilage degeneration (Remst et al., 2014; Blaney Davidson et al., 2009).

Activation of these two distinct pathways depends on different factors, such as TGF-β concentration, inflammation, and iCa^{2+}. For instance, low concentrations of TGF-β stimulate Smad2/3 signaling, which helps maintain the chondrogenic phenotype (Remst et al., 2014; X. Yang et al., 2001). In contrast, high concentrations of TGF-β would stimulate Smad1/5/8 signaling,

which causes chondrocyte hypertrophy (Remst et al., 2014; Blaney Davidson et al., 2009).

Not only the concentration but also the duration of TGF-β3 exposure is important. Studies have shown that BM-MSCs have been reported to gradually increase cartilage-specific matrix gene expression over time (H.-J. Kim et al., 2008; Mauck et al., 2006). Therefore, chondrogenic differentiation mediated by TGF-β requires precise regulation of both its concentration and the timing of exposure.

Although research is still ongoing to determine the optimal TGF-β concentration and exposure duration. Some studies have already demonstrated successful chondrogenic induction under varying conditions. For instance, one study showed that just a single day of exposure to 10 ng/mL TGF-β1 was sufficient to initiate differentiation (Futrega et al., 2021). While another study induced chondrogenic differentiation of BM-MSCs by culturing them for 35 days with 5 ng/mL of TGF-β3 (Z. Yang et al., 2012). However, it is currently standard practice to culture BM-MSCs for 21 days with 10 ng/mL TGF-β3 to achieve effective chondrogenic differentiation (Fonteneau et al., 2017; Futrega et al., 2021; Kiliç et al., 2007; Ruiz et al., 2019; Thorpe et al., 2010; Uzieliene, Bialaglovyte, Miksiunas, et al., 2023).

Overall, TGF-β3 remains a key regulator of chondrogenic differentiation, with its effects tightly dependent on concentration, exposure time, and the activated signaling pathway. These aspects are essential for understanding its role in cartilage development and related cellular processes.

1.5.2 Interleukin-1 Beta

IL-1β, like TGF-β3, belongs to the cytokines but differs in its function, acting as a proinflammatory cytokine. It is a part of the IL-1 family that plays a central role in regulating immune and inflammatory responses (Lopez-Castejon & Brough, 2011; Ren & Torres, 2009). It was first identified in 1984 as a factor produced by monocytes essential for host defense and immune responses (Auron et al., 1984). Although IL-1β can be produced by multiple cell types, its production has been most extensively studied in immune cells, including monocytes (Auron et al., 1984; Dasu et al., 2007), macrophages (H.-I. Huang et al., 2022) and lymphocytes (Lekshmi et al., 2012). Importantly, IL-1β is synthesized as an inactive precursor (pro-IL-1β) and requires cleavage by caspase-1 within the inflammasome complex to become biologically active (Lopez-Castejon & Brough, 2011; Modi et al., 2023; H. Zhang et al., 2023).

As one of the earliest mediators released upon infection or tissue injury, IL-1β modulates both local and systemic immune responses. It triggers the acute phase response through an interleukin-6 autocrine loop, involving the activation of NF-κB and CCAAT/enhancer-binding protein β (Kramer et al., 2008). It also enhances adaptive immunity by promoting T-helper cell responses and B-cell activation (Lipsky, 1985). At the systemic level, IL-1β participates in fever induction through central mechanisms by activating the sympathetic nervous system, which stimulates heat production in brown adipose tissue (Dascombe et al., 1989). This response helps create an unfavorable environment for infectious microorganisms and enhances lymphocyte function, which in mammals is more effective at elevated temperatures (Lin et al., 2019). Beyond immune regulation, IL-1β exerts broader effects on cellular physiology, including the control of proliferation, differentiation, and apoptosis in diverse cell types (Eller et al., 1995; C. Guo et al., 2016; Y. Li et al., 2020; Mahr et al., 2000; X. Wang et al., 2007; Yoon et al., 2023).

The role of IL-1β in regulating immune and inflammatory responses means that its imbalance can contribute to pathological conditions. Overexpression of this cytokine has been associated with various disorders, such as atherosclerosis (Kamari et al., 2007), diabetes (Mendiola & Cardona, 2018), cancer (Litmanovich et al., 2018), and a wide range of acute and chronic inflammatory disorders. Since the 1980s, IL-1β has been recognized as an effective inducer of an animal model of arthritis. The single intraarticular injection (in rabbit knee) of IL-1 is sufficient to reproduce, within 24 hours, the characteristic features of chronic erosive arthritis (Henderson & Pettipher, 1988; Pettipher et al., 1986). This model allows scientists to observe how the disease progresses over time, including changes in the synovial lining, cartilage, and bone.

Now it is known that IL-1β promotes OA and joint degeneration by downregulating cartilage matrix components such as type II collagen and aggrecan, while simultaneously upregulating catabolic enzymes such as MMP-1, MMP-3 and MMP13 in chondrocytes (Afifah et al., 2019; Kobayashi et al., 2005). Beyond its catabolic effects on cartilage matrix components, IL-1β also interferes with chondrogenic signaling pathways and stem cell differentiation.

IL-1β suppresses TGF-β-induced chondrogenesis of BM-MSCs (Wehling et al., 2009). IL-1β signals through various overlapping pathways with TGF-β, including Ca^{2+} signaling, and the Smad1/5/8 and Smad2/3 pathways. During inflammation, IL-1β inhibits Smad2/3 signaling (Baugé et al., 2007;

N. Thielen et al., 2021) while increasing Smad 1/5/8 signaling (L. Lu et al., 2020). It also decreases *Sox9* expression at both mRNA and protein levels, thereby inhibiting chondrocyte proliferation and differentiation via a *Sox9*-dependent pathway in mouse chondrocytic cell line (Murakami et al., 2000).

Despite its catabolic effects in chondrogenesis, some studies indicate a more complex role for IL-1β, showing that some concentrations can stimulate anabolic processes. For instance, IL-1β at concentrations between 10^{-10} and 10^{-8} g/mL significantly increased synovial MSCs proliferation in 2D culture, and pretreatment enhanced chondrogenic pellet formation and glycosaminoglycan (GAG) production after 14 days *in vitro* (Matsumura et al., 2017). Similarly, low doses of IL-1β have been reported to promote GAG accumulation and bone morphogenetic protein 2 expression during BM-MSC chondrogenesis, whereas higher doses impair ECM production and inhibit chondrogenic differentiation (Mumme et al., 2012).

In summary, although IL-1β usually inhibits cartilage formation, it can also support certain repair processes. This dual behavior highlights the need for a deeper understanding of IL-1β signaling in order to design more effective therapeutic strategies for cartilage repair and inflammatory joint diseases.

1.6 Calcium Homeostasis and Signaling in Chondrogenesis

Ca^{2+} signaling pathways regulate nearly all aspects of cellular function, including proliferation and differentiation (Mestril et al., 2021). Consequently, considerable attention has been directed toward understanding Ca^{2+} homeostasis in BM-MSC over the past decades. Research in this field has explored the mechanisms responsible for Ca^{2+} influx and efflux, as well as the signaling cascades that convert Ca^{2+} fluctuations into specific cellular outcomes (Kawano et al., 2002; Matta & Zakany, 2013). Although substantial progress has been made in characterizing Ca^{2+} homeostasis and ion channel composition in both BM-MSCs and mature chondrocytes (Lv et al., 2018; Matta & Zakany, 2013), the precise role of these mechanisms during the differentiation of BM-MSCs into chondrocytes remains insufficiently understood. Given that undifferentiated BM-MSCs and mature chondrocytes possess a distinct but partially overlapping set of Ca^{2+} channels and receptors regulating iCa^{2+}, it is reasonable to assume that both Ca^{2+} homeostasis and ion channel composition undergo dynamic changes during differentiation and contribute to the regulation of this process.

It has been demonstrated that Ca^{2+} takes part in chondrogenic differentiation. Pharmacological inhibition or genetic deletion of Ca^{2+} channels reduces the expression of key chondrogenic differentiation markers, including *Sox9* and *Col2a1* (Atsuta et al., 2019). Elevation of iCa^{2+} by ionophore, which facilitates Ca^{2+} entry into cells, improved the chondrogenic differentiation of chicken MSCs (Matta et al., 2008). An increase in extracellular Ca^{2+} concentration to physiologically relevant (8 mM) has been shown to enhance GAG and collagen type II production formation during chondrogenic differentiation of BM-MSCs. Importantly, this enhancement was achieved without hypertrophic side effects (Hammersen et al., 2023). On the other hand, elevated iCa^{2+} can activate Ca^{2+}/calmodulin-dependent protein kinase II (CaMKII) associated with chondrogenic hypertrophy (Saitta et al., 2019; Wuttisiriboon et al., 2023).

The regulation of iCa^{2+} depends mainly on Ca^{2+} entry from two sources: the extracellular space through channels located in the plasma membrane, and Ca^{2+} release from internal stores.

A broad range of plasma membrane Ca^{2+} channels can be classified into the following main groups:

- VGCCs, subdivided into several subtypes based on their characteristics, including L-, P/Q-, N-, R-, and T-type channels;
- ligand- or receptor-operated calcium channels;
- calcium release-activated calcium channels, which link external calcium entry to internal calcium release through store-operated mechanisms (Matta & Zakany 2013).

Another significant source of cytosolic Ca^{2+} is the intracellular Ca^{2+} stores, where release occurs through two main channel types:

- the inositol 1,4,5-trisphosphate receptor;
- the ryanodine receptor.

Ca^{2+} release from these intracellular stores is typically voltage-independent but agonist-dependent.

Since elevated iCa^{2+} can be cytotoxic, cells have evolved efficient mechanisms to tightly regulate and reduce cytosolic Ca^{2+} levels. The reduction of iCa^{2+} is achieved through several major pathways, including:

- removal across the plasma membrane;
- uptake into intracellular stores;
- buffering by calcium-binding proteins.

Removal of Ca^{2+} across the plasma membrane is primarily mediated by two key systems. One of the most important mechanisms is the sodium–calcium exchanger (NCX), an electrogenic antiporter that utilizes the electrochemical gradient of Na^{+} to drive Ca^{2+} efflux. Typically, three Na^{+} ions enter the cell in exchange for the export of one Ca^{2+} ion, making this process energetically favorable under physiological conditions. NCX is widely expressed across various cell types and plays a crucial role in maintaining low basal cytosolic Ca^{2+} concentrations, particularly in excitable cells (Xue et al., 2023).

In addition to NCX, Ca^{2+} removal is mediated by the plasma membrane Ca^{2+}-ATPase (PMCA), a high-affinity transport system that actively pumps Ca^{2+} out of the cell using energy derived from ATP hydrolysis. This process operates against the Ca^{2+} concentration gradient and is typically coupled with the counter-transport of protons (H^{+}). PMCA is especially important for fine-tuning iCa^{2+} and maintaining Ca^{2+} homeostasis under resting conditions (Brini & Carafoli, 2011).

Another major mechanism for reducing iCa^{2+} involves its sequestration into intracellular organelles, primarily ER and mitochondria. Uptake of Ca^{2+} into the ER is mediated by the sarco/endoplasmic reticulum Ca^{2+}-ATPase (SERCA), which actively transports Ca^{2+} from the cytosol into the ER lumen using ATP. This process is essential for both the termination of Ca^{2+} signaling and the replenishment of intracellular Ca^{2+} stores (Brini & Carafoli, 2011; H. Xu & Van Remmen, 2021). Mitochondria also contribute to Ca^{2+} buffering by taking up Ca^{2+} through the mitochondrial calcium uniporter, particularly under conditions of elevated iCa^{2+}(D'Angelo & Rizzuto, 2023).

In addition to transport mechanisms, iCa^{2+} levels are further regulated by calcium-binding proteins, such as calmodulin, calbindin, and parvalbumin, which act as buffers by reversibly binding free Ca^{2+} ions. These proteins modulate both the amplitude and duration of Ca^{2+} signals and play an essential role in shaping downstream signaling pathways (Cruikshank et al., 2001; Timofeeva & Volynski, 2015).

1.7 TGF-β and IL-1β Impact Calcium Homeostasis

Cytokines used to induce chondrogenic differentiation, as well as those present in inflamed or degenerating cartilage, can profoundly modulate iCa^{2+} homeostasis, thereby influencing the downstream signaling pathways that regulate chondrogenesis and cartilage maintenance. It has been demonstrated that TGF-β mediates elevation of iCa^{2+} (Alevizopoulos et al., 1997; Cailotto et al., 2011; Muldoon et al., 1988; Nesti et al., 2007). IL-1β also mediates the

elevation of iCa^{2+} in bovine chondrocytes (LUO et al., 1997). In turn, elevated iCa^{2+} activates CaMKII, which directly interacts with Smads (Eapen et al., 2013; Saitta et al., 2019; Wicks et al., 2000). Activated CaMKII leads to the activation of the Smad1/5/8 and inactivation Smad2/3 pathways (Saitta et al., 2019).

It has been demonstrated that TGF-β induces Ca^{2+} influx in murine fibroblasts, mesangial cells, insulinoma cells, chondrocytes, and human pulmonary fibroblasts (Alevizopoulos et al., 1997; Ishiyama et al., 1996; McGowan et al., 2002; Mukherjee et al., 2012). In fibroblasts, TGF-β mediates iCa^{2+} elevation, which involves both Ca^{2+} influx across the cell membrane as well as Ca^{2+} release from the ER (Alevizopoulos et al., 1997; Mukherjee et al., 2012). TGF-β led to a significant elevation in iCa^{2+} in rat chondrocytes via a few types of voltage-gated Ca^{2+} channels (Cailotto et al., 2011), while IL-1β was shown to mediate iCa^{2+} elevation in rat chondrocytes via the transient receptor potential ankyrin 1 (TRPA1) cation channel (Yin et al., 2018). The TGF-β-mediated increase in iCa^{2+} may depend on Ca^{2+} entry through L-VGCCs in insulinoma cells (Ishiyama et al., 1996; Lv et al., 2019).

In excitable cells, there is substantial evidence that TGF-β and IL-1β modulate L-VGCCs, particularly $Ca_{V1.2}$. For example, TGF-β reduces the number of functional L-VGCCs at the myoblast plasma membrane by approximately 90% (Mejia-Luna & Avila, 2004), suppresses the L-type calcium currents ($I_{Ca,L)}$ in cardiac myocytes, and decreases atrial $Ca_{V1.2}$ mRNA levels (Avila et al., 2007). TGF-β has also been shown to downregulate $Ca_{V1.2}$ expression in cortical neurons (Z. Liu et al., 2018). IL-1β has been reported to reduce I_{CaL} in mouse cardiomyocytes (El Khoury et al., 2014) and to decrease the density of I_{CaL} in mouse cardiomyocytes without affecting $Ca_{V1.2}$ expression (Khoury & Fiset, 2012). IL-1β caused a concentration-dependent decrease in the peak I_{CaL} in rat ventricular myocytes (S. Liu & Schreur, 1995). In contrast, the literature remains limited, and there are insufficient studies directly assessing how TGF-β and IL-1β regulate $Ca_{V1.2}$ function in non-excitable cells, including chondrocytes and MSCs.

1.8 L-VGCCs Structure, Distribution, and Function

L-VGCCs are high-voltage-activated channels known for their long-lasting activation and sensitivity to dihydropyridine drugs. L-VGCCs include four isoforms of the pore forming α_1 subunit – α_{1S} ($Ca_{V1.1}$), α_{1C} ($Ca_{V1.2}$), α_{1D} ($Ca_{V1.3}$), and α_{1F} ($Ca_{V1.4}$) - encoded by *CACNA1S, CACNA1C, CACNA1D*, and *CACNA1F,* respectively (Figure 4).

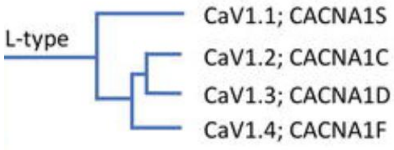

Figure 4. The relationship among the members of the L-VGCCs (modified from Feng et al., 2018)**.**

From a structural standpoint, L-VGCCs are hetero-oligomeric assemblies composed of five subunits (Figure 5):

- α_1 (170 kDa),
- β (50–78 kDa),
- α_2 (150 kDa),
- δ (17–25 kDa),
- γ (32 kDa).

The α_1 subunit forms a pore of L-VGCCs, creating the ion-conducting pathway for Ca^{2+}. This subunit consists of four intervening transmembrane domains (DI-DIV). Each of the four transmembrane domains of the α_1 subunit is formed from six transmembrane α-helices (S1–S6), where S1–S4 helices are known as the voltage-sensing domain (VSD), and S5–S6 form the pore domain (PD) (Figure 5).

The β subunit is located on the intracellular side of the channel.

The α_2 and δ subunits are encoded by a single gene but are later split into two parts: extracellular α_2 and a the transmembrane δ. These two parts remain linked by a disulfide bond and together form the $\alpha_2\delta$ subunit (T. Feng et al., 2018).

The β, $\alpha_2\delta$, and γ act as auxiliary subunits that modulate L-VGCCs function. In general, they enhance activation and deactivation kinetics and markedly increase the maximal ionic current conductance (Dolphin, 2013).

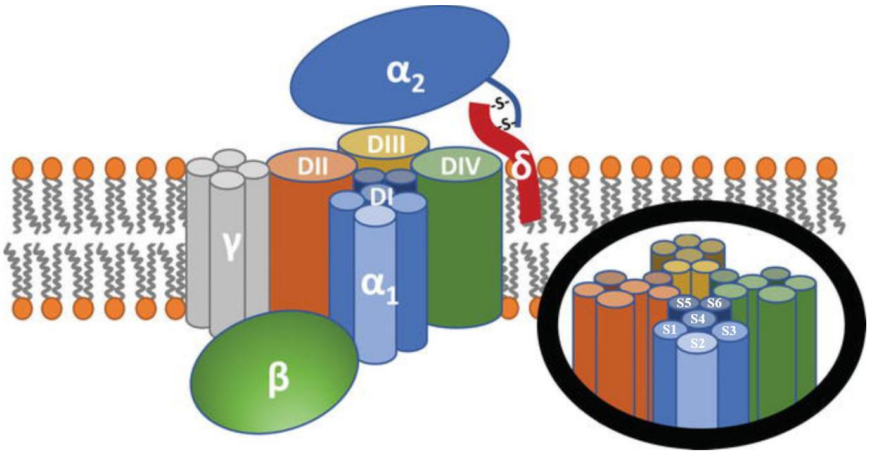

Figure 5. L-VGCCs structure: the pore-forming α1 subunit and auxiliary subunits (β, $\alpha_2\delta$, and γ). The circled inset depicts a detailed view of the α1 transmembrane domains (modified from Feng et al., 2018).

Not all L-VGCC isoforms share the same subunit composition. For example, $Ca_{V1.2}$ and $Ca_{V1.3}$ lack the transmembrane γ subunit and are composed of four subunits (Striessnig et al., 2014). Differences in subunit composition contribute to isoform-specific biophysical properties, including differences in activation threshold, activation and inactivation kinetics, peak current, and the midpoint of voltage-dependent activation ($V_{1/2}$). $Ca_{V1.3}$ channels have been reported to exhibit faster activation and slower inactivation kinetics compared to $Ca_{V1.2}$, with differences of up to ~30% and ~36%, respectively (Christel et al., 2012).

In terms of voltage dependence, $Ca_{V1.2}$ channels activated at relatively depolarized potentials (around -35 mV) and reached peak current at approximately 10 mV (Heubach et al., 2004) with $V_{1/2}$ around -5 mV (Lipscombe, 2002). In contrast, $Ca_{V1.3}$ channels activate at significantly more hyperpolarized potentials (around −60 mV), peak at approximately −20 mV (W. Xu & Lipscombe, 2001) with $V_{1/2}$ of around -30 mV (Figure 6) (Lipscombe, 2002).

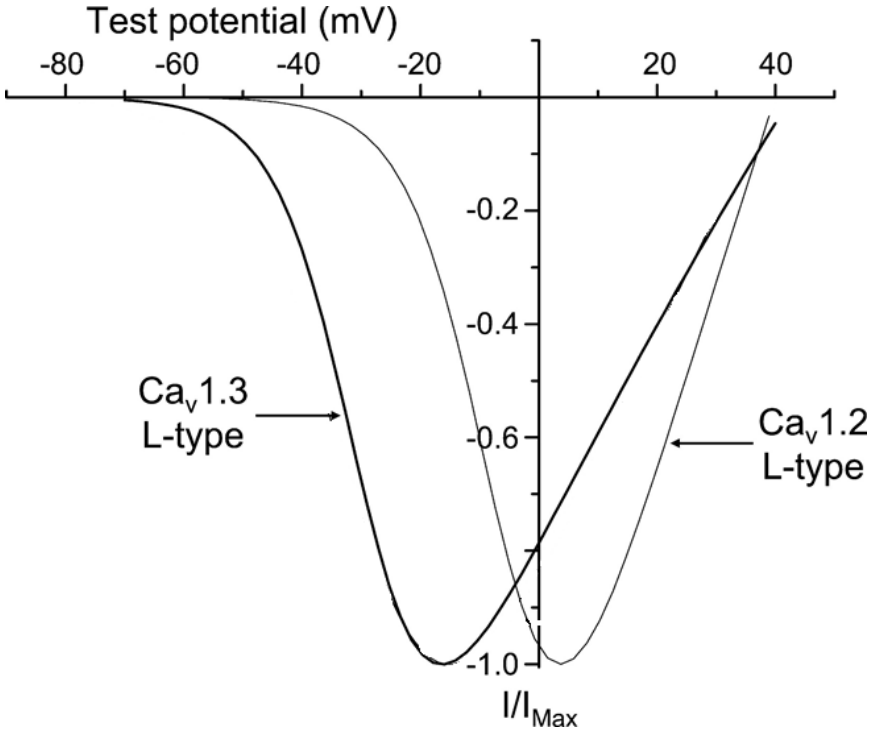

Figure 6. Normalized, peak current-voltage relationships for $Ca_{V1.2}$ and $Ca_{V1.3}$ (modified from Lipscombe, 2002)**.**

The distribution of L-VGCCs isoforms is highly heterogeneous across tissues, consistent with their divergent physiological roles in different cell types. For example, all L-VGCCs isoforms have been identified in lymphocytes, supporting a potential role for these channels in endocrine-related functions (Gomes et al., 2004). $Ca_{V1.1}$ is expressed predominantly in skeletal muscle, where it contributes to muscle contraction. In addition, $Ca_{V1.1}$ has been reported to be co-expressed with ryanodine receptors in GABAergic neurons (Hofmann et al., 2014). $Ca_{V1.2}$ is the most abundant subtype of L-VGCCs in the mammalian brain (Hell et al., 1993). In addition, $Ca_{V1.2}$ is the main L-VGCCs in cardiomyocytes and supports excitation–contraction coupling. $Ca_{V1.3}$ is expressed in the pancreas and kidney, where it is linked to endocrine secretion, and in the cochlea, where it helps regulate auditory transduction. $Ca_{V1.4}$ is expressed predominantly in retinal cells and supports normal visual function (Baumann et al., 2004).

Several L-VGCC isoforms may be expressed in the same cells yet contribute to different physiological functions. In this context, $Ca_{V1.2}$ and

$Ca_{V1.3}$ display a highly overlapping expression profile and often occur in the same cell types, such as cardiomyocytes and neurons (Striessnig et al., 2014).

The α1 subunit of $Ca_{V1.2}$ is highly expressed in human BM-MSCs (Heubach et al., 2004; Uzieliene, Bironaite, Miksiunas, et al., 2023). $Ca_{V1.2}$ expression has also been reported in chondrocytes (Atsuta et al., 2019; Matta et al., 2015; Uzieliene, Bironaite, Miksiunas, et al., 2023). The existing reports suggest that $Ca_{V1.2}$ signaling may influence proliferation and differentiation in both chondrocytes and BM-MSCs. For example, nifedipine, a specific L-VGCC blocker, has been shown to tend to reduce proliferation in BM-MSCs and to significantly decrease proliferation in chondrocytes. This reduction in proliferation may reflect a shift toward chondrogenic differentiation, accompanied by cell cycle arrest (Beier et al., 1999). Consistent with this interpretation, nifedipine treatment promoted chondrogenic differentiation, as evidenced by increased ECM production in both chondrocytes and BM-MSCs. Interestingly, BayK8644, a L-VGCC agonist, also stimulated cartilage ECM production in both cell types. However, its effects were markedly weaker than those observed with nifedipine (Uzieliene et al., 2019).

1.9 Long QT Syndrome

LQTS is an abnormal prolongation of the QT interval on an electrocardiogram (ECG) (Figure 7A), a serious inherited arrhythmia disorder and an important cause of sudden cardiac death in children and young adults. This condition has a tendency to develop syncope and ventricular arrhythmias, most often triggered by physical exertion or emotional stress (Moss, 2003). According to the 2015 European Society of Cardiology guidance, the corrected QT interval (QTc) ≥480 ms (sex-independent) is considered diagnostic for LQTS (Figure 7B) (Priori et al., 2015).

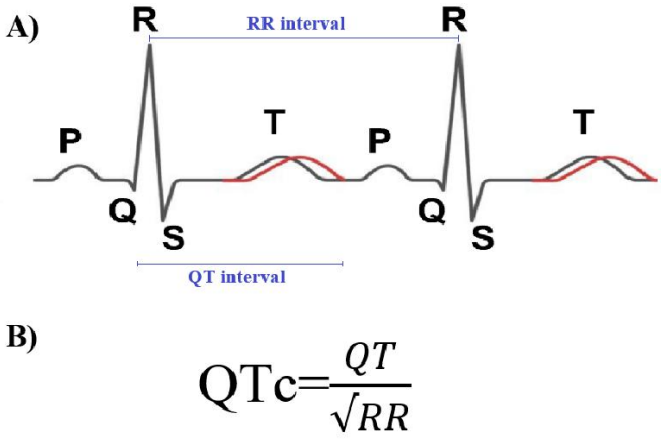

Figure 7. A) Representative ECG trace illustrating a cardiac cycle. The basic pattern of heart's electrical activity recorded on an ECG consists of the P–QRS–T waveform. These components represent the cardiac electrical cycle, where the P wave reflects atrial depolarization, the QRS complex represents rapid ventricular depolarization, the ST segment corresponds to the plateau phase of the ventricular action potential, and the T wave reflects ventricular repolarization. QT interval = Q wave to end of T wave. RR interval = time from two consecutive R waves.
The grey trace depicts a normal ECG waveform, while the red trace shows QT interval prolongation characteristic of LQTS (modified from Kekenes-Huskey et al., 2022).
B) Bezett`s Formula, where the corrected QT interval (QTc) is the QT interval divided by the square root of the RR interval.

The risk of QT prolongation is influenced by multiple factors, including age, electrolyte disturbances, medications, and diseases such as psychiatric comorbidities, diabetes mellitus, or epilepsy (Diercks et al., 2004; Fenichel et al., 2004; Ferreira Felix et al., 2025; Marstrand et al., 2019; Roden et al., 1986; Surges et al., 2010). In addition, long QT can be congenital, most often due to pathogenic variants in ion-channel genes, or acquired, arising secondary to external or clinical factors.

Nowadays, three major genes and ten minor LQTS-susceptibility genes have been implicated in LQTS, and together they account majority of genetically confirmed cases (Tester & Ackerman, 2014). The ten minor LQTS-susceptibility genes include *AKAP9, CACNA1C, CALM1, CALM2, CAV3, KCNE1, KCNE2, KCNJ5, SCN4B, SNTA1* (Tester & Ackerman, 2014).

Variants in the three major LQTS genes, *KCNQ1, KCNH2, and SCN5A*, typically cause LQT1, LQT2, and LQT3, respectively, and together account for ~90% of genotype-positive (molecularly confirmed) LQTS cases (Kapplinger et al., 2009; Tester et al., 2005). Among these, *KCNQ1* mutations are the most frequent, representing the major cause of inherited LQTS

(Fernandes et al., 2015). In fact, *KCNQ1*-related LQTS alone accounts for approximately 45% of all cases, making it the most common of the three principal LQTS subtypes (Morgat et al., 2024).

1.10 Structure and Function of the $Kv_{7.1}$ Channel and Accessory β-Subunits of the KCNE Family

KCNQ1 encodes the pore-forming α-subunit of the voltage-gated potassium channel $Kv_{7.1}$, comprising 676 amino acids and a molecular weight of 75 kD (Craig et al., 2015). Four pore-forming α-subunits form a functional $Kv_{7.1}$ channel. Each α-subunit contains six transmembrane-spanning segments (S1-S6) with four VSD segments (S1-S4), two PD (S5-S6) segments, two cytoplasmic loops (S2-S3 and S4-S5), and an intracellular C-terminal helix (Figure 7). $Kv_{7.1}$ expressed alone generates a typical delayed rectifier potassium current characterized by rapid activation ($\tau_{activation} \approx 80-100$ ms at 60 mV), delayed partial inactivation (~60% of the channels are inactivated at 60 mV under steady-state conditions), and relatively slow deactivation kinetics (Wrobel et al., 2012).

$Kv_{7.1}$ can co-assemble with KCNE regulatory β-subunits (KCNE1–5), which dramatically alter the channel's biophysical properties (Kasuya et al., 2024; Wrobel et al., 2012). For example, KCNE2 reduces $Kv_{7.1}$ channel current amplitude, induces instantaneous activation, rapid partial deactivation, and produces a linear current–voltage relationship (Tinel, 2000). KCNE3 exerts similar effects but, unlike KCNE2, retains some time-dependent gating at positive potentials and increases current density (Melman et al., 2001; Schroeder et al., 2000). KCNE4 markedly reduces channel currents at physiologically relevant membrane potentials (Grunnet et al., 2002). KCNE5 induces a depolarizing shift in the voltage dependence of activation, with a threshold of ~+40 mV (Angelo et al., 2002).

KCNE1 consists of only 130 amino acids and has a molecular weight of 15.7 kD (Craig et al., 2014; Sanguinetti et al., 1996). It contains a single α-helical transmembrane domain, with an extracellular N-terminal helix and an intracellular C-terminal helix (Figure 8) (J. Wu et al., 2016).

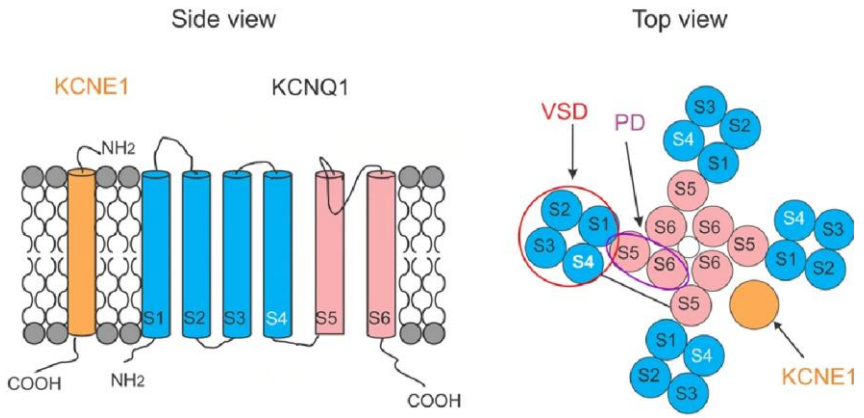

Figure 8. Schematic side and top view of one KCNQ1 and one KCNE1 subunit (shown in orange), and top view of the $K_{V7.1}$ channel (four KCNQ1 subunits) and one KCNE1 subunit (shown in orange). Segments S1–S4 form VSD (blue), while S5–S6 constitute PD (pink) (modified from Wu et al., 2021).

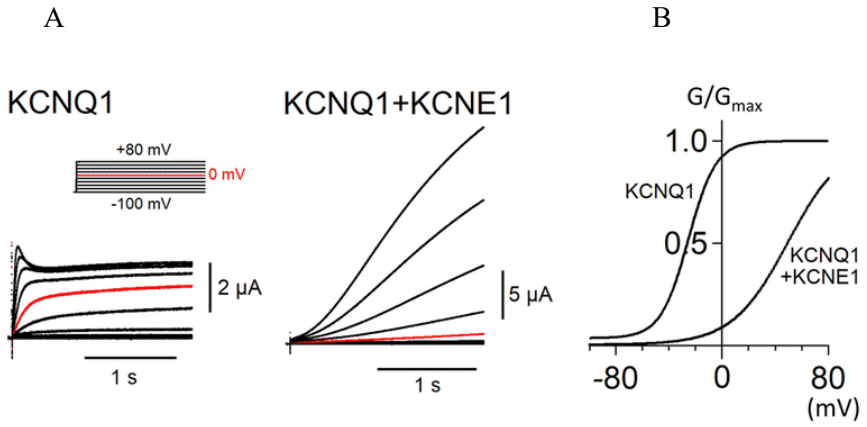

Figure 9. A) Representative whole-cell current traces and B) G–V relationships of current mediated through $K_{V7.1}$ channels (encoded by *KCNQ1)* expressed in *Xenopus* oocytes, with or without *KCNE1* co-expression. The currents recorded at 0 mV are highlighted in red for comparison (modified from Nakajo, 2019).

The function of the $K_{V7.1}$ channel is modulated by the KCNE1 subunit through several mechanisms (Ponce-Balbuena & Deschênes, 2021; Schwartz et al., 2021). Co-expression of the channel with the KCNE1 subunit increases current amplitude by 10 times and single-channel conductance while eliminating the inactivation of the $K_{V7.1}$ channel (Figure 9A). In addition, association with KCNE1 markedly slows channel activation kinetics, often

resulting in a double-exponential time course that is much slower than that of the α-subunits alone, particularly at intermediate potentials (Chan et al., 2012). KCNE1 typically increases the activation time constant to the range of hundreds of milliseconds to several seconds, essential for cardiac action potential repolarization. Also, KCNE1 shifts the voltage dependence of channel activation toward more depolarized potentials (Figure 9B) (Nakajo, 2019; X. Wu et al., 2021).

1.11 $K_{V7.1}$ Channel Role in the Cardiac Action Potential

In the heart, $K_{V7.1}$ channels co-assembled with the KCNE1 β-subunit mediate I_{Ks} during ventricular cardiac action potential repolarization, thereby contributing to repolarization regulation (Jespersen et al., 2005). These channels remain closed at the negative diastolic membrane potential but open in response to membrane depolarization during systole.

The ventricular action potential is traditionally divided into five phases, from phase 0 to phase 4 (Figure 10):

- Phase 0, the rapid depolarization phase, occurs when fast voltage-gated sodium channels open, generating a sharp inward sodium current.
- Phase 1, the initial repolarization, results from a brief outward potassium current carried by transient outward potassium channels.
- Phase 2, known as the plateau phase, reflects a delay in membrane repolarization due to sustained inward calcium influx through L-VGCCs, which are activated when the membrane potential reaches approximately –40 mV.
- Phase 3, or repolarization, begins as delayed rectifier potassium channels (I_{Kr} and I_{Ks}) become open while L-VGCCs become closed.
- Phase 4, the resting phase, corresponds to returning to the resting membrane potential (Santana et al., 2010).

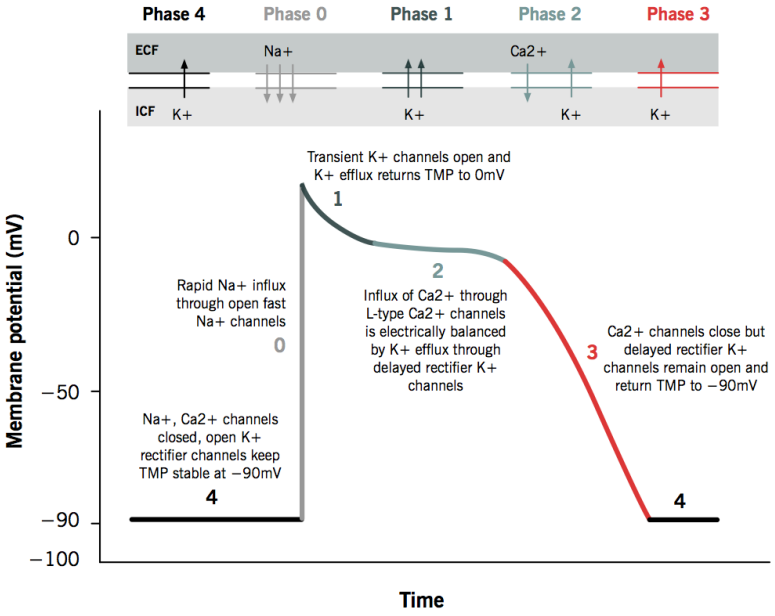

Figure 10. Overview of the ventricular action potential phases and associated ionic currents.

Top panel: Schematic representation of ionic fluxes during each phase of the ventricular action potential. Arrows indicate the direction of sodium, calcium, and potassium movement across the cell membrane in extracellular (ECF) and intracellular (ICF) fluid.

Bottom panel: Graphical representation of the ventricular action potential phases: phase 0 – depolarization; phase 1 – early repolarization; phase 2 – plateau; phase 3 - repolarization; phase 4 – resting phase (Physiology of Cardiac Conduction and Contractility – McMaster Pathophysiology Review, 2013).

1.12 Long QT Syndrome Caused by Mutations in the *KCNQ1* Gene

I_{Ks} play a critical role in shortening the QT interval during increases in heart rate. Mutations in *KCNQ1* lead to the formation of dysfunctional $Kv_{7.1}$ α-subunits, resulting in impaired channel function and altered I_{Ks}, which in turn causes delayed ventricular repolarization and QT interval prolongation, which creates conditions strongly predisposing to arrhythmias (Tristani-Firouzi et al., 2001).

Genetic defects in ion channel genes disrupt channel behavior through several distinct pathways. Most cases of LQTS follow a dominant inheritance pattern, in which one mutated and one normal allele are present. A large proportion of these mutations are missense variants, caused by single-nucleotide changes, which lead to the substitution of one amino acid. Such

substitutions often produce misfolded subunits that cannot assemble properly, leading to the accelerated degradation of the channel complex. This dominant-negative interference reduces the number of functional channels to well below 50%.

Dominant-negative effects may also occur when the substituted amino acid is critical for channel function (Tristani-Firouzi et al., 2001). *KCNQ1* variants located in the transmembrane VSD or PD are generally associated with more severe clinical manifestations (Brewer et al., 2025). Carriers of such variants typically exhibit an average QTc of 480 ± 32 ms (J. N. Johnson & Ackerman, 2009) and a high incidence of cardiac events, whereas normal QTc values are usually ≤450 ms for men and ≤460 ms for women (Figure 11).

For example, several pathogenic *KCNQ1* variants in the PD region have been reported with marked QT prolongation (QTc: 540 ms), including p.(Ala371Thr) (QTc: 506 ms) (Donger et al., 1997; Jongbloed et al., 1999), p.(Leu374His) (QTc: >500 ms), and (Ser373Pro) (Hammami Bomholtz et al., 2020). By contrast, carriers of p.(Arg555Cys) in the same domain exhibit a less pronounced QT prolongation (459 ± 33 ms) and a lower incidence of symptoms and sudden deaths (Donger et al., 1997).

Collectively, these observations suggest that variant location alone does not reliably predict clinical severity or the underlying mechanism. Therefore, each *KCNQ1* variant should be evaluated on a case-by-case basis, ideally including dedicated functional characterization.

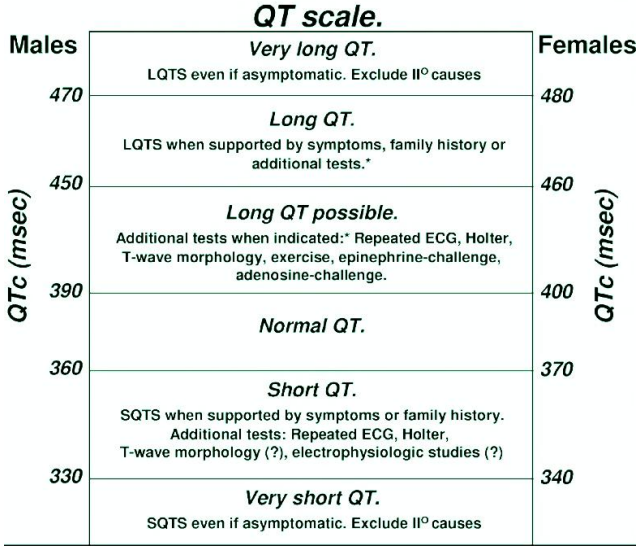

Figure 11. "QT scale" illustrating the spectrum of QT intervals, from very short to very long (Viskin, 2009). Definitions and additional tests are provided in the figure text.

1.13 Functional Signatures of Pathogenic *KCNQ1* Variants in LQT1

As of today, approximately 3,000 *KCNQ1* variants are registered in the ClinVar database (Landrum et al., 2016), with many submissions annotated as variants of uncertain significance or with conflicting pathogenicity assessments (Figure 12). This highlights the need for functional evidence capable of distinguishing pathogenic from benign variation.

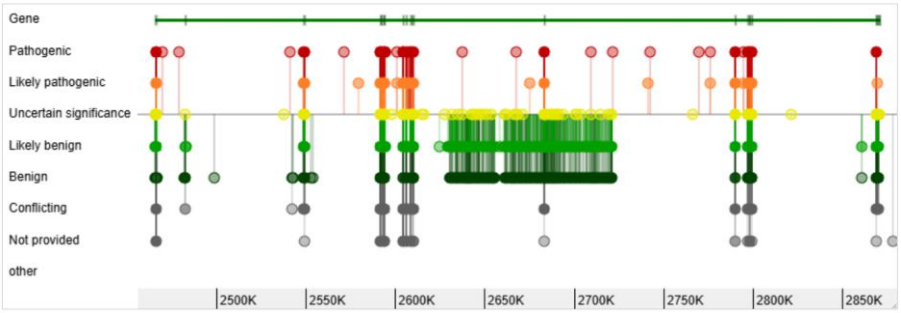

Figure 12. ClinVar entries for KCNQ1. Graphical view of variant distribution and clinical significance categories (NCBI ClinVar accessed on 12 January 2026).

KCNQ1 variants associated with LQTS generally impair $Kv_{7.1}$ channel function, leading to alterations in $I_{Ks,}$ most commonly through loss-of-function (LOF). In 2025, a study evaluated the functional impact of 61 *KCNQ1* variants distributed across all domains of the channel, including the N-terminal domain, the membrane-integral VSD, PD, and multiple cytosolic regions, such as the calmodulin-binding HA/HB helices, as well as the HC and HD helices and the distal C-terminus. Functional assessment of *KCNQ1* variants, which encode the pore-forming α-subunits of the $Kv_{7.1}$ channel, based on peak current density and $V_{1/2}$, demonstrated that 91% exhibited LOF, defined as a reduction in current to less than 65% of the maximal wild-type current, and more than half of the variants showed severe LOF, with currents reduced to less than 25% of wild-type levels (Figure 13). Furthermore, some variants significantly shifted the voltage dependence of channel activation, as reflected by changes in $V_{1/2}$ (Brewer et al., 2025).

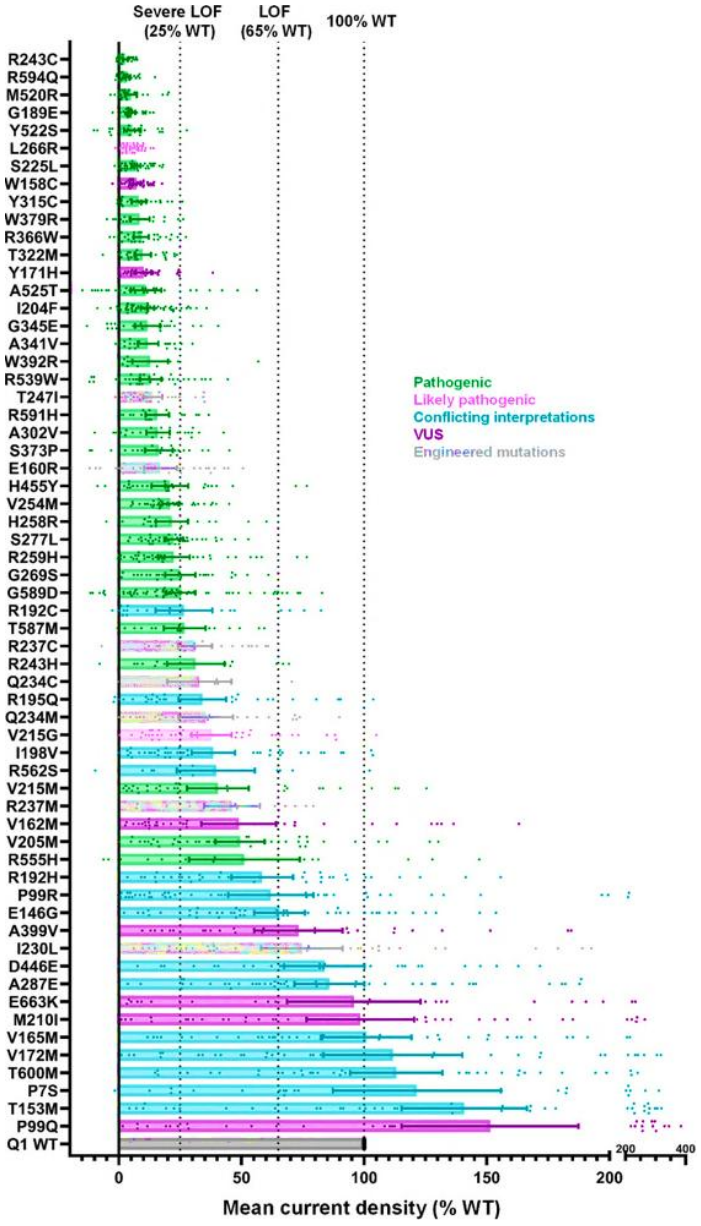

Figure 13. Comparison of mean current density of the $Kv_{7.1}$ channel in 61 variants spanning the KCNQ1 protein sequence. The data are color-coded by variant classification: pathogenic mutations in green, variants of uncertain significance (VUS) in dark purple, conflicting interpretations in cyan, likely pathogenic mutations in light purple, and engineered mutations in light gray. Data are ordered from highest to lowest current density measured at the end of a 2000-ms pulse to +60 mV. Mean current density values are given as % WT. Error bars denote mean and standard deviation (modified from Brewer et al., 2025).

Importantly, although variants were distributed across all structural regions of the *KCNQ1* gene encoding the α-subunit of the $Kv_{7.1}$ channel, most resulted in LOF irrespective of their location. This indicates that pathogenicity cannot be reliably predicted based solely on variant localization, underscoring the need for individual functional characterization.

Although most *KCNQ1* variants result in LOF of the $Kv_{7.1}$ channel, this effect is not universal. In a study by (Rinné et al., 2023), eight of nine *KCNQ1* variants (G119R, delF166, delG186_L187, V254L, I421E, R539L, and R591C) when co-expressed with β-subunit KCNE1, exhibited a significant reduction in I_{Ks} mediated by channel complexes (Figure 14A, B, C), with only one (L273V**)** showing a significant rightward shift in $V_{1/2}$ of a channel. In contrast, only one of the nine variants (G430fs*28) did not significantly alter channel current amplitudes (Figure 14A, B, D).

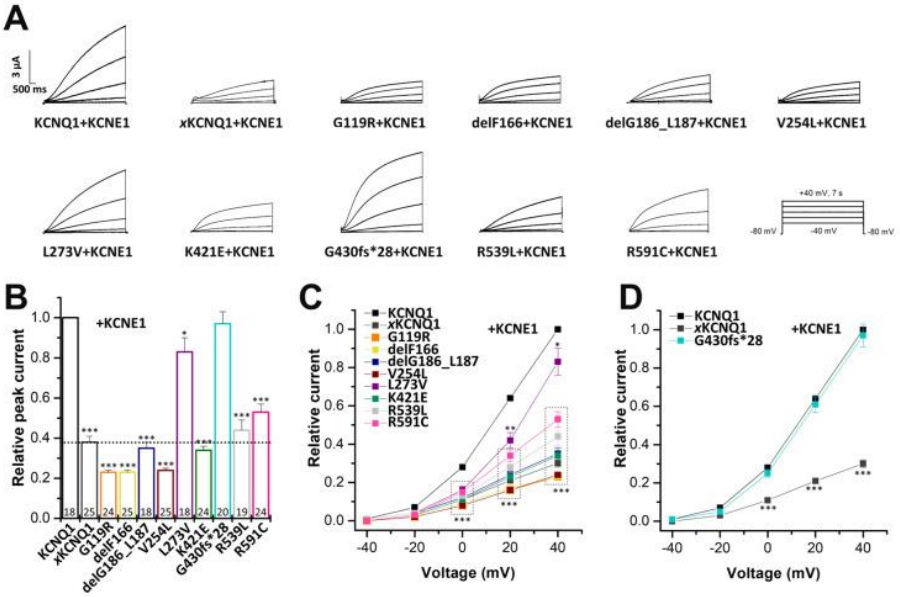

Figure 14. Electrophysiological properties of nine *KCNQ1* variants encoding the $Kv_{7.1}$ channel α-subunits, co-expressed with β-subunit KCNE1 in *Xenopus laevis* oocytes. (A) Representative whole-cell current traces recorded from wild-type *KCNQ1* and the nine *KCNQ1* variants. (**B**) Normalized current densities at +40 mV. (**C**) Current-voltage relationships of variants exhibiting significantly reduced and (**D**) unchanged current amplitudes compared to wild-type KCNQ1. *x*KCNQ1 – endogenous I_{Ks} recorded by the injection of *KCNE1* alone. Data are shown as mean ± standard error of mean (SEM). Statistical significance was evaluated using a two-tailed Student's *t*-test. *** $p < 0.001$, ** $p < 0.01$, * $p < 0.05$ (Rinné et al., 2023).

Furthermore, the functional impact of *KCNQ1* variants on $Kv_{7.1}$ channel-mediated I_{Ks} can depend on zygosity. While the homozygous condition was discussed above, in the heterozygous state, seven of nine variants (G119R, delG186_L187, V254L, I421E, R539L, R591C, and L273V) caused a significant reduction in I_{Ks} mediated by $Kv_{7.1}$ (Figure 15A, B, C), and three of these (delG186_L187, L273V, and R539L) exhibited a rightward shift in $V_{1/2}$ of the channel. The remaining two variants (delF166 and G430fs*28) showed no notable differences from wild-type I_{Ks} mediated by $Kv_{7.1}$ (Figure 15A, B, D) (Rinné et al., 2023).

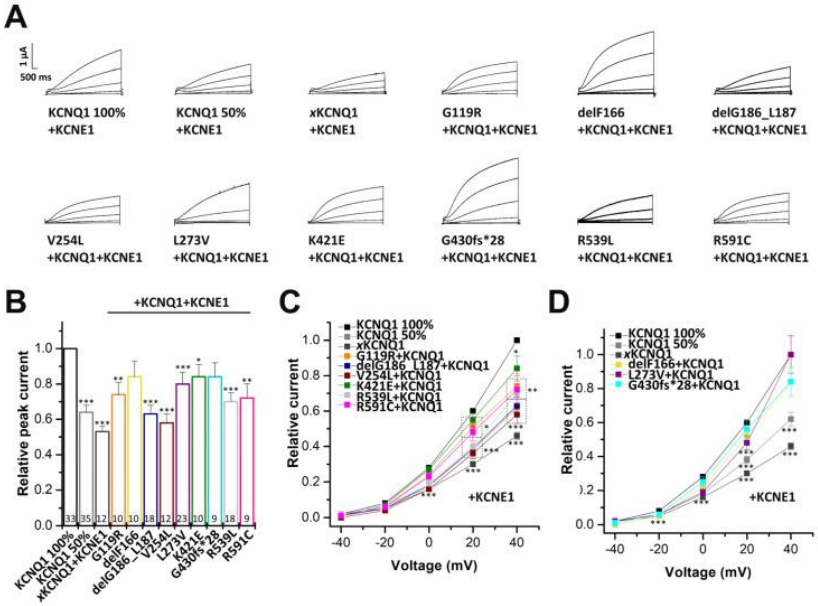

Figure 15. Electrophysiological properties of nine heterozygous *KCNQ1* variants encoding the $Kv_{7.1}$ channel α-subunits, co-expressed with equal amounts of wild-type *KCNQ1,* in the presence of β-subunit KCNE1 in *Xenopus laevis* oocytes. (A) Representative whole-cell current traces recorded from wild-type *KCNQ1* (100 and 50%) and the nine heterozygous *KCNQ1* variants. (**B**) Normalized current densities at +40 mV. (**C**) Current-voltage relationships of variants exhibiting significantly reduced and (**D**) unchanged current amplitudes compared to wild-type KCNQ1 100%. *x*KCNQ1 – endogenous I_{Ks} recorded by the injection of KCNE1 alone. Data are shown as mean ± SEM. Statistical significance was evaluated using a two-tailed Student's *t*-test. *** $p < 0.001$, ** $p < 0.01$, * $p < 0.05$ (Rinné et al., 2023).

Collectively, reduced I_{Ks} amplitude and $V_{1/2}$ are consistent functional signatures of pathogenic *KCNQ1* variants in LQT1. The effects are often zygosity-dependent, with homozygous variants showing stronger reductions and gating changes than heterozygous ones, providing a reliable basis for distinguishing pathogenic from benign variants.

METHODS

2.1 Whole-cell Patch-clamp Analysis of Ion Channel Activity

The patch-clamp technique in whole-cell configuration was used to directly assess ion channel activity in this study.

Cells were seeded onto 12 mm glass coverslips, transferred into a 33 mm Petri dish containing recording solution optimized for either $I_{Ca,L}$, or I_{Ks} measurements, and placed under a Nikon FN-S2N microscope (Nikon Corporation, Tokyo, Japan). Patch pipettes were pulled from borosilicate glass capillaries using a Flaming/Brown micropipette puller (Model P-1000; Sutter Instrument Co., USA) and had a resistance of 2–8 MΩ when filled with the pipette solution.

Whole-cell patch-clamp recordings were performed at room temperature (21 ± 1°C). A cell-attached configuration was first established by forming a high-resistance (gigaseal) between the patch pipette and the cell membrane using gentle suction (Figure 16A). The whole-cell configuration was subsequently achieved by applying additional suction to disrupt the membrane patch beneath the pipette tip (Figure 16B).

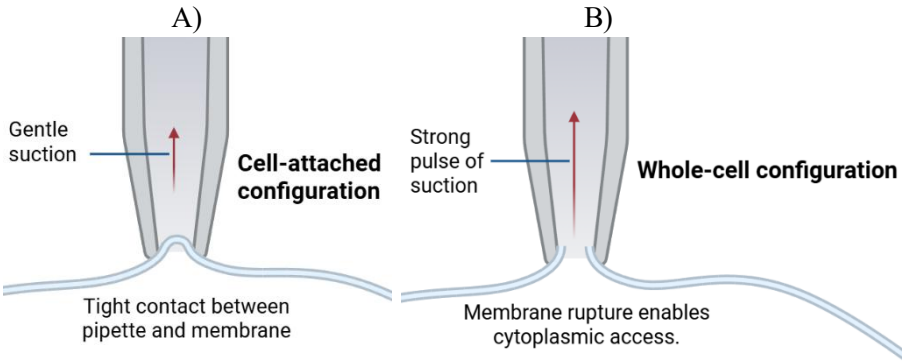

Figure 16. Patch-clamp configurations. A) Cell-attached configuration with gigaseal formation. B) Whole-cell configuration following membrane rupture and cytoplasmic access.

Recordings were obtained in voltage-clamp mode using a Multiclamp 700B amplifier (Molecular Devices) controlled by pCLAMP 10.5 software (Molecular Devices).

$I_{Ca,L}$, or I_{Ks} were recorded using specific voltage-clamp protocols consisting of defined holding potentials and depolarizing voltage steps, as described below. Steady-state current was measured at the end of each depolarizing pulse, when the current reached a stable level and transient

components were minimized (Gray & Santin, 2023). These values were used to assess whole-cell ionic current.

2.2 The Effect of TGF-β3 and IL-1β on L-VGCCs and Ca^{2+} Homeostasis in Osteoarthritic Chondrocytes and hBM-MSCs During Chondrogenesis

The research was conducted in collaboration with the Innovative Medicine Center (IMC) and the Department of Neurobiology and Biophysics, Institute of Biosciences, Life Sciences Center, Vilnius University. This component of the research was partly funded by the EU HORIZON-WIDERA-2021-ACCESS-03-01 program: "Twinning for Promoting Excellence, Ability and Knowledge to develop novel approaches for targeting inflammatory and degenerative age-related joint diseases" (Grant No. 101079489 – TWINFLAG).

hBM-MSCs and primary chondrocytes were obtained from voluntary adult donors who provided written informed consent. All procedures involving hBM-MSCs and chondrocytes were performed in accordance with the regulations of the institutional Bioethics Committee under permission No. 158200-14-741-257, approved on June 9, 2014.

2.2.1 Isolation and Culture of hBM-MSCs and Chondrocytes

Human tissue samples were obtained from Vilnius University Hospital Santaros Klinikos. Articular cartilage samples were obtained as tissues removed during articular surgery from 4 patients with OA (aged 64 ± 14 years) without systemic, acute or chronic comorbidities.

Chondrocytes were isolated and cultured according to the established protocols as previously reported (Uzieliene et al., 2019). Briefly, cartilage samples were washed in PBS with 1% penicillin-streptomycin (PS) (Gibco, Life Technologies, Waltham, MA, USA), chopped into small pieces, incubated in low glucose (1 g/L) DMEM (Capricorn Scientific, Ebsdorfergrund, Germany) with 1% PS at 37 °C in 5% CO_2. After, samples were washed and enzymatically digested: first with pronase for 1 h, then with a type II collagenase solution at 10 mL/g of tissue for 4 h, both at 37 °C in 5% CO_2. Isolated chondrocytes were cultured in complete medium, consisting of low glucose DMEM, 1% PS and 10% fetal bovine serum (FBS), in a 37 °C incubator with 5% CO_2, changing the medium twice a week.

hBM-MSCs were isolated from 3 donors with OA (aged 52 ± 10 years) according to established IMC protocols, after joint replacement surgical

procedures. hBM-MSCs were incubated under the same conditions as chondrocytes, with the addition of 1 ng/mL of fibroblast growth factor 2 (Sigma Aldrich, Burlington, MA, USA) to maintain their stem cell potential and to avoid spontaneous differentiation. Isolated hBM-MSCs were cultured with complete medium in a 37 °C incubator with 5% CO_2, changing the medium twice a week.

Passage 2–3 (P2–P3) of hBM-MSCs and chondrocytes were used for all experiments.

2.2.2 Chondrogenic Differentiation

The proliferation medium consisted of DMEM containing 1 g/L glucose, supplemented with 10% FBS and 1% PS. The chondrogenic differentiation medium, applied to both hBM-MSCs and chondrocytes, was composed of high-glucose DMEM (4.5 g/L), 1% PS, 1% insulin-transferrin-selenium supplement (Gibco, Life Technologies, Waltham, MA, USA), 350 nM L-proline (Carl Roth, Karlsruhe, Germany), 100 nM dexamethasone (Sigma Aldrich, Burlington, MA, USA), and 170 nM ascorbic acid-2-phosphate (Sigma Aldrich, Burlington, MA, USA).

Cells cultured in the chondrogenic medium were treated for 24 hours with either 10 ng/mL TGF-β3 (Gibco, Life Technologies) or 10 ng/mL IL-1β (ProSpec, Ness-Ziona, Israel). A concentration of 10 ng/mL TGF-β3 was selected for all experiments, as it represents a commonly used dose to promote chondrogenic differentiation (Uzieliene et al., 2021). Likewise, IL-1β was applied at 10 ng/mL, based on previous studies showing that this concentration effectively induces early degenerative alterations in human chondrocytes (Shakibaei et al., 2005). A 24-hour incubation time was consistently applied across all conditions to capture initial cellular responses.

2.2.3 Intracellular Calcium Level Measurement

The evaluation of iCa^{2+} levels was performed by seeding hBM-MSCs and chondrocytes in 6-well plates 200,000 cells/well. After the cells reached 95% confluence, subsequent incubation with IL-1β or TGF-β3, hBM-MSCs and chondrocytes were detached with 0.25% trypsin-EDTA, counted, and transferred at a density of 100,000 cells/vial into new 1.5 mL vials. These cells were then stained with Cal-520 dye (1 μM) (Interchim, Montlucon, France) for 30 min, washed with PBS, and measured using the Luminex Guava Flow cytometer (Luminex Corporation, Austin, TX, USA). The data were analyzed using FlowJo software, version 10 (FlowJo Corp., Ashland, OR, USA).

2.2.4 Electrophysiological Recording of hBM-MSCs and Chondrocytes

To study $I_{Ca,L}$, we used a modified Ca^{2+}-free Krebs–Ringer solution as recording containing (in mM): 150 NaCl, 5.4 KCl, 10 $BaCl_2$, 2 $MgCl_2$, 11 glucose, and 10 HEPES, with pH adjusted to 7.4 using NaOH. In this solution, Ca^{2+} was replaced with Ba^{2+} to enhance L-VGCC-mediated current amplitude, as Ba^{2+} permeates L-type channels more efficiently and reduces Ca^{2+}-dependent inactivation, thereby facilitating current detection (Hess & Tsien, 1984; Heubach et al., 2004).

The pipette solution contained the following components (in mM): 130 KCl, 10 Na aspartate, 3 MgATP, 0.2 $CaCl_2$, 2 ethylene glycol tetraacetic acid (EGTA), and 5 4-(2-hydroxyethyl)-1-piperazineethanesulfonic acid (HEPES), adjusted to pH 7.3 with KOH (Fabiato and Fabiato 1979; Heubach et al. 2004).

Nifedipine (10 μM) and Bay-K8644 (10 μM), used respectively as an L-VGCC blocker and activator, were added to the external solution prior to measurements. Both compounds were obtained from Sigma Aldrich (Burlington, MA, USA).

To isolate $I_{Ca,L}$, membrane currents were recorded using a voltage-clamp protocol that started from a holding potential of -40 mV and applied depolarizing steps of 100 ms duration in 10 mV increments up to +10 mV (Heubach et al., 1999) (Figure 17A).

Given that the observed peak influx of Ca^{2+} ions through L-VGCCs is noted at membrane potentials of 0 and +10 mV (Heubach et al., 2004; Zhao et al., 2009), we used three subthreshold potentials (−30, −20, −10 mV) to evaluate the leak conductance, which were linearly extrapolated at 0 and +10 mV (Figure 17B) and then subtracted from experimental data. Leak subtraction isolated the voltage-dependent current component, namely, the leak-subtracted current.

A

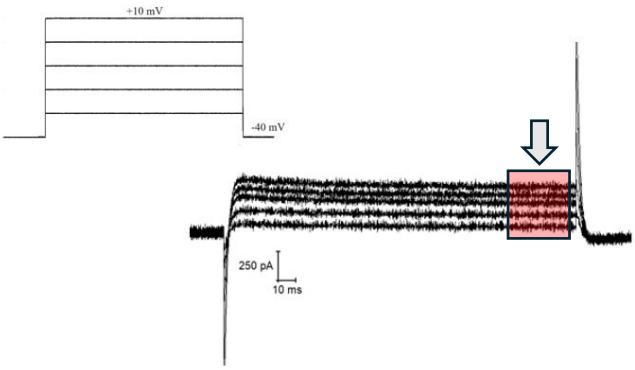

B

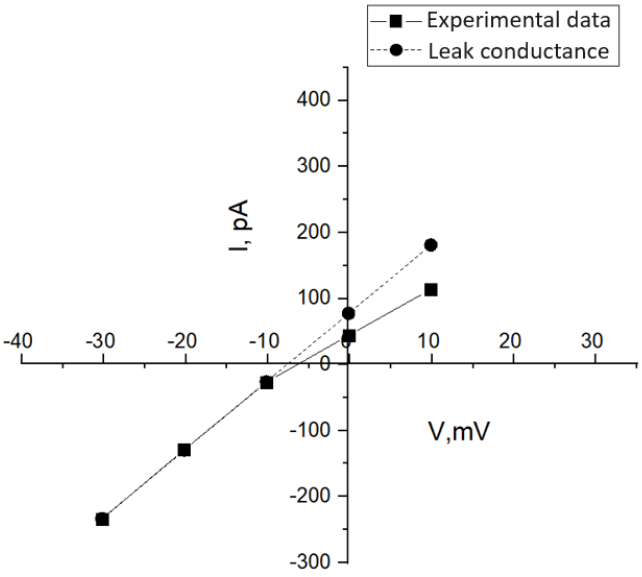

Figure 17. Inward current patch-clamp recorded in whole-cell configuration. A) The voltage-clamp protocol and representative examples of whole-cell current traces recorded in hBM-MSCs. The arrow indicates 30 ms at the end of voltage steps used for steady-state current measurement to assess whole-cell ionic current. B). An example of current–voltage relationships obtained from a single hBM-MSC demonstrated an inward current.

The leak-subtracted and normalized to the leak current (I_{LSN}) at +10 mV was used to evaluate the functional activity of L-VGCCs in both hBM-MSCs

and chondrocytes. Negative I_{LSN} indicates the presence of inward voltage-gated current, while positive I_{LSN} – outward voltage-gated current.

Our approach for determining the leak conductance involved using three data points (−30, −20, −10 mV) where a minor $I_{Ca,L}$ was already present (Heubach et al., 2004; Zhao et al., 2009). This implies that the obtained values of I_{LSN} at +10 mV may be under-evaluated.

2.2.5 Gene Expression Analysis of Key Ca^{2+} Regulators

hBM-MSCs and chondrocytes were seeded in 6-well plates using 200,000 cell/well density. When cells reached 95% confluence, they were treated with IL-1β or TGF-β3. After, the cells were lysed using LTR lysis buffer (Qiagen, 74104, Hilden, Germany) and RNA was extracted according to the manufacturer's instructions. The RNA concentration and purity of all samples were measured with SpectraMax i3 (Molecular Devices, San Jose, CA, USA). RNA was reverse-transcribed with a Maxima cDNA synthesis kit including dsDNase treatment (Thermo Fisher Scientific, Waltham, MA, USA). RT-qPCR reaction mixes were prepared with Maxima Probe qPCR Master Mix (Thermo Fisher Scientific, Waltham, MA, USA) and TaqMan Gene expression Assays (*RPS9*–Hs02339424_g1, *B2M*–Hs00984230_m1, *CACNA1C*–Hs00167681_m1, *ATP2A2*–Hs00544877_m1 (Thermo Fisher Scientific, Waltham, MA, USA)), and ran on the Agilent Aria MX instrument (Agilent Technologies, Santa Clara, CA, USA)) in technical triplicates starting with a denaturation step at 95 °C for 10 min followed by 40 cycles at 95 °C for 15 s of denaturation and 60 s for annealing and extension.

Relative levels of gene transcripts were calculated by subtracting the threshold cycle (Ct) of the normalizer (the geometric mean of the two housekeeping genes *RPS9* and *B2M*) from the Ct of the gene of interest, giving the dCt values that were subsequently transformed to 2-dCt values and multiplied by 1000 to scale-up for better graphical representation.

2.3 LQT1: Clinical and Functional Characterization of *KCNQ1* Variant C.1111G > C

The research was conducted at the Institute of Biosciences, Life Sciences Center, Vilnius University, and Vilnius University Hospital Santaros Klinikos. This part of the work was funded by the Research Council of Lithuania through the ATGC project (Grant No. S-MIP-21-15; PI: EP). The research was conducted under the approval of the Vilnius Regional Biomedical Research Ethics Committee of Lithuania (Protocol Code 2020/1-

1182-669, approval date January 28, 2020; and Protocol Code 2021/9-1373-849, approval date September 21, 2021).

All procedures involving human participants adhered to the ethical principles outlined in the Helsinki Declaration. All subjects provided written informed consent prior to participation, and all biological samples were anonymized and coded before laboratory processing to ensure confidentiality and compliance with ethical standards.

2.3.1 Clinical Evaluation of Carriers of the Heterozygous KCNQ1 c.1111G>C Variant

Five Lithuanian families with the rare pathogenic *KCNQ1* variant NM_000218.3:c.1111G > C were identified at Vilnius University Hospital Santaros Klinikos. Clinical evaluation of nine adults was performed between December 2022 and December 2023 during their follow-up according to the study protocol. Clinical evaluation included anamnesis of disease-related symptoms, collection of family history, 12-lead ECGs at exercise stress test (EST).

2.3.2 Transfection of HEK293 Cells

Human embryonic kidney (HEK293) cells were seeded in 24-well plates (Thermo Scientific Biolite 24-well Multidish) at a density of 80000 cells/ml, a day before the transfection. According to the manufacturer's protocol, the Lipofectamine® 3000 Transfection Reagent (Thermo Fisher Scientific) was used for transient transfection. *KCNE1* coding plasmid was pIRES_EGFP_GA_KCNE1, it was a gift from Al George (Addgene plasmid # 173160; http://n2t.net/addgene:173160; RRID: Addgene_173160). Cells were transfected with different plasmid combinations (*KCNQ1*_wt+*KCNE1*, *KCNQ1*_mut+*KCNE1*), maintaining the plasmid DNA amount recommended by the manufacturer. After transfection, cells were returned to the incubator (37 °C, 5 % CO_2) and allowed to express the transgene for 24–48 hours before electrophysiological analysis.

2.3.3 Electrophysiological Recording of Transfected HEK293 Cells

Whole-cell voltage-clamp recordings were performed in HEK293 cells 2-3 days after transfection with either wild-type *KCNQ1* (WT) or the *KCNQ1* p.(Ala371Pro) variant, co-expressed with the *KCNE1* subunit, to assess $K_{V7.1}$ channel function.

The HEK293 cell line was chosen due to its consistent morphology (Ooi et al., 2016), adhesion characteristics (Inada et al., 2016), and widespread use in ion channel research (Thomas & Smart, 2005), making it a well-established model for functional analysis.

Plasmids encoding *KCNQ1* (together with cyan-excitable orange fluorescent protein 1 **(**CyOFP1)) and *KCNE1* (together with enhanced green fluorescent protein (EGFP)) were used to identify transfected cells for the voltage-clamp recordings (Figure 18).

Fluorescence microscopy was used to identify successfully transfected cells. CyOFP1 fluorescence was visualized using a G-2A filter set (excitation 510–560 nm, emission 590 nm) while EGFP fluorescence was detected using a B-2A filter set (excitation 450–490 nm, emission 520 nm) (Nikon Corporation, Tokyo, Japan). Images were acquired with an exposure time of 2 s. Cells exhibiting both types of fluorescent markers (CyOFP1 and EGFP), indicating successful transfection, were selected for the electrophysiological recordings (Figure 18).

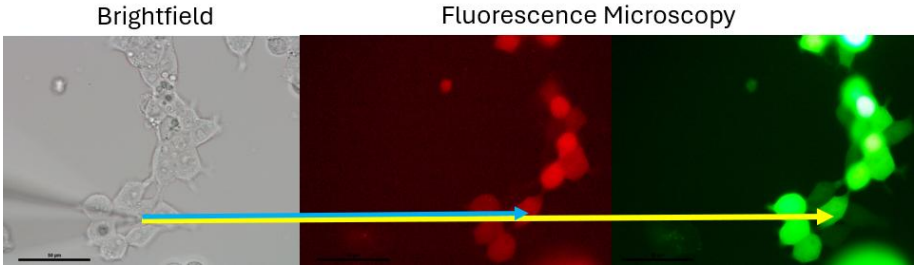

Figure 18. *Left:* Light microscopy image showing a cell patched with a patch pipette. *Right:* Fluorescence microscopy image of the same field of view, with blue arrow indicating the CyOFP1-positive (with *KCNQ1*) and yellow arrow indicating the EGFP-positive patched cell (with *KCNE1*).

The pipette solution contained (in mM): 140 KCl, 1 Na2-ATP, 2 EGTA, 10 HEPES, 0.1 $CaCl_2$, 1 $MgCl_2$, and 10 glucose, with pH adjusted to 7.4 using KOH.

Tyrode's solution was used as the recording solution (in mM): 140 NaCl, 4 KCl, 2 $CaCl_2$, 1 $MgCl_2$, 10 HEPES, and 10 glucose, with pH adjusted to 7.4 using NaOH.

Chromanol 293B, dissolved in dimethyl sulfoxide at a final concentration of 10 μM, was used as a specific inhibitor of $Kv_{7.1}$ channels.

Membrane currents were recorded using the voltage-clamp protocol that starts from a holding potential of -90 mV and depolarizing steps of 2-s duration and applied in 20 mV increments up to +70 mV (Figure 19A).

The activation threshold for the $Kv_{7.1}$-mediated current was near -40 mV (Aidery et al., 2012, p. 1). To assess leak conductance, currents at three subthreshold potentials (-90, -70, and -50 mV) were used for the linear extrapolation of leak currents at -30 – +70 mV (Figure 19B). Leak subtraction resulted in the isolation of the voltage-dependent current component. The voltage-dependent current components were normalized to the cell membrane capacitance to obtain current densities (pA/pF).

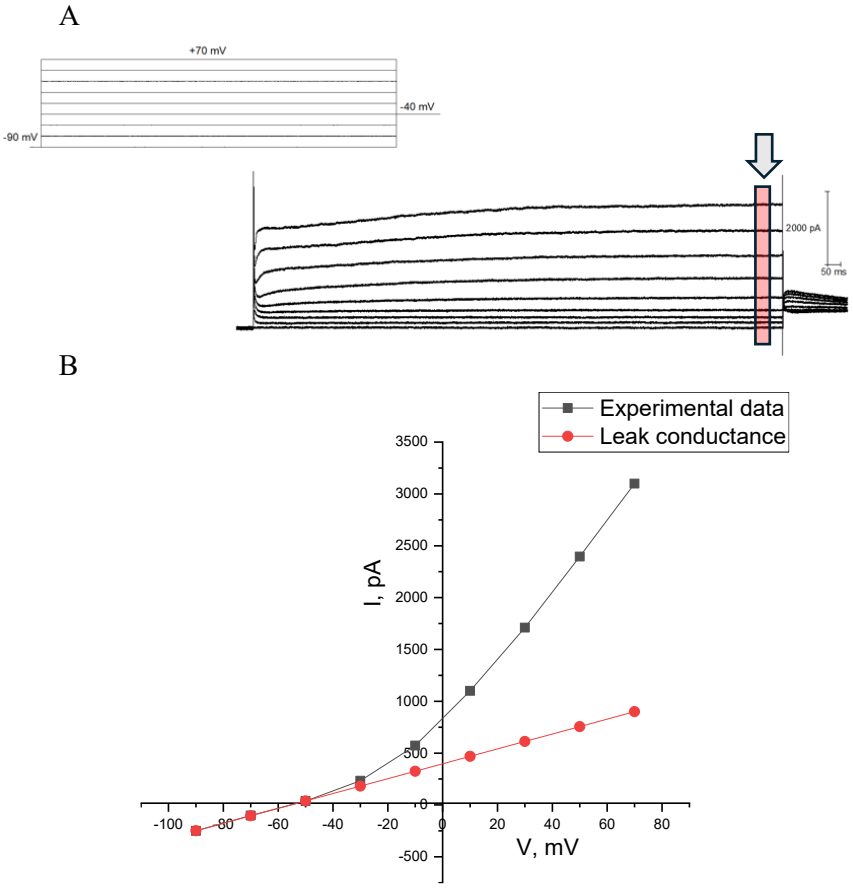

Figure 19. Autward current patch-clamp recorded in whole-cell configuration. A) The voltage-clamp protocol and representative examples of whole-cell current traces recorded in HEK293 cells transfected with wild-type *KCNQ1* co-expressed with the *KCNE1* subunit. The arrow indicates 50 ms at the end of the voltage steps used for steady-state current measurement to assess whole-cell ionic current. B) An example of a current–voltage relationship obtained from a HEK293 cell showed an outward current.

Current densities were also used to generate conductance-voltage (G-V) curves to determine the voltage dependence of channel activation. To obtain G-V curves, the change in current (ΔI) was divided by the change in membrane potential (ΔV) at each voltage step.

The G_{max} and $V_{1/2}$ were obtained by fitting the G/G_{max} curve with a Boltzmann equation.

$$G(V) = G_{min} + \frac{(G_{max} - G_{min})}{1+\exp(\frac{V - V_{1/2}}{s})} \quad (1)$$

G_{min} is the minimal conductance, G_{max} is the maximal conductance, $V_{1/2}$ is midpoint of voltage-dependent activation and *s* is the slope factor.

2.4 Statistical Analysis

The Shapiro-Wilk test (Origin Pro) was used to assess normality. In the first project, the data followed a normal distribution. Statistical difference between groups was evaluated using one-way analysis of variance (ANOVA) with OriginPro software, version 9.5 (OriginLab Corporation, Northampton, MA, USA), while the difference between two groups was assessed using a Student's unpaired two-tailed *t*-test (Microsoft Excel). In the text, data are presented as mean ± standard deviation (SD).

In the second project, the data did not follow a normal distribution. Therefore, statistical analysis was performed using the non-parametric Kruskal-Wallis test (Origin Pro) to evaluate differences among multiple groups, while the Mann-Whitney U test (Origin Pro) was used for comparisons between two groups. Statistical significance was defined as * $p \leq 0.05$. In the figures, significance levels are indicated in the respective legends. Results are presented as mean ± SEM, with "n" representing the number of cells.

2.5 Authors' Contributions

Isolation and culture of hBM-MSCs and chondrocytes, evaluation of iCa^{2+}, and gene expression analysis in hBM-MSCs and chondrocytes were performed by colleagues from IMC. Clinical evaluation of *KCNQ1* p.(Ala371Pro) variant carriers was conducted at Vilnius University Hospital Santaros Klinikos. Cell transfection was performed by colleagues from the Department of Biochemistry and Molecular Biology at the Institute of Biosciences, Vilnius University, Vilnius, Lithuania. All electrophysiological recordings, including data acquisition and analysis, were performed by the thesis author.

RESULTS

The results of this dissertation are based on two published peer-reviewed journal articles.

The first study investigated the effect of TGF-β3 and IL-1β on L-VGCCs and Ca^{2+} homeostasis in osteoarthritic chondrocytes and hBM-MSCs during chondrogenesis. Ca^{2+} homeostasis is examined across three aspects: iCa^{2+}, $I_{Ca,L,}$ and the expression of *CACNA1C* and *ATP2A2*.

The second study focused on LQT1: clinical and functional characterization of *KCNQ1* variant c.1111G > C. This part integrates clinical data from variant carriers with direct electrophysiological investigation of currents mediated by the mutant $Kv_{7.1}$ channel containing the *KCNQ1* variant.

3.1 The Effect of TGF-β3 and IL-1β on L-VGCCs and Ca^{2+} Homeostasis in Osteoarthritic Chondrocytes and hBM-MSCs During Chondrogenesis

3.1.1 TGF-B3 Causes an Increase in Intracellular Ca^{2+} Concentration

Ca^{2+} channels appear to play a pivotal role in chondrogenic differentiation (Uzieliene et al., 2018). Consistent with this, iCa^{2+} are known to change during this process, indicating that Ca^{2+} homeostasis is actively regulated during chondrogenesis (Fodor et al., 2013; Matta & Zakany, 2013). Because TGF-β3 is routinely used to induce chondrogenesis (Uzieliene et al., 2019; Wee et al., 2022; Xia et al., 2017) – and IL-1β is a key inflammatory mediator relevant to osteoarthritic conditions (Kobayashi et al., 2005) - we first examined how these cytokines affect iCa^{2+} in hBM-MSCs and chondrocytes during chondrogenic differentiation.

TGF-β3 significantly increased iCa^{2+} in both hBM-MSCs and chondrocytes, whereas IL-1β did not cause significant changes compared to chondrogenic media alone (Figure 20).

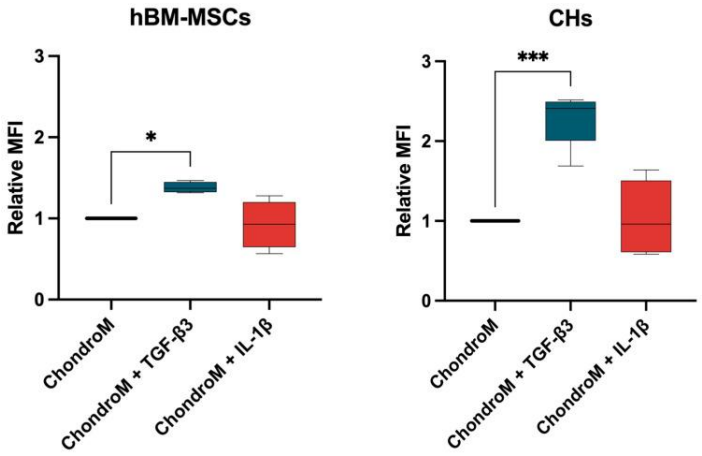

Figure 20. iCa^{2+}levels in hBM-MSCs and chondrocytes (CHs). Median fluorescence intensity (MFI) is presented as a ratio to non-stained control. Data are presented as mean ± SD. * $p < 0.05$, *** $p < 0.001$.

3.1.2 TGF-β3 Induces Nifedipine-sensitive $I_{Ca,L}$ in hBM-MSCs

In insulinoma cells, the TGF-β3-mediated increase in iCa^{2+} depends on Ca^{2+} entry through L-VGCCs (Ishiyama et al., 1996). Moreover, previous studies have shown that only a small fraction of undifferentiated hBM-MSCs demonstrated a small $I_{Ca,L}$ (Heubach et al., 2004; Kawano et al., 2002). However, the functional role of L-VGCCs in extracellular Ca^{2+} entry in hBM-MSCs is currently unknown. To investigate how TGF-β3 can cause elevation of iCa^{2+} in hBM-MSCs, we examined its impact on the functional activity of L-VGCCs in chondrogenic media. Additionally, the influence of IL-1β on L-VGCCs functional activity in hBM-MSCs was tested.

hBM-MSCs cultivated in proliferation media did not show significant I_{LSN} (0.006 ± 0.04) in n = 22 cells (Figure 21).

Because chondrogenic media are supplemented with high glucose DMEM, 1% PS, insulin-transferrin-selenium, L-proline, dexamethasone, and other bioactive compounds – each of which could potentially influence ion channel function (Levitan et al., 1991; Y. Liu et al., 2001; L. Wang et al., 2021) – the effect of chondrogenic media alone on L-VGCCs functional activity was evaluated.

Cultivation in chondrogenic media did not show significant effects on I_{LSN} in hBM-MSCs (−0.01 ± 0.03; n = 12), compared to the proliferation media (Figure 21).

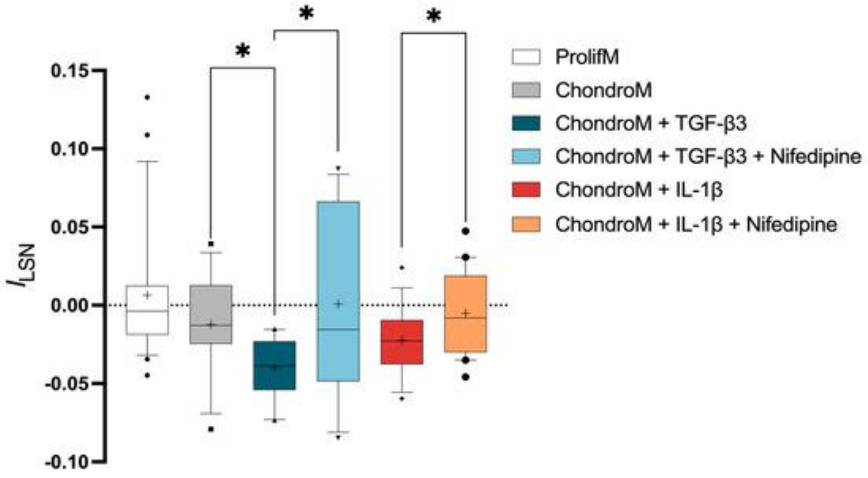

Figure 21. I_{LSN} in hBM-MSCs. The current was measured in cells cultivated in proliferation media (ProlifM) and chondrogenic media (ChondroM) with TGF-β3 (10 ng/mL) or IL-1β (10 ng/mL) with or without nifedipine. Data are shown as a box with whiskers, indicating the median (50th), upper (90th), and lower (10th) percentiles. Outliers are represented with individual marks outside the whiskers. *p< 0.05. The number of cells in each condition is specified in the text.

The exposure of hBM-MSCs to TGF-β3 caused significant negative I_{LSN} (−0.04 ± 0.02; n = 14), compared to chondrogenic media alone (Figure 17). TGF-β3-mediated negative I_{LSN} was sensitive to nifedipine, an L-VGCC blocker (0.0007 ± 0.06; n = 12) (Figure 21).

The exposure of hBM-MSCs to IL-1β showed a tendency to cause negative, but not statistically significant, I_{LSN} compared to chondrogenic media (−0.02 ± 0.02; n = 16) (Figure 21). Nifedipine resulted in significantly reduced I_{LSN} (−0.005 ± 0.03; n = 20) (Figure 21).

3.1.3 L-VGCCs do not Mediate TGF-β3-induced Inward Current in Chondrocytes

To investigate how TGF-β3 can cause the elevation of iCa^{2+} in chondrocytes, we examined its impact on the functional activity of L-VGCCs. Additionally, we investigated how IL-1β influenced L-VGCCs functional activity in chondrocytes.

Chondrocytes cultivated in proliferation media did not show significant I_{LSN} (−0.007 ± 0.02; n = 42) (Figure 22A). The application of Bay-K8644, an activator of L-VGCCs, to proliferation media did not result in a significant change in I_{LSN} (−0.01 ± 0.01; n = 16) (Figure 22B).

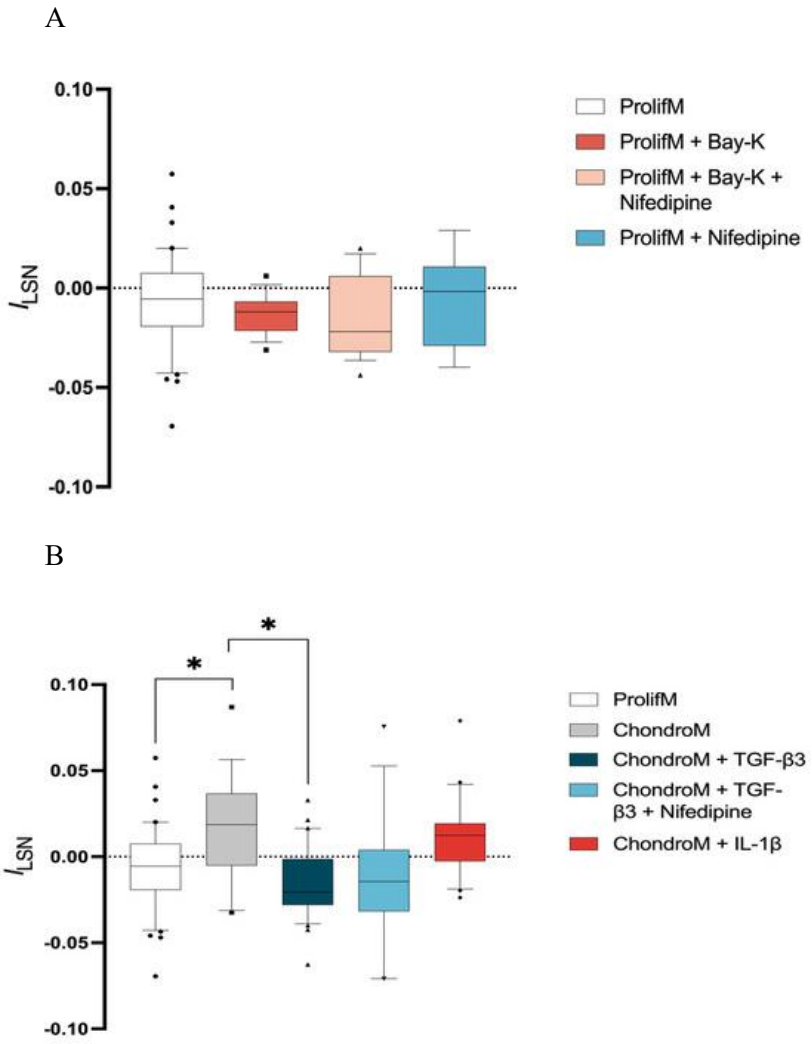

Figure 22. I_{LSN} in chondrocytes. The current was measured in cells cultivated A) in proliferation media (ProlifM) with Bay-K8644, nifedipine, or both; B) in proliferation and chondrogenic media (ChondroM) with TGF-β3 (10 ng/mL) or IL-1β (10 ng/mL) with or without nifedipine. Data are shown as a box with whiskers, indicating the median (50th), upper (90th), and lower (10th) percentiles. Outliers are represented with individual marks outside the whiskers. *$p < 0.05$. The number of cells in each condition is specified in the text.

The inward current could be compensated by voltage-gated potassium currents (Mobasheri et al., 2012). Moreover, the lack of changes in I_{LSN} after the application of Bay-K8644 may indicate that the majority of L-VGCCs were already activated. This hypothesis was tested by the application of

nifedipine. Nonetheless, applying nifedipine or a combination of Bay-K8644 with nifedipine did not result in a significant change in I_{LSN} (−0.006 ± 0.02; n = 9, −0.01 ± 0.02; n = 18, respectively) (Figure 22A).

Incubation of chondrocytes in chondrogenic media caused significantly positive I_{LSN} (0.02 ± 0.03; n = 18), indicating the activation of voltage-gated outward current (Figure 22B).

The exposure of chondrocytes to TGF-β3 caused significantly negative I_{LSN} (−0.02 ± 0.01; n = 31) compared with chondrocytes cultivated in chondrogenic media alone (Figure 22B). TGF-β3-mediated negative I_{LSN} was not sensitive to nifedipine (−0.01 ± 0.04; n = 16) (Figure 22B).

The exposure of chondrocytes to IL-1β did not change I_{LSN} (0.01 ± 0.02; n = 20) when compared to chondrogenic media alone (Figure 22B).

3.1.4 TGF-β3 and IL-1β Differentially Regulate *CACNA1C* and *ATP2A2* Expression

Evidence indicates that both TGF-β3 and elevated iCa^{2+} levels can modulate Ca^{2+} homeostasis at the gene expression level (C. M. Johnson et al., 1997; Y. Liu et al., 2001; Ranganathan et al., 2007). To explore this regulatory axis, we examined how these factors affect the expression of key Ca^{2+} regulators. Specifically, we focused on the expression of *CACNA1C* and *ATP2A2. CACNA1C* encodes the L-VGCC subunit $Ca_{V1.2}$, a major pathway for Ca^{2+} influx into cells, whereas *ATP2A2* encodes the SERCA pump responsible for Ca^{2+} reuptake into the ER and restoration of basal iCa^{2+}. This approach allows us to evaluate Ca^{2+} influx and reuptake mechanisms in hBM-MSCs and chondrocytes. Additionally, we evaluated the effects of IL-1β on *CACNA1C* and *ATP2A2* expressions.

CACNA1C expression was significantly downregulated in chondrocytes in response to both TGF-β3 and IL-1β; whereas no changes were detected in hBM-MSCs (Figure 23A).

ATP2A2 expression was significantly increased in hBM-hMSCs in response to both TGF-β3 and IL-1β. In chondrocytes, *ATP2A2* expression increased significantly only following exposure to TGF-β3 (Figure 23B).

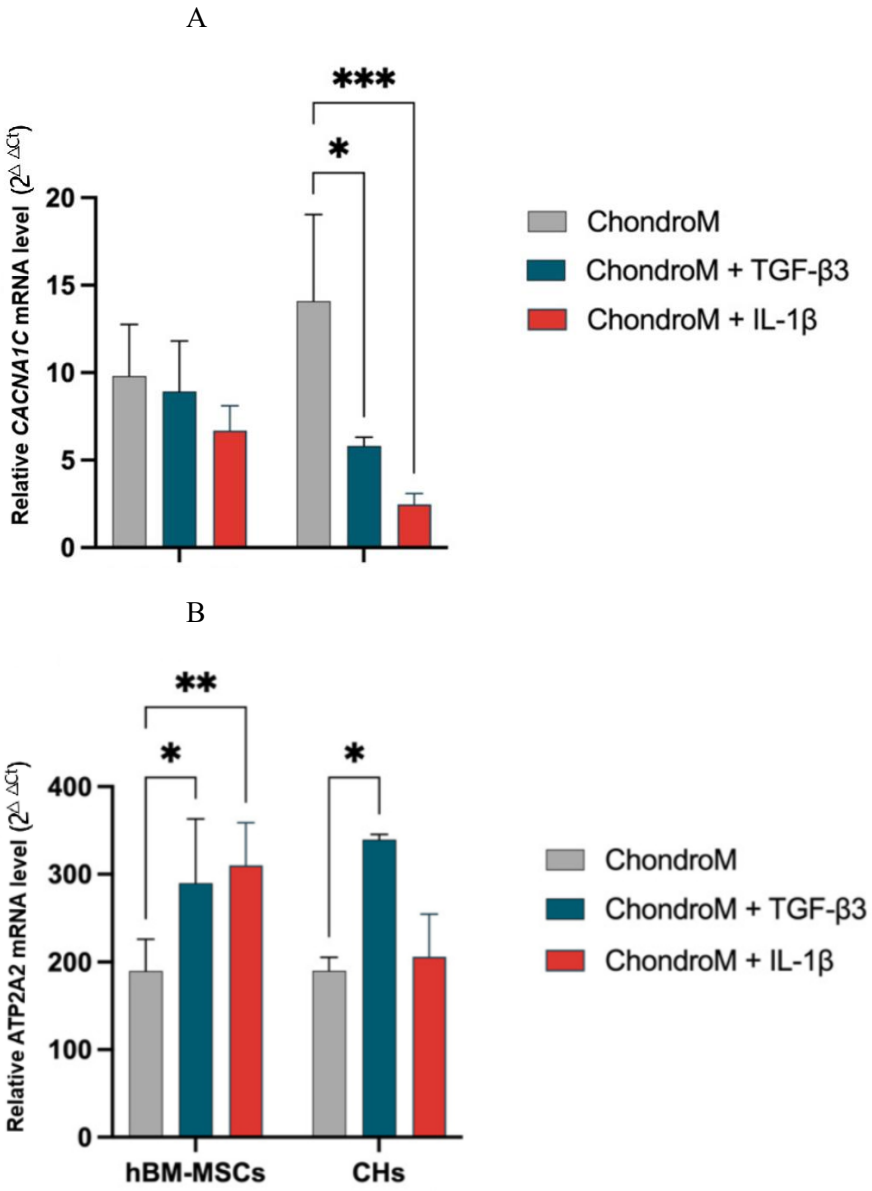

Figure 23. The effect of IL-1β (10 ng/mL) and TGF-β3 (10 ng/mL) on hBM-MSCs and chondrocyte (CHs) $Cav_{1.2}$ (*CACNA1C*) and SERCA2 pump (*ATP2A2*) gene expression. The expression ratio of A) *CACNA1C* and B) *ATP2A2*, were analyzed in chondrogenic media (ChondroM) with (10 ng/mL) and IL-1β (10 ng/mL). Relative transcript level after normalization to the geometric mean of housekeeping *B2M* and *RPS9* genes are shown. Data are presented as mean ± SD. * $p < 0.05$, ** $p < 0.01$, *** $p < 0.001$.

3.2 LQT1: Clinical and Functional Characterization of *KCNQ1* Variant c.1111G > C

3.2.1 Clinical Characterization of Individuals Carrying the Heterozygous *KCNQ1* c.1111G>C Variant

Long QT syndrome is a rare inherited cardiac disorder for which establishing a definitive diagnosis can be challenging and time-consuming due to genetic heterogeneity. In clinical practice, genetic testing is most commonly focused on the three major genes – *KCNQ1*, *KCNH2*, and *SCN5A* (Kapa et al., 2009). In this study, probands were referred for genetic testing based on long QT features identified during cardiological assessment. This approach enabled the identification of nine heterozygous carriers of the *KCNQ1* variant c.1111G>C [p.(Ala371Pro)], which encodes the $Kv_{7.1}$ channel α-subunit, across five unrelated Lithuanian families, including five males (56%) and four females (44%), aged 18-47 years at the time of clinical evaluation. Four individuals (44%) were symptomatic: one reported multiple syncopal episodes during physical activity (competitive sports), while three experienced exertion-provoked arrhythmic presyncope. Symptom onset occurred during childhood or adolescence (10-16 years). In addition, three families reported sudden cardiac death events (one female at 34 years and two males at 53 and 59 years), underscoring the clinical relevance of the phenotype. During peak exercise on 12-lead ECG testing, most carriers (89%) demonstrated QTc prolongation >480 ms. Collectively, these findings support an association between *KCNQ1* variant c.1111G>C, which encodes the $Kv_{7.1}$ channel α-subunit, and a long QT syndrome phenotype characterized by exertion-related symptoms, exercise-induced QTc prolongation, and familial occurrence of sudden cardiac death.

Overall, the clinical evaluation revealed a consistent, load-dependent QTc prolongation, indicating impaired ventricular repolarization. As ventricular repolarization is critically dependent on I_{Ks}, these findings prompted further direct electrophysiological investigation of the identified *KCNQ1* variant on $Kv_{7.1}$ channel function using patch-clamp techniques.

3.2.2 *KCNQ1* Variant Reduces Current Density of $Kv_{7.1}$ channels

In the heart, the functional $Kv_{7.1}$ channels are assembled with KCNE1 subunits, which substantially alter the function and biophysical properties of the channel. KCNE1 notably enhances $Kv_{7.1}$ channels current amplitude (Barhanin et al., 1996; Nakajo & Kubo, 2015; Sanguinetti et al., 1996). Given

this, we examined how the *KCNQ1* p.(Ala371Pro) variant influences the electrophysiological properties of $K_{V7.1}$ channels by comparing cells expressing wild-type or *KCNQ1* p.(Ala371Pro) variant co-expressed with *KCNE1*.

Significant differences in current densities between the tested groups were observed even at +10 mV and became progressively larger with increasing depolarization steps (Fig. 24B). At +30 mV, $K_{V7.1}$-mediated current density was significantly higher in cells expressing wild-type *KCNQ1* with *KCNE1* (15.80 ± 1.09, pA/pF, n=11) compared to those expressing *KCNQ1* p.(Ala371Pro) variant with KCNE1 (10.84 ± 0.48 pA/pF, n=24, Figure 24B). At +70 mV, this difference was even higher, 33.92 ± 2.44 pA/pF, n=11 in the wild-type group and 19.87 ± 0.86 pA/pF, n=24 in the *KCNQ1* p.(Ala371Pro) variant group (Figure 24B). These findings demonstrate that the *KCNQ1* p.(Ala371Pro) variant led to a partial LOF of $K_{V7.1}$ channels.

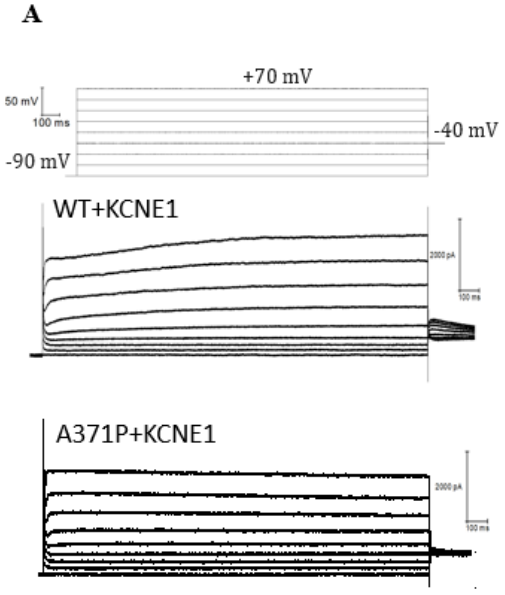

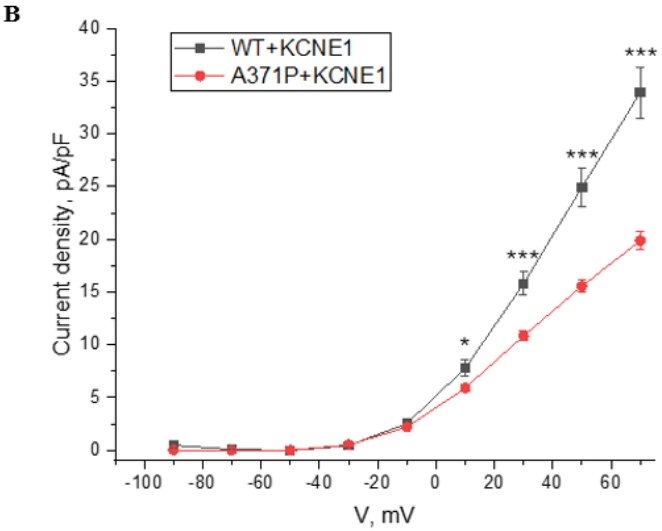

Figure 24. Patch clamp analysis of I_{Ks} in HEK293 cells transfected with wild-type *KCNQ1* (WT) or *KCNQ1* p.(Ala371Pro) variant (A371P) co-expressed with *KCNE1*. A) *Upper panel*: The voltage-clamp protocol that starts from a holding potential of -90 mV and depolarizing steps of 2-s duration and applied in 20 mV increments up to +70 mV. *Lower panels*: Representative whole-cell current traces. B) Dependence of current density on membrane potential (I–V) for the indicated groups. The number of cells in each condition is specified in the text. Data are shown as mean ± SEM. * $p \leq 0.05$, *** $p \leq 0.005$.

3.2.3 Chromanol Sensitivity of Altered $Kv_{7.1}$ Channels

To verify the origin of observed outward currents, we tested the sensitivity of these currents to chromanol 293B, a selective $Kv_{7.1}$ blocker. The current density observed in cells co-expressing wild-type *KCNQ1* with *KCNE1* was significantly reduced by chromanol to 10.70 ± 3.98 pA/pF, (n=6; Figure 25) at +70 mV, confirming the contribution of currents mediated by $Kv_{7.1}$ channels. Moreover, *KCNQ1* p.(Ala371Pro) variant co-expressed with *KCNE1* was also sensitive to chromanol: current density was significantly reduced to 10.86 ± 1.45 pA/pF, at +70 mV (n=7; Figure 25). These results suggest that, although the *KCNQ1* p.(Ala371Pro) variant reduces $Kv_{7.1}$-mediated current, the channel remains chromanol sensitive.

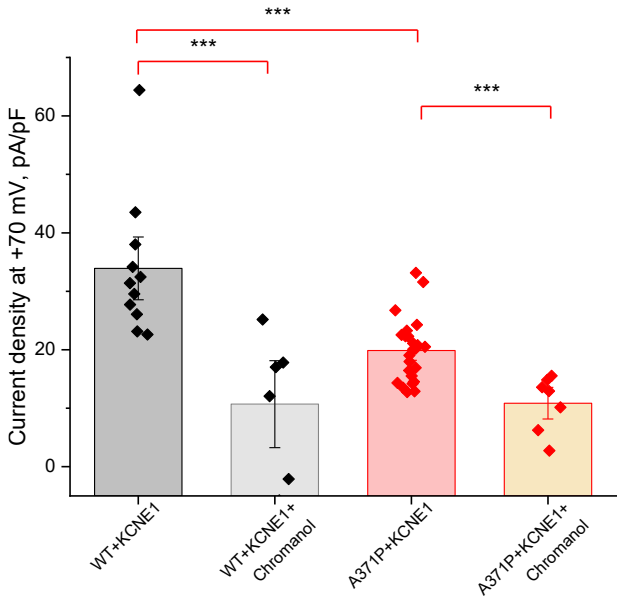

Figure 25. Current densities (pA/pF) at +70 mV in HEK293 cells transfected with wild-type *KCNQ1* (WT) or *KCNQ1* p.(Ala371Pro) variant (A371P) co-expressed with *KCNE1* with and without Chromanol 293B (10 µM). Chromanol 293B was applied to block the $Kv_{7.1}$-mediated current. Bars represent mean ± SEM; each diamond corresponds to an individual cell. *** $p \leq 0.005$.

3.2.4 A371P Reduces $Kv_{7.1}$ Channel Conductance without Altering Voltage Dependence

The reduced current density in cells expressing the *KCNQ1* p.(Ala371Pro) variant co-expressed with *KCNE1* may result from decreased $Kv_{7.1}$ channel conductance or altered voltage dependency. However, *KCNQ1* p.(Ala371Pro) variant did not alter the voltage dependence of $Kv_{7.1}$ channel activation compared to wild-type ($V_{1/2}$: -21.16 ± 1.57 mV, n=24 for A371P+KCNE1 vs -15.49 ± 2.10 mV, n=11 for WT+KCNE1; Figure 26C). In contrast, the maximal conductance (G_{max}) of the $Kv_{7.1}$ channel was significantly reduced by the variant (0.27 ± 0.01 nS/pF, n=24) compared to the wild-type (0.51 ± 0.04 nS/pF, n=11) (Figure 26A, B). These findings demonstrate that *KCNQ1* p.(Ala371Pro) variant disrupts normal $Kv_{7.1}$ channel gating by decreasing maximal conductance.

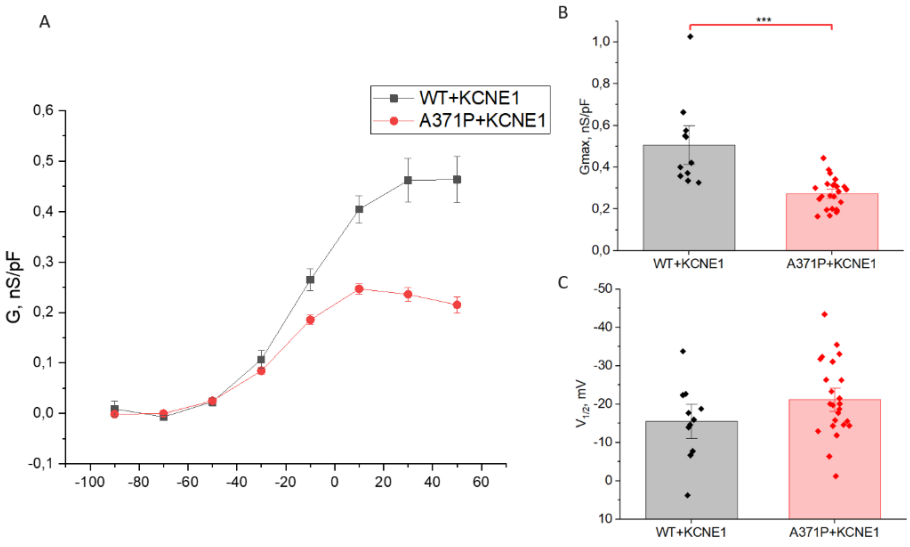

Figure 26. Activation of currents mediated in HEK293 cells transfected with wild-type *KCNQ1* (WT) or *KCNQ1* p.(Ala371Pro) variant (A371P) co-expressed with *KCNE1*. A) Voltage dependence of conductance. Symbols with error bars represent mean ± SEM. B) The maximal conductance (G_{max}). C) Midpoint of activation ($V_{1/2}$). Bars represent mean ± SEM; each diamond corresponds to an individual cell. *** $p \leq 0.005$.

DISCUSSION

In this study, we investigated two distinct mechanisms regulating voltage-gated ion channel function: modulation by external factors and alteration by genetic variation. Specifically, we evaluated the effects of cytokines on Ca^{2+} homeostasis with a focus on L-VGCCs encoded by *CACNA1C*, and to assess the functional consequences of the rare *KCNQ1* variant c.1111G>C [p.(Ala371Pro)] on $Kv_{7.1}$ channel function.

Three aspects of Ca^{2+} homeostasis were evaluated to assess the functional contribution of L-VGCCs under 24 h exposure to 10 ng/mL of TGF-β3 and 10 ng/mL of IL-1β in both hBM-MSCs and chondrocytes:

1. iCa^{2+} levels,
2. $I_{Ca,L}$, providing insights as to whether Ca^{2+} is entering cells through the L-VGCCs,
3. expression of *CACNA1C* and *ATP2A2* genes, which represent the cellular responses to the altered iCa^{2+} levels seeking to restore homeostasis.

Cytokines modulation of ion channel function is dose- and time-dependent, with distinct cellular outcomes observed depending on the intensity and duration of stimulation (Almuraikhi et al., 2025; Rudzitis et al., 2025; Zhou et al., 2011). In the present study, cells were exposed to 10 ng/mL of TGF-β3 for all experiments as it is a standard concentration used to induce chondrogenic differentiation (Uzieliene et al., 2021). Similarly, 10 ng/mL IL-1β was chosen based on the literature as it demonstrated early degenerative changes in human chondrocytes (Shakibaei et al., 2005). The 24 h incubation period was selected for all experiments to study early changes in cells.

We observed an increase in iCa^{2+} in both hBM-MSCs and chondrocytes following exposure to TGF-β3. The $I_{Ca,L}$ in BM-hMSCs, but not in chondrocytes, was enhanced by TGF-β3. *CACNA1C* gene expression was significantly reduced in chondrocytes by both TGF-β3 and IL-1β, which also showed tendencies for a reduction in the *CACNA1C* gene in hBM-MSCs. The gene expression of *ATP2A2* was increased by TGF-β3 and IL-1β in hBM-MSCs, while in chondrocytes, just by TGF-β3.

Among three isoforms of TGF-β observed in mammals, TGF-β1 or TGF-β3 are used for the induction of chondrogenesis (Uzieliene et al., 2019; Wee et al., 2022; Xia et al., 2017). We chose to use TGF-β3 because it was shown to have a higher potential to induce chondrogenic differentiation than TGF-β1 (Barry et al., 2001).

TGF-β3 mediated a significant elevation in iCa^{2+} in both hBM-MSCs and chondrocytes (Shelest et al., 2025). Previous studies reported an elevation in iCa^{2+} as early as within 1 min after incubation with TGF-β1 in chondrocytes (Cailotto et al., 2011). Moreover, an increase in iCa^{2+} mediated by TGF-β has been observed in other cell types, including neurons (Y. Li et al., 2022; X. Zhang et al., 2015), osteoblasts (Nesti et al., 2007), and fibroblasts (Alevizopoulos et al., 1997; Muldoon et al., 1988).

IL-1β has been shown to increase intracellular Ca^{2+} levels in rat chondrocytes via TRPA1 (Yin et al., 2018). Our research demonstrated that a 24 h exposure to 10 ng/mL IL-1β does not cause a change in iCa^{2+} in hBM-MSCs and chondrocytes, which corresponds to a previous study in this type of cells (Uzieliene et al., 2019).

The regulation of iCa^{2+} in cells depends on Ca^{2+} entering through channels located on the plasma membrane, with L-VGCCs being one of them. In chondrocytes, L-VGCC activation is associated with the pathogenesis of OA, making them potential therapeutic targets for alleviating OA severity. The increase in iCa^{2+} mediated by TGF-β3 may be related to changes in the functional activity of L-VGCCs. Therefore, we explored L-VGCCs' functional activity by investigating I_{LSN} at +10 mV, which corresponds to the peak of the $I_{Ca,L}$ (Zhao et al., 2009). The leak subtraction enabled the isolation of $I_{Ca,L}$ from other (mainly potassium) currents present in the hBM-MSCs (Heubach et al., 2004) and chondrocytes (Clark et al., 2011), while normalization minimized the effect of cell size. Incubation of hBM-MSCs with TGF-β3 resulted in an increased nifedipine-sensitive inward current, suggesting activation of L-VGCCs. This activation can result from a complex cascade reaction stimulated by TGF-β3. For example, it has been demonstrated that TGF-β increased β-adrenergic signaling (Rosenkranz et al., 2002). The stimulation of β-adrenergic receptors is known to activate $I_{Ca,L}$ (Ganesan et al., 2006).

The incubation of hBM-MSCs with IL-1β displayed a tendency to increase the inward nifedipine-sensitive current; however, this increase was not statistically significant.

The inhibition of L-VGCCs with nifedipine was reported to downregulate the proliferation of chondrocytes (Uzieliene et al., 2019), suggesting the functional involvement of these channels. However, in our study, L-VGCCs activity was not detected in chondrocytes incubated in proliferation media. Notably, we observed a significant increase in outward currents when chondrocytes were incubated in chondrogenic media. We suppose that components of chondrogenic media, such as dexamethasone (Levitan et al.,

1991; L. Wang et al., 2021), high glucose concentration (Chu et al., 2009), or streptomycin (Iscla et al., 2014), could enhance potassium outward currents, which might explain our observations. Further, incubation of chondrocytes with TGF-β3 resulted in inward currents that were not sensitive to nifedipine. One possible reason for this could be the downregulation in potassium channel expression by TGF-β (Kaur et al., 2013). The total membrane current is a sum of inward and outward currents. Therefore, the downregulation of potassium outward currents will result in the total inward membrane current.

Our data showed that neither the application of proliferation nor chondrogenic media, TGF-β3 nor IL-1β stimulation, has changed L-VGCCs activity in chondrocytes.

In summary, our findings in hBM-MSCs indicate that TGF-β3 exposure elevates iCa^{2+}, at least partially, due to enhanced $I_{Ca,L}$ (Figure 27, left). While the expression of *CACNA1C*, a subunit of L-VGCCs, remains unchanged, we suggest that TGF-β3 exposure increases the functional activity of the L-VGCCs already present. Moreover, TGF-β3 results in the upregulation of *ATP2A2* expression (Figure 24, left). Upregulation of *ATP2A2* may provide the initial step in a cellular response for the reduction in elevated iCa^{2+}. In chondrocytes, TGF-β3 exposure also elevates iCa^{2+} but without changes in $I_{Ca,L}$ (Figure 27, right), indicating different pathways for iCa^{2+} elevation than in hBM-MSCs. Moreover, TGF-β3 downregulates *CACNA1C* expression while upregulating *ATP2A2* (Figure 24, right). This suggests involvement of two mechanisms of elevated iCa^{2+} reduction in chondrocytes: by enhancing Ca^{2+} reuptake from the cytosol into the ER through *ATP2A2* upregulation and by downregulation of *CACNA1C*.

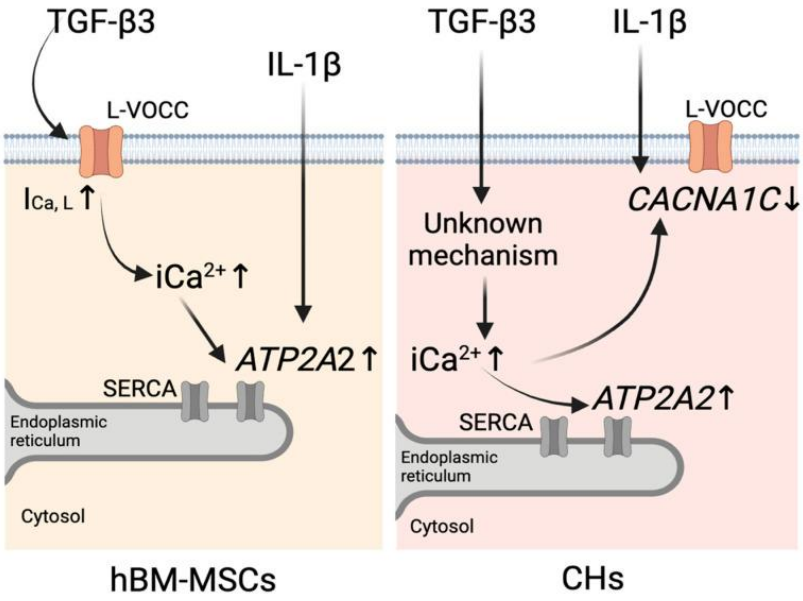

Figure 27. Schematic representation of the proposed mechanisms of calcium homeostasis regulation by TGF-β3 and IL-1β in hBM-MSCs (left) and chondrocytes (CHs) (right). In hBM-MSCs, TGF-β3 increases intracellular calcium (iCa^{2+}) levels by enhancing L-type calcium current ($I_{Ca,L}$), which leads to *ATP2A2* upregulation. IL-1β upregulates *ATP2A2* expression. In CHs, TGF-β3 increases iCa^{2+} via an unknown mechanism, which leads to upregulation of *ATP2A2* and downregulation of *CACNA1C*. IL-1β downregulates *CACNA1C* expression. The image was created with BioRender.com (www.biorender.com, accessed on 26 February 2025).

In contrast to extracellular factors, genetic alterations in ion channels represent a fundamentally different level of regulation, characterized by persistent, structurally determined effects on channel activity. This distinction is especially critical in excitable tissues, where genetically encoded changes in ion channel function directly shape membrane excitability and electrical stability (Enkvetchakul, 2010). For instance, in the heart, $Kv_{7.1}$ channels, assembled with the auxiliary β-subunit KCNE1, generate I_{Ks}, which plays a crucial role in ventricular repolarization and the shaping of the cardiac action potential (Jespersen et al., 2005). Mutations in the *KCNQ1,* which encodes the $Kv_{7.1}$ channel α-subunit, alter I_{Ks}, leading to delayed ventricular repolarization and prolonging the QT interval, thereby increasing the risk of arrhythmias (Tristani-Firouzi et al., 2001).

The p.Ala371Pro variant is located in the HA helix of *KCNQ1*, a region previously shown to undergo conformational changes required for proper channel function and to interact with calmodulin (Bileisiene et al., 2025;

Brewer et al., 2025). This substitution is predicted to disrupt the protein structure. Therefore, we evaluated its functional impact by direct electrophysiological recordings of channel currents. Our results showed that the *KCNQ1* p.(Ala371Pro) variant, when co-expressed with KCNE1, reduced the $Kv_{7.1}$ channel current density at +70 mV by about 40%. The maintained chromanol sensitivity indicates that mutant channels remain functional, and, in combination with reduced current density, indicates a partial loss-of-function mechanism. The reduction in current density observed with the *KCNQ1* p.(Ala371Pro) variant co-expressed with *KCNE1* is consistent with previous studies showing that various *KCNQ1* variants decrease $Kv_{7.1}$-mediated currents. For example, mutations in the C-terminal region of *KCNQ1* co-expressed with *KCNE1*, such as p.(Arg555Cys), not only reduce channel current density but also cause a marked rightward shift in the voltage dependence of channel activation (Chouabe et al., 1997). Similarly, several other C-terminal mutants co-expressed with KCNE1, including p.(Arg555His), p.(Ala590Thr), and p.(Gly589Asp), have been shown to reduce current mediated by the $Kv_{7.1}$ channel and shift the voltage dependence of channel activation to more positive potentials (Aromolaran et al., 2014; Kinoshita et al., 2014; Piippo et al., 2001). In contrast, some mutations, such as p.(Pro535Thr), do not alter channel voltage dependence but reduce maximal conductance (González-Garrido et al., 2021). In this study, the *KCNQ1* p.(Ala371Pro) variant did not affect the voltage dependence of activation but reduced the channel's maximal conductance by 42.9 %. The reported mutation results in a partial loss of function of $Kv_{7.1}$ channels, which is compatible with observed LQT1 phenotypic features (Figure 28).

In our electrophysiological experiments, we investigated the homozygous form of the p.(Ala371Pro) variant, yet in clinical settings, both homozygous and heterozygous carriers are observed. This distinction is clinically relevant, as differences in zygosity can influence the severity of the phenotype and may involve mechanisms such as dominant negative effects. In this study, we focused on the direct impact of the p.(Ala371Pro) variant on potassium currents. Whether the p.(Ala371Pro) variant exerts a dominant negative effect is currently unknown. Heterozygous patients often exhibit a very mild phenotype, while homozygous individuals show more severe symptoms (Kinoshita et al., 2014). However, dominant-negative effects cannot be excluded, as illustrated by the ΔF275 mutation, which strongly suppresses $Kv_{7.1}$-mediated current and leads to an LQT1 phenotype (Aizawa et al., 2007). Therefore, our study addressed the variant`s direct functional consequences,

while the potential effects of heterozygosity and dominant-negative interactions remain important topics for future investigation.

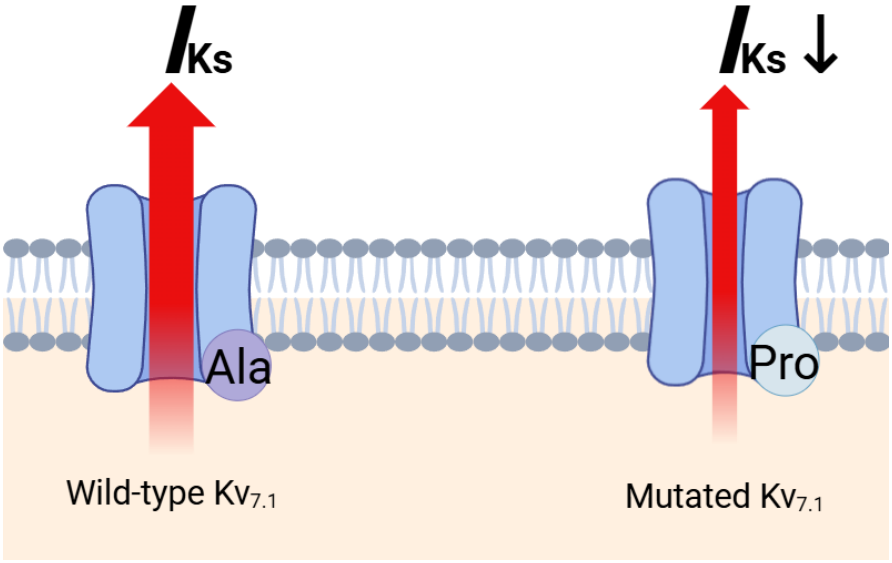

Figure 28. Schematic representation of reduced current mediated by the mutated $Kv_{7.1}$ channel encoded by the *KCNQ1* p.(Ala371Pro) variant. Compared to wild-type $Kv_{7.1}$ channels, channels carrying the p.(Ala371Pro) variant exhibit reduced current, indicating decreased channel conductance. The substitution of alanine with proline at position 371 likely alters channel structure and impairs ion permeation, consistent with a loss-of-function effect. The image was created with BioRender.com (www.biorender.com, accessed on 1 April 2026).

CONCLUSION

- TGF-β3 increases intracellular Ca^{2+} in a cell-type-dependent manner: in hBM-MSCs via functional activation of L-VGCCs, whereas in chondrocytes through L-VGCC-independent mechanisms. IL-1β does not significantly affect Ca^{2+} levels or L-VGCC activity in either cell type.
- Regulation of genes encoding Ca^{2+}-handling proteins differs between cell types: expression of *CACNA1C*, which encodes the pore-forming α1C subunit $Cav_{1.2}$ of L-VGCCs, remains unchanged in hBM-MSCs but is downregulated in chondrocytes following TGF-β3 and IL-1β exposure. In contrast, expression of *ATP2A2*, encoding SERCA2, is upregulated in hBM-MSCs by both cytokines, and in chondrocytes selectively by TGF-β3.
- The KCNQ1 p.(Ala371Pro) variant causes a loss-of-function of the $Kv_{7.1}$ channel by reducing I_{Ks} conductance without altering voltage-dependent activation.

LIST OF REFERENCES

Abula, K., Muneta, T., Miyatake, K., Yamada, J., Matsukura, Y., Inoue, M., Sekiya, I., Graf, D., Economides, A. N., Rosen, V., & Tsuji, K. (2015). Elimination of BMP7 from the developing limb mesenchyme leads to articular cartilage degeneration and synovial inflammation with increased age. *FEBS Letters*, *589*(11), 1240–1248. https://doi.org/10.1016/j.febslet.2015.04.004

Afifah, E., Mozef, T., Sandra, F., Arumwardana, S., Rihibiha, D., Nufus, H., Rizal, R., Amalia, A., Bachtiar, I., Murti, H., & Widowati, W. (2019). Induction of Matrix Metalloproteinases in Chondrocytes by Interleukin IL-1β as an Osteoarthritis Model. *Journal of Mathematical and Fundamental Sciences*, *51*, 103–111. https://doi.org/10.5614/j.math.fund.sci.2019.51.2.1

Aidery, P., Kisselbach, J., Schweizer, P. A., Becker, R., Katus, H. A., & Thomas, D. (2012). Impaired ion channel function related to a common *KCNQ1* mutation—Implications for risk stratification in long QT syndrome 1. *Gene*, *511*(1), 26–33. https://doi.org/10.1016/j.gene.2012.09.041

Aizawa, Y., Ueda, K., Scornik, F., Cordeiro, J. M., Wu, Y., Desai, M., Guerchicoff, A., Nagata, Y., Iesaka, Y., Kimura, A., Hiraoka, M., & Antzelevitch, C. (2007). A novel mutation in KCNQ1 associated with a potent dominant negative effect as the basis for the LQT1 form of the long QT syndrome. *Journal of Cardiovascular Electrophysiology*, *18*(9), 972–977. https://doi.org/10.1111/j.1540-8167.2007.00889.x

Alevizopoulos, A., Dusserre, Y., Rüegg, U., & Mermod, N. (1997). Regulation of the Transforming Growth Factor β-responsive Transcription Factor CTF-1 by Calcineurin and Calcium/ Calmodulin-dependent Protein Kinase IV*. *Journal of Biological Chemistry*, *272*(38), 23597–23605. https://doi.org/10.1074/jbc.272.38.23597

Alford, J. W., & Cole, B. J. (2005). Cartilage Restoration, Part 1: Basic Science, Historical Perspective, Patient Evaluation, and Treatment Options. *The American Journal of Sports Medicine*, *33*(2), 295–306. https://doi.org/10.1177/0363546504273510

Almuraikhi, N., Alkhamees, L., Tareen, S., Alshammari, H., & Muthurangan, M. (2025). Dose-Dependent Effects of TGF-β Inhibition on Osteoblast Differentiation and Wound Healing. *Current Issues in Molecular Biology*, *47*(5), 360. https://doi.org/10.3390/cimb47050360

Angelo, K., Jespersen, T., Grunnet, M., Nielsen, M. S., Klaerke, D. A., & Olesen, S.-P. (2002). KCNE5 Induces Time- and Voltage-Dependent Modulation of the KCNQ1 Current. *Biophysical Journal*, *83*(4), 1997–2006. https://doi.org/10.1016/S0006-3495(02)73961-1

Aromolaran, A. S., Subramanyam, P., Chang, D. D., Kobertz, W. R., & Colecraft, H. M. (2014). LQT1 mutations in KCNQ1 C-terminus assembly domain suppress IKs using different mechanisms.

Cardiovascular Research, *104*(3), 501–511. https://doi.org/10.1093/cvr/cvu231

Atsuta, Y., Tomizawa, R. R., Levin, M., & Tabin, C. J. (2019). L-type voltage-gated Ca2+ channel CaV1.2 regulates chondrogenesis during limb development. *Proceedings of the National Academy of Sciences of the United States of America*, *116*(43), 21592–21601. https://doi.org/10.1073/pnas.1908981116

Auron, P. E., Webb, A. C., Rosenwasser, L. J., Mucci, S. F., Rich, A., Wolff, S. M., & Dinarello, C. A. (1984). Nucleotide sequence of human monocyte interleukin 1 precursor cDNA. *Proceedings of the National Academy of Sciences*, *81*(24), 7907–7911. https://doi.org/10.1073/pnas.81.24.7907

Avila, G., Medina, I. M., Jiménez, E., Elizondo, G., & Aguilar, C. I. (2007). Transforming growth factor-β1 decreases cardiac muscle L-type Ca2+ current and charge movement by acting on the Cav1.2 mRNA. *American Journal of Physiology-Heart and Circulatory Physiology*, *292*(1), H622–H631. https://doi.org/10.1152/ajpheart.00781.2006

Barbero, A., Grogan, S., Schäfer, D., Heberer, M., Mainil-Varlet, P., & Martin, I. (2004). Age related changes in human articular chondrocyte yield, proliferation and post-expansion chondrogenic capacity. *Osteoarthritis and Cartilage*, *12*(6), 476–484. https://doi.org/10.1016/j.joca.2004.02.010

Barhanin, J., Lesage, F., Guillemare, E., Fink, M., Lazdunski, M., & Romey, G. (1996). K(V)LQT1 and lsK (minK) proteins associate to form the I(Ks) cardiac potassium current. *Nature*, *384*(6604), 78–80. https://doi.org/10.1038/384078a0

Barry, F., Boynton, R. E., Liu, B., & Murphy, J. M. (2001). Chondrogenic differentiation of mesenchymal stem cells from bone marrow: Differentiation-dependent gene expression of matrix components. *Experimental Cell Research*, *268*(2), 189–200. https://doi.org/10.1006/excr.2001.5278

Battegay, E. J., Raines, E. W., Seifert, R. A., Bowen-Pope, D. F., & Ross, R. (1990). TGF-beta induces bimodal proliferation of connective tissue cells via complex control of an autocrine PDGF loop. *Cell*, *63*(3), 515–524. https://doi.org/10.1016/0092-8674(90)90448-n

Baugé, C., Girard, N., Lhuissier, E., Bazille, C., & Boumediene, K. (2013). Regulation and Role of TGFβ Signaling Pathway in Aging and Osteoarthritis Joints. *Aging and Disease*, *5*(6), 394–405. https://doi.org/10.14336/AD.2014.0500394

Baugé, C., Legendre, F., Leclercq, S., Elissalde, J. M., Pujol, J. P., Galéra, P., & Boumédiene, K. (2007). Interleukin-1beta impairment of transforming growth factor beta1 signaling by down-regulation of transforming growth factor beta receptor type II and up-regulation of Smad7 in human articular chondrocytes. *Arthritis and Rheumatism*, *56*(9), 3020–3032. https://doi.org/10.1002/art.22840

Baumann, L., Gerstner, A., Zong, X., Biel, M., & Wahl-Schott, C. (2004). Functional characterization of the L-type Ca2+ channel Cav1.4alpha1 from mouse retina. *Investigative Ophthalmology & Visual Science*, *45*(2), 708–713. https://doi.org/10.1167/iovs.03-0937

Beier, F., Leask, T. A., Haque, S., Chow, C., Taylor, A. C., Lee, R. J., Pestell, R. G., Ballock, R. T., & LuValle, P. (1999). Cell cycle genes in chondrocyte proliferation and differentiation. *Matrix Biology: Journal of the International Society for Matrix Biology*, *18*(2), 109–120. https://doi.org/10.1016/s0945-053x(99)00009-8

Bhat, S., Viswanathan, P., Chandanala, S., Prasanna, S. J., & Seetharam, R. N. (2021). Expansion and characterization of bone marrow derived human mesenchymal stromal cells in serum-free conditions. *Scientific Reports*, *11*(1), 3403. https://doi.org/10.1038/s41598-021-83088-1

Bijlenga, P., Liu, J. H., Espinos, E., Haenggeli, C. A., Fischer-Lougheed, J., Bader, C. R., & Bernheim, L. (2000). T-type alpha 1H Ca2+ channels are involved in Ca2+ signaling during terminal differentiation (fusion) of human myoblasts. *Proceedings of the National Academy of Sciences of the United States of America*, *97*(13), 7627–7632. https://doi.org/10.1073/pnas.97.13.7627

Bileisiene, N., Shelest, A., Petraityte, G., Alaburda, A., Sasnauskiene, A., Jasinevicius, A., Kairys, V., Dapkunas, J., Mikstiene, V., Zitkute, V., Maldziene, Z., Barysiene, J., & Preiksaitiene, E. (2025). Long QT syndrome type 1: Clinical and functional characterization of KCNQ1 variant c.1111G > C. *BMC Cardiovascular Disorders*, *25*, 841. https://doi.org/10.1186/s12872-025-05335-x

Blaney Davidson, E. N., Remst, D. F. G., Vitters, E. L., van Beuningen, H. M., Blom, A. B., Goumans, M.-J., van den Berg, W. B., & Van der Kraan, P. M. (2009). Increase in ALK1/ALK5 Ratio as a Cause for Elevated MMP-13 Expression in Osteoarthritis in Humans and Mice1. *The Journal of Immunology*, *182*(12), 7937–7945. https://doi.org/10.4049/jimmunol.0803991

Brewer, K. R., Vanoye, C. G., Huang, H., Clowes Moster, K. R., Desai, R. R., Hayes, J. B., Burnette, D. T., George, A. L., & Sanders, C. R. (2025). Integrative analysis of KCNQ1 variants reveals molecular mechanisms of type 1 long QT syndrome pathogenesis. *Proceedings of the National Academy of Sciences*, *122*(8), e2412971122. https://doi.org/10.1073/pnas.2412971122

Brini, M., & Carafoli, E. (2011). The Plasma Membrane Ca2+ ATPase and the Plasma Membrane Sodium Calcium Exchanger Cooperate in the Regulation of Cell Calcium. *Cold Spring Harbor Perspectives in Biology*, *3*(2), a004168. https://doi.org/10.1101/cshperspect.a004168

Browe, D. C., Burdis, R., Díaz-Payno, P. J., Freeman, F. E., Nulty, J. M., Buckley, C. T., Brama, P. A. J., & Kelly, D. J. (2022). Promoting endogenous articular cartilage regeneration using extracellular matrix

scaffolds. *Materials Today Bio*, *16*, 100343. https://doi.org/10.1016/j.mtbio.2022.100343
Browning, J. A., Saunders, K., Urban, J. P. G., & Wilkins, R. J. (2004). The influence and interactions of hydrostatic and osmotic pressures on the intracellular milieu of chondrocytes. *Biorheology*, *41*(3–4), 299–308.
Cailotto, F., Reboul, P., Sebillaud, S., Netter, P., Jouzeau, J.-Y., & Bianchi, A. (2011). Calcium Input Potentiates the Transforming Growth Factor (TGF)-β1-dependent Signaling to Promote the Export of Inorganic Pyrophosphate by Articular Chondrocyte. *The Journal of Biological Chemistry*, *286*(22), 19215–19228. https://doi.org/10.1074/jbc.M110.175448
Chan, P. J., Osteen, J. D., Xiong, D., Bohnen, M. S., Doshi, D., Sampson, K. J., Marx, S. O., Karlin, A., & Kass, R. S. (2012). Characterization of KCNQ1 atrial fibrillation mutations reveals distinct dependence on KCNE1. *The Journal of General Physiology*, *139*(2), 135–144. https://doi.org/10.1085/jgp.201110672
Chen, D., Kim, D. J., Shen, J., Zou, Z., & O'Keefe, R. J. (2020). Runx2 plays a central role in Osteoarthritis development. *Journal of Orthopaedic Translation*, *23*, 132–139. https://doi.org/10.1016/j.jot.2019.11.008
Chen, N., Wu, R. W. H., Lam, Y., Chan, W. C. W., & Chan, D. (2023). Hypertrophic chondrocytes at the junction of musculoskeletal structures. *Bone Reports*, *19*, 101698. https://doi.org/10.1016/j.bonr.2023.101698
Chen, S., Fu, P., Cong, R., Wu, H., & Pei, M. (2015). Strategies to minimize hypertrophy in cartilage engineering and regeneration. *Genes & Diseases*, *2*(1), 76–95. https://doi.org/10.1016/j.gendis.2014.12.003
Chen, T., Weng, W., Liu, Y., Aspera-Werz, R. H., Nüssler, A. K., & Xu, J. (2021). Update on Novel Non-Operative Treatment for Osteoarthritis: Current Status and Future Trends. *Frontiers in Pharmacology*, *12*, 755230. https://doi.org/10.3389/fphar.2021.755230
Chen, X., & Xu, L. (2011). Mechanism and Regulation of Nucleocytoplasmic Trafficking of Smad. *Cell & Bioscience*, *1*, 40. https://doi.org/10.1186/2045-3701-1-40
Chin, S. P., Ng, W.-C., Tai, L., Mohd, M. A., Then, K. Y., & Cheong, S. K. (2025). Umbilical Cord-derived Mesenchymal Stem Cells (CLV-100) Infusion in Healthy Subjects: A 5-Year Follow-up Study on Safety and Immunomodulatory Effect. *Regenerative Engineering and Translational Medicine*. https://doi.org/10.1007/s40883-025-00384-2
Choi, Y. S., Park, J. K., Kang, E. H., Lee, Y.-K., Kim, T. K., Chung, J.-H., Zimmerer, J. M., Carson, W. E., Song, Y. W., & Lee, Y. J. (2013). Cytokine signaling-1 suppressor is inducible by IL-1beta and inhibits the catabolic effects of IL-1beta in chondrocytes: Its implication in the paradoxical joint-protective role of IL-1beta. *Arthritis Research & Therapy*, *15*(6), R191. https://doi.org/10.1186/ar4381

Chouabe, C., Neyroud, N., Guicheney, P., Lazdunski, M., Romey, G., & Barhanin, J. (1997). Properties of KvLQT1 K+ channel mutations in Romano-Ward and Jervell and Lange-Nielsen inherited cardiac arrhythmias. *The EMBO Journal*, *16*(17), 5472–5479. https://doi.org/10.1093/emboj/16.17.5472

Christel, C. J., Cardona, N., Mesirca, P., Herrmann, S., Hofmann, F., Striessnig, J., Ludwig, A., Mangoni, M. E., & Lee, A. (2012). Distinct localization and modulation of Cav1.2 and Cav1.3 L-type Ca2+ channels in mouse sinoatrial node. *The Journal of Physiology*, *590*(Pt 24), 6327–6341. https://doi.org/10.1113/jphysiol.2012.239954

Chu, K., Cheng, Q., Chen, C., Au, L., Seto, S. W., Tuo, Y., Motin, L., Kwan, Y., & Leung, P. S. (2009). Angiotensin II exerts glucose-dependent effects on Kv currents in mouse pancreatic -cells via angiotensin II type 2 receptors. *American Journal of Physiology. Cell Physiology*, *298*, C313-23. https://doi.org/10.1152/ajpcell.00575.2008

Clark, R. B., Kondo, C., Belke, D. D., & Giles, W. R. (2011). Two-pore domain K+ channels regulate membrane potential of isolated human articular chondrocytes. *The Journal of Physiology*, *589*(21), 5071–5089. https://doi.org/10.1113/jphysiol.2011.210757

Colombini, A., Perucca Orfei, C., Kouroupis, D., Ragni, E., De Luca, P., ViganÒ, M., Correa, D., & de Girolamo, L. (2019). Mesenchymal stem cells in the treatment of articular cartilage degeneration: New biological insights for an old-timer cell. *Cytotherapy*, *21*(12), 1179–1197. https://doi.org/10.1016/j.jcyt.2019.10.004

Craig, A. F., Sahu, I. D., Zhang, R., Dunagan, M. M., Meiberg, A. G., Harmon, C. N., McCarrick, R. M., & Lorigan, G. A. (2014). Determining the Structural Topology of KCNE1 in a Lipid Bilayer using Electron Paramagentic Resonance (EPR) Spectroscopy. *Biophysical Journal*, *106*(2), 266a. https://doi.org/10.1016/j.bpj.2013.11.1556

Craig, A. F., Sahu, I. D., Zhang, R., Dunagan, M. M., Wang, K., McCarrick, R. M., & Lorigan, G. A. (2015). Probing the Protein-Protein Interactions between KCNQ1 and KCNE1 using Electron Paramagnetic Resonance (EPR) Spectroscopy. *Biophysical Journal*, *108*(2), 615a. https://doi.org/10.1016/j.bpj.2014.11.3349

Cruikshank, S. J., Killackey, H. P., & Metherate, R. (2001). Parvalbumin and calbindin are differentially distributed within primary and secondary subregions of the mouse auditory forebrain. *Neuroscience*, *105*(3), 553–569. https://doi.org/10.1016/s0306-4522(01)00226-3

Daheshia, M., & Yao, J. Q. (2008). The Interleukin 1β Pathway in the Pathogenesis of Osteoarthritis. *The Journal of Rheumatology*, *35*(12), 2306–2312. https://doi.org/10.3899/jrheum.080346

D'Angelo, D., & Rizzuto, R. (2023). The Mitochondrial Calcium Uniporter (MCU): Molecular Identity and Role in Human Diseases. *Biomolecules*, *13*(9). https://doi.org/10.3390/biom13091304

Dascombe, M. J., Rothwell, N. J., Sagay, B. O., & Stock, M. J. (1989). Pyrogenic and thermogenic effects of interleukin 1 beta in the rat. *American Journal of Physiology-Endocrinology and Metabolism*, *256*(1), E7–E11. https://doi.org/10.1152/ajpendo.1989.256.1.E7

Dasu, M. R., Devaraj, S., & Jialal, I. (2007). High glucose induces IL-1β expression in human monocytes: Mechanistic insights. *American Journal of Physiology-Endocrinology and Metabolism*, *293*(1), E337–E346. https://doi.org/10.1152/ajpendo.00718.2006

de Larco, J. E., & Todaro, G. J. (1978). Growth factors from murine sarcoma virus-transformed cells. *Proceedings of the National Academy of Sciences of the United States of America*, *75*(8), 4001–4005. https://doi.org/10.1073/pnas.75.8.4001

Degala, S., Williams, R., Zipfel, W., & Bonassar, L. J. (2012). Calcium signaling in response to fluid flow by chondrocytes in 3D alginate culture. *Journal of Orthopaedic Research: Official Publication of the Orthopaedic Research Society*, *30*(5), 793–799. https://doi.org/10.1002/jor.21571

Derynck, R., Jarrett, J. A., Chen, E. Y., Eaton, D. H., Bell, J. R., Assoian, R. K., Roberts, A. B., Sporn, M. B., & Goeddel, D. V. (1985). Human transforming growth factor-beta complementary DNA sequence and expression in normal and transformed cells. *Nature*, *316*(6030), 701–705. https://doi.org/10.1038/316701a0

Derynck, R., Turley, S. J., & Akhurst, R. J. (2021). TGFβ biology in cancer progression and immunotherapy. *Nature Reviews Clinical Oncology*, *18*(1), 9–34. https://doi.org/10.1038/s41571-020-0403-1

Diercks, D. B., Shumaik, G. M., Harrigan, R. A., Brady, W. J., & Chan, T. C. (2004). Electrocardiographic manifestations: Electrolyte abnormalities. *The Journal of Emergency Medicine*, *27*(2), 153–160. https://doi.org/10.1016/j.jemermed.2004.04.006

Dolphin, A. C. (2013). The α2δ subunits of voltage-gated calcium channels. *Biochimica Et Biophysica Acta*, *1828*(7), 1541–1549. https://doi.org/10.1016/j.bbamem.2012.11.019

Donger, C., Denjoy, I., Berthet, M., Neyroud, N., Cruaud, C., Bennaceur, M., Chivoret, G., Schwartz, K., Coumel, P., & Guicheney, P. (1997). KVLQT1 C-Terminal Missense Mutation Causes a Forme Fruste Long-QT Syndrome. *Circulation*, *96*(9), 2778–2781. https://doi.org/10.1161/01.CIR.96.9.2778

Dreier, R. (2010). Hypertrophic differentiation of chondrocytes in osteoarthritis: The developmental aspect of degenerative joint disorders. *Arthritis Research & Therapy*, *12*(5), 216. https://doi.org/10.1186/ar3117

Du, X., Cai, L., Xie, J., & Zhou, X. (2023). The role of TGF-beta3 in cartilage development and osteoarthritis. *Bone Research*, *11*(1), Article 1. https://doi.org/10.1038/s41413-022-00239-4

Eapen, A., Kulkarni, R., Ravindran, S., Ramachandran, A., Sundivakkam, P., Tiruppathi, C., & George, A. (2013). Dentin Phosphophoryn Activates

Smad Protein Signaling through Ca2+-Calmodulin-dependent Protein Kinase II in Undifferentiated Mesenchymal Cells. *The Journal of Biological Chemistry*, *288*(12), 8585–8595. https://doi.org/10.1074/jbc.M112.413997

El Khoury, N., Mathieu, S., & Fiset, C. (2014). Interleukin-1β Reduces L-type Ca2+ Current through Protein Kinase Cϵ Activation in Mouse Heart*. *Journal of Biological Chemistry*, *289*(32), 21896–21908. https://doi.org/10.1074/jbc.M114.549642

Eller, M. S., Yaar, M., Ostrom, K., Harkness, D. D., & Gilchrest, B. A. (1995). A role for interleukin-1 in epidermal differentiation: Regulation by expression of functional versus decoy receptors. *Journal of Cell Science*, *108*(8), 2741–2746. https://doi.org/10.1242/jcs.108.8.2741

Enkvetchakul, D. (2010). Genetic Disorders of Ion Channels. *Missouri Medicine*, *107*(4), 270–275.

Eyre, D. R. (1991). The collagens of articular cartilage. *Seminars in Arthritis and Rheumatism*, *21*(3, Supplement 2), 2–11. https://doi.org/10.1016/0049-0172(91)90035-X

Fabiato, A., & Fabiato, F. (1979). Calculator programs for computing the composition of the solutions containing multiple metals and ligands used for experiments in skinned muscle cells. *Journal De Physiologie*, *75*(5), 463–505.

Faramarzi, H., Mehrabani, D., Fard, M., Akhavan, M., Zare, S., Bakhshalizadeh, S., Manafi, A., Kazemnejad, S., & Shirazi, R. (2016). The Potential of Menstrual Blood-Derived Stem Cells in Differentiation to Epidermal Lineage: A Preliminary Report. *World Journal of Plastic Surgery*, *5*(1), 26–31.

Feng, T., Kalyaanamoorthy, S., Barakat, K., Feng, T., Kalyaanamoorthy, S., & Barakat, K. (2018). L-Type Calcium Channels: Structure and Functions. In *Ion Channels in Health and Sickness*. IntechOpen. https://doi.org/10.5772/intechopen.77305

Feng, X.-H., & Derynck, R. (2005). SPECIFICITY AND VERSATILITY IN TGF-β SIGNALING THROUGH SMADS. *Annual Review of Cell and Developmental Biology*, *21*(Volume 21, 2005), 659–693. https://doi.org/10.1146/annurev.cellbio.21.022404.142018

Fenichel, R. R., Malik, M., Antzelevitch, C., Sanguinetti, M., Roden, D. M., Priori, S. G., Ruskin, J. N., Lipicky, R. J., & Cantilena, L. R. (2004). Drug-induced torsades de pointes and implications for drug development. *Journal of Cardiovascular Electrophysiology*, *15*(4), 475–495. https://doi.org/10.1046/j.1540-8167.2004.03534.x

Fernandes, M., Martins Ribeiro, S., Sanfins, V., & Lourenço, A. (2015). Long QT syndrome with mutations in three genes: A rare case. *Revista Portuguesa de Cardiologia (English Edition)*, *34*(5), 359.e1-359.e5. https://doi.org/10.1016/j.repce.2014.10.006

Fernández-Iglesias, Á., Fuente, R., Gil-Peña, H., Alonso-Durán, L., Santos, F., & López, J. M. (2021). The Formation of the Epiphyseal Bone Plate

Occurs via Combined Endochondral and Intramembranous-Like Ossification. *International Journal of Molecular Sciences*, *22*(2), Article 2. https://doi.org/10.3390/ijms22020900

Ferreira Felix, I., Karlinski Vizentin, V., Neves, R., Bains, S., Bos, J. M., Giudicessi, J. R., & Ackerman, M. J. (2025). The Risk of Breakthrough Cardiac Events Associated With Psychiatric Medications in Patients With Diagnosed and Clinically Treated Long QT Syndrome. *JACC: Clinical Electrophysiology*, *11*(12), 2660–2669. https://doi.org/10.1016/j.jacep.2025.08.002

Fodor, J., Matta, C., Oláh, T., Juhász, T., Takács, R., Tóth, A., Dienes, B., Csernoch, L., & Zákány, R. (2013). Store-operated calcium entry and calcium influx *via* voltage-operated calcium channels regulate intracellular calcium oscillations in chondrogenic cells. *Cell Calcium*, *54*(1), 1–16. https://doi.org/10.1016/j.ceca.2013.03.003

Foncuberta, M. C., Cagnoni, P. J., Brandts, C. H., Mandanas, R., Fields, K., Derigs, H. G., Reed, E., Sonis, S. T., Fay, J., LeVeque, F., Pouillart, P., Schrezenmeier, H., Emmons, R., Thiel, E., & Investigators in TGF-beta3/OM Study Protocols 203/205. (2001). Topical transforming growth factor-beta3 in the prevention or alleviation of chemotherapy-induced oral mucositis in patients with lymphomas or solid tumors. *Journal of Immunotherapy (Hagerstown, Md.: 1997)*, *24*(4), 384–388. https://doi.org/10.1097/00002371-200107000-00014

Fonteneau, G., Bony, C., Goulabchand, R., Maria, A. T. J., Le Quellec, A., Rivière, S., Jorgensen, C., Guilpain, P., & Noël, D. (2017). Serum-Mediated Oxidative Stress from Systemic Sclerosis Patients Affects Mesenchymal Stem Cell Function. *Frontiers in Immunology*, *8*, 988. https://doi.org/10.3389/fimmu.2017.00988

Fülber, J., Agreste, F. R., Seidel, S. R. T., Sotelo, E. D. P., Barbosa, Â. P., Michelacci, Y. M., & Baccarin, R. Y. A. (2021). Chondrogenic potential of mesenchymal stem cells from horses using a magnetic 3D cell culture system. *World Journal of Stem Cells*, *13*(6), 645–658. https://doi.org/10.4252/wjsc.v13.i6.645

Furler, R. L., Nixon, D. F., Brantner, C. A., Popratiloff, A., & Uittenbogaart, C. H. (2018). TGF-β Sustains Tumor Progression through Biochemical and Mechanical Signal Transduction. *Cancers*, *10*(6), 199. https://doi.org/10.3390/cancers10060199

Futrega, K., Robey, P. G., Klein, T. J., Crawford, R. W., & Doran, M. R. (2021). A single day of TGF-β1 exposure activates chondrogenic and hypertrophic differentiation pathways in bone marrow-derived stromal cells. *Communications Biology*, *4*(1), 1–12. https://doi.org/10.1038/s42003-020-01520-0

Gale, A. L., Linardi, R. L., McClung, G., Mammone, R. M., & Ortved, K. F. (2019). Comparison of the Chondrogenic Differentiation Potential of Equine Synovial Membrane-Derived and Bone Marrow-Derived

Mesenchymal Stem Cells. *Frontiers in Veterinary Science*, *6*, 178. https://doi.org/10.3389/fvets.2019.00178

Ganesan, A. N., Maack, C., Johns, D. C., Sidor, A., & O'Rourke, B. (2006). β-Adrenergic Stimulation of L-type Ca2+ Channels in Cardiac Myocytes Requires the Distal Carboxyl Terminus of α1C but Not Serine 1928. *Circulation Research*, *98*(2), e11–e18. https://doi.org/10.1161/01.RES.0000202692.23001.e2

Gavenis, K., Schumacher, C., Schneider, U., Eisfeld, J., Mollenhauer, J., & Schmidt-Rohlfing, B. (2009). Expression of ion channels of the TRP family in articular chondrocytes from osteoarthritic patients: Changes between native and in vitro propagated chondrocytes. *Molecular and Cellular Biochemistry*, *321*(1–2), 135–143. https://doi.org/10.1007/s11010-008-9927-x

Goldberg, A., Mitchell, K., Soans, J., Kim, L., & Zaidi, R. (2017). The use of mesenchymal stem cells for cartilage repair and regeneration: A systematic review. *Journal of Orthopaedic Surgery and Research*, *12*, 39. https://doi.org/10.1186/s13018-017-0534-y

Gomes, B., Savignac, M., Moreau, M., Leclerc, C., Lory, P., Guery, J.-C., & Pelletier, L. (2004). Lymphocyte calcium signaling involves dihydropyridine-sensitive L-type calcium channels: Facts and controversies. *Critical Reviews in Immunology*, *24*(6), 425–447. https://doi.org/10.1615/critrevimmunol.v24.i6.30

González-Garrido, A., Domínguez-Pérez, M., Jacobo-Albavera, L., López-Ramírez, O., Guevara-Chávez, J. G., Zepeda-García, O., Iturralde, P., Carnevale, A., & Villarreal-Molina, T. (2021). Compound Heterozygous KCNQ1 Mutations Causing Recessive Romano–Ward Syndrome: Functional Characterization by Mutant Co-expression. *Frontiers in Cardiovascular Medicine*, *8*. https://doi.org/10.3389/fcvm.2021.625449

Gray, M., & Santin, J. M. (2023). Series resistance errors in whole cell voltage clamp measured directly with dual patch-clamp recordings: Not as bad as you think. *Journal of Neurophysiology*, *129*(5), 1177–1190. https://doi.org/10.1152/jn.00476.2022

Grunnet, M., Jespersen, T., Rasmussen, H. B., Ljungstrøm, T., Jorgensen, N. K., Olesen, S., & Klaerke, D. A. (2002). KCNE4 is an inhibitory subunit to the KCNQ1 channel. *The Journal of Physiology*, *542*(1), 119–130. https://doi.org/10.1113/jphysiol.2002.017301

Guo, C., Yang, X.-G., Wang, F., & Ma, X.-Y. (2016). IL-1α induces apoptosis and inhibits the osteoblast differentiation of MC3T3-E1 cells through the JNK and p38 MAPK pathways. *International Journal of Molecular Medicine*, *38*(1), 319–327. https://doi.org/10.3892/ijmm.2016.2606

Guo, X., Xi, L., Yu, M., Fan, Z., Wang, W., Ju, A., Liang, Z., Zhou, G., & Ren, W. (2023). Regeneration of articular cartilage defects: Therapeutic strategies and perspectives. *Journal of Tissue Engineering*, *14*, 20417314231164765. https://doi.org/10.1177/20417314231164765

Hammami Bomholtz, S., Refaat, M., Buur Steffensen, A., David, J.-P., Espinosa, K., Nussbaum, R., Wojciak, J., Hjorth Bentzen, B., Scheinman, M., & Schmitt, N. (2020). Functional phenotype variations of two novel KV7.1 mutations identified in patients with Long QT syndrome. *Pacing and Clinical Electrophysiology*, *43*(2), 210–216. https://doi.org/10.1111/pace.13870

Hammersen, T., Buchert, J., Zietzschmann, S., Diederichs, S., & Richter, W. (2023). Inverse Regulation of Cartilage Neogenesis at Physiologically Relevant Calcium Conditions by Human Articular Chondrocytes and Mesenchymal Stromal Cells. *Cells*, *12*(12), 1659. https://doi.org/10.3390/cells12121659

Hanna, H., Mir, L. M., & Andre, F. M. (2018). In vitro osteoblastic differentiation of mesenchymal stem cells generates cell layers with distinct properties. *Stem Cell Research & Therapy*, *9*(1), 203. https://doi.org/10.1186/s13287-018-0942-x

Haque, S., & Morris, J. C. (2017). Transforming growth factor-β: A therapeutic target for cancer. *Human Vaccines & Immunotherapeutics*, *13*(8), 1741–1750. https://doi.org/10.1080/21645515.2017.1327107

He, Q., Shi, J., Liu, W., Zhao, W., Wang, Z., Liu, K., Zhao, D., Wang, S., Guo, Y., Cheng, L., & Gao, Y. (2022). TGF-β1-induced bone marrow mesenchymal stem cells (BMSCs) migration via histone demethylase KDM6B mediated inhibition of methylation marker H3K27me3. *Cell Death Discovery*, *8*(1), 339. https://doi.org/10.1038/s41420-022-01132-z

Heine, U., Munoz, E. F., Flanders, K. C., Ellingsworth, L. R., Lam, H. Y., Thompson, N. L., Roberts, A. B., & Sporn, M. B. (1987). Role of transforming growth factor-beta in the development of the mouse embryo. *The Journal of Cell Biology*, *105*(6 Pt 2), 2861–2876. https://doi.org/10.1083/jcb.105.6.2861

Hell, J. W., Westenbroek, R. E., Warner, C., Ahlijanian, M. K., Prystay, W., Gilbert, M. M., Snutch, T. P., & Catterall, W. A. (1993). Identification and differential subcellular localization of the neuronal class C and class D L-type calcium channel alpha 1 subunits. *Journal of Cell Biology*, *123*(4), 949–962. https://doi.org/10.1083/jcb.123.4.949

Henderson, B., & Pettipher, E. R. (1988). Comparison of the in vivo inflammatory activities after intra-articular injection of natural and recombinant IL-1α and IL-1β in the rabbit. *Biochemical Pharmacology*, *37*(21), 4171–4176. https://doi.org/10.1016/0006-2952(88)90112-8

Hess, P., & Tsien, R. W. (1984). Mechanism of ion permeation through calcium channels. *Nature*, *309*(5967), Article 5967. https://doi.org/10.1038/309453a0

Heubach, J. F., Graf, E. M., Leutheuser, J., Bock, M., Balana, B., Zahanich, I., Christ, T., Boxberger, S., Wettwer, E., & Ravens, U. (2004). Electrophysiological properties of human mesenchymal stem cells. *The Journal of Physiology*, *554*(3), 659–672. https://doi.org/10.1113/jphysiol.2003.055806

https://doi.org/10.1113/jphysiol.2003.055806
Heubach, J. F., Trebeß, I., Wettwer, E., Himmel, H. M., Michel, M. C., Kaumann, A. J., Koch, W. J., Harding, S. E., & Ravens, U. (1999). L-type calcium current and contractility in ventricular myocytes from mice overexpressing the cardiac β2-adrenoceptor1. *Cardiovascular Research*, *42*(1), 173–182. https://doi.org/10.1016/S0008-6363(98)00262-4
Hofmann, F., Flockerzi, V., Kahl, S., & Wegener, J. W. (2014). L-type CaV1.2 calcium channels: From in vitro findings to in vivo function. *Physiological Reviews*, *94*(1), 303–326. https://doi.org/10.1152/physrev.00016.2013
Hu, L., Yin, C., Zhao, F., Ali, A., Ma, J., & Qian, A. (2018). Mesenchymal Stem Cells: Cell Fate Decision to Osteoblast or Adipocyte and Application in Osteoporosis Treatment. *International Journal of Molecular Sciences*, *19*(2), 360. https://doi.org/10.3390/ijms19020360
Hu, Q., & Ecker, M. (2021). Overview of MMP-13 as a Promising Target for the Treatment of Osteoarthritis. *International Journal of Molecular Sciences*, *22*(4), 1742. https://doi.org/10.3390/ijms22041742
Huang, H.-I., Chio, C.-C., Lin, J.-Y., Chou, C.-J., Lin, C.-C., Chen, S.-H., & Yu, L.-S. (2022). EV-A71 induced IL-1β production in THP-1 macrophages is dependent on NLRP3, RIG-I, and TLR3. *Scientific Reports*, *12*(1), 21425. https://doi.org/10.1038/s41598-022-25458-x
Huang, T., Schor, S. L., & Hinck, A. P. (2014). Biological Activity Differences between TGF-β1 and TGF-β3 Correlate with Differences in the Rigidity and Arrangement of Their Component Monomers. *Biochemistry*, *53*(36), 5737–5749. https://doi.org/10.1021/bi500647d
Hunziker, E. B., Quinn, T. M., & Häuselmann, H.-J. (2002). Quantitative structural organization of normal adult human articular cartilage. *Osteoarthritis and Cartilage*, *10*(7), 564–572. https://doi.org/10.1053/joca.2002.0814
Inada, M., Izawa, G., Kobayashi, W., & Ozawa, M. (2016). 293 cells express both epithelial as well as mesenchymal cell adhesion molecules. *International Journal of Molecular Medicine*, *37*(6), 1521–1527. https://doi.org/10.3892/ijmm.2016.2568
Inayama, M., Suzuki, Y., Yamada, S., Kurita, T., Yamamura, H., Ohya, S., Giles, W. R., & Imaizumi, Y. (2015). Orai1–Orai2 complex is involved in store-operated calcium entry in chondrocyte cell lines. *Cell Calcium*, *57*(5), 337–347. https://doi.org/10.1016/j.ceca.2015.02.005
Iscla, I., Wray, R., Wei, S., Posner, B., & Blount, P. (2014). Streptomycin potency is dependent on MscL channel expression. *Nature Communications*, *5*(1), 4891. https://doi.org/10.1038/ncomms5891
Ishiyama, N., Shibata, H., Kanzaki, M., Shiozaki, S., Miyazaki, J., Kobayashi, I., & Kojima, I. (1996). Calcium as a second messenger of the action of transforming growth factor-beta on insulin secretion. *Molecular and Cellular Endocrinology*, *117*(1), 1–6. https://doi.org/10.1016/0303-7207(95)03726-8

Jahn, M., Rauh, O., Fauth, T., & Buerger, C. (2021). Cell Volume Regulation in the Epidermis | Cell Physiol Biochem. *Cellular Physiology & Biochemistry*, *55*(S1), 57–70.

Jaiswal, N., Haynesworth, S. E., Caplan, A. I., & Bruder, S. P. (1997). Osteogenic differentiation of purified, culture-expanded human mesenchymal stem cells in vitro. *Journal of Cellular Biochemistry*, *64*(2), 295–312.

Jenei-Lanzl, Z., Meurer, A., & Zaucke, F. (2019). Interleukin-1β signaling in osteoarthritis – chondrocytes in focus. *Cellular Signalling*, *53*, 212–223. https://doi.org/10.1016/j.cellsig.2018.10.005

Jespersen, T., Grunnet, M., & Olesen, S.-P. (2005). The KCNQ1 Potassium Channel: From Gene to Physiological Function. *Physiology*, *20*(6), 408–416. https://doi.org/10.1152/physiol.00031.2005

Johnson, C. M., Hill, C. S., Chawla, S., Treisman, R., & Bading, H. (1997). Calcium Controls Gene Expression via Three Distinct Pathways That Can Function Independently of the Ras/Mitogen-Activated Protein Kinases (ERKs) Signaling Cascade. *The Journal of Neuroscience*, *17*(16), 6189–6202. https://doi.org/10.1523/JNEUROSCI.17-16-06189.1997

Johnson, J. N., & Ackerman, M. J. (2009). QTc: How long is too long? *British Journal of Sports Medicine*, *43*(9), 657–662. https://doi.org/10.1136/bjsm.2008.054734

Johnstone, B., Hering, T. M., Caplan, A. I., Goldberg, V. M., & Yoo, J. U. (1998). In vitro chondrogenesis of bone marrow-derived mesenchymal progenitor cells. *Experimental Cell Research*, *238*(1), 265–272. https://doi.org/10.1006/excr.1997.3858

Kamari, Y., Werman-Venkert, R., Shaish, A., Werman, A., Harari, A., Gonen, A., Voronov, E., Grosskopf, I., Sharabi, Y., Grossman, E., Iwakura, Y., Dinarello, C. A., Apte, R. N., & Harats, D. (2007). Differential role and tissue specificity of interleukin-1alpha gene expression in atherogenesis and lipid metabolism. *Atherosclerosis*, *195*(1), 31–38. https://doi.org/10.1016/j.atherosclerosis.2006.11.026

Kapa, S., Tester, D. J., Salisbury, B. A., Harris-Kerr, C., Pungliya, M. S., Alders, M., Wilde, A. A. M., & Ackerman, M. J. (2009). Genetic Testing for Long QT Syndrome—Distinguishing Pathogenic Mutations from Benign Variants. *Circulation*, *120*(18), 1752–1760. https://doi.org/10.1161/CIRCULATIONAHA.109.863076

Kapplinger, J. D., Tester, D. J., Salisbury, B. A., Carr, J. L., Harris-Kerr, C., Pollevick, G. D., Wilde, A. A. M., & Ackerman, M. J. (2009). Spectrum and prevalence of mutations from the first 2,500 consecutive unrelated patients referred for the FAMILION long QT syndrome genetic test. *Heart Rhythm*, *6*(9), 1297–1303. https://doi.org/10.1016/j.hrthm.2009.05.021

Kasuya, G., Zempo, B., Yamamoto, Y., Ryu, K., Ono, F., & Nakajo, K. (2024). Identification of KCNE6, a new member of the KCNE family of

potassium channel auxiliary subunits. *Communications Biology*, *7*(1). https://doi.org/10.1038/s42003-024-07352-6
Kaur, K., Zarzoso, M., Ponce-Balbuena, D., Guerrero-Serna, G., Hou, L., Musa, H., & Jalife, J. (2013). TGF-β1, Released by Myofibroblasts, Differentially Regulates Transcription and Function of Sodium and Potassium Channels in Adult Rat Ventricular Myocytes. *PLOS ONE*, *8*(2), e55391. https://doi.org/10.1371/journal.pone.0055391
Kawai, F. (2024). Somatic ion channels and action potentials in olfactory receptor cells and vomeronasal receptor cells. *Journal of Neurophysiology*, *131*(3), 455–471. https://doi.org/10.1152/jn.00137.2023
Kawano, S., Shoji, S., Ichinose, S., Yamagata, K., Tagami, M., & Hiraoka, M. (2002). Characterization of Ca(2+) signaling pathways in human mesenchymal stem cells. *Cell Calcium*, *32*(4), 165–174. https://doi.org/10.1016/s0143416002001240
Kehrl, J. H., Roberts, A. B., Wakefield, L. M., Jakowlew, S., Sporn, M. B., & Fauci, A. S. (1986). Transforming growth factor beta is an important immunomodulatory protein for human B lymphocytes. *Journal of Immunology (Baltimore, Md.: 1950)*, *137*(12), 3855–3860.
Kekenes-Huskey, P. M., Burgess, D. E., Sun, B., Bartos, D. C., Rozmus, E. R., Anderson, C. L., January, C. T., Eckhardt, L. L., & Delisle, B. P. (2022). Mutation-Specific Differences in Kv7.1 (KCNQ1) and Kv11.1 (KCNH2) Channel Dysfunction and Long QT Syndrome Phenotypes. *International Journal of Molecular Sciences*, *23*(13), 7389. https://doi.org/10.3390/ijms23137389
Khoury, N. E., & Fiset, C. (2012). Interleukin-1β Modulates Cardiac L-Type Calcium Channel via PKC Signalling Pathways in Mice. *Biophysical Journal*, *102*(3), 338a. https://doi.org/10.1016/j.bpj.2011.11.1855
Kiliç, E., Ceyhan, T., & Cetinkaya, D. U. (2007). [Evaluation of differentiation potential of human bone marrow-derived mesenchymal stromal cells to cartilage and bone cells]. *Acta Orthopaedica Et Traumatologica Turcica*, *41*(4), 295–301.
Kim, H.-J., Kim, Y.-J., & Im, G.-I. (2008). Is Continuous Treatment with Transforming Growth Factor-Beta Necessary to Induce Chondrogenic Differentiation in Mesenchymal Stem Cells? *Cells Tissues Organs*, *190*(1), 1–10. https://doi.org/10.1159/000153041
Kim, J., & Lee, J. (2017). Role of transforming growth factor-β in muscle damage and regeneration: Focused on eccentric muscle contraction. *Journal of Exercise Rehabilitation*, *13*(6), 621–626. https://doi.org/10.12965/jer.1735072.536
Kim, J., Shapiro, L., & Flynn, A. (2015). The clinical application of mesenchymal stem cells and cardiac stem cells as a therapy for cardiovascular disease. *Pharmacology & Therapeutics*, *151*, 8–15. https://doi.org/10.1016/j.pharmthera.2015.02.003

Kinoshita, K., Komatsu, T., Nishide, K., Hata, Y., Hisajima, N., Takahashi, H., Kimoto, K., Aonuma, K., Tsushima, E., Tabata, T., Yoshida, T., Mori, H., Nishida, K., Yamaguchi, Y., Ichida, F., Fukurotani, K., Inoue, H., & Nishida, N. (2014). A590T mutation in KCNQ1 C-terminal helix D decreases IKs channel trafficking and function but not Yotiao interaction. *Journal of Molecular and Cellular Cardiology*, *72*, 273–280. https://doi.org/10.1016/j.yjmcc.2014.03.019

Kobayashi, M., Squires, G. R., Mousa, A., Tanzer, M., Zukor, D. J., Antoniou, J., Feige, U., & Poole, A. R. (2005). Role of interleukin-1 and tumor necrosis factor alpha in matrix degradation of human osteoarthritic cartilage. *Arthritis and Rheumatism*, *52*(1), 128–135. https://doi.org/10.1002/art.20776

Kramer, F., Torzewski, J., Kamenz, J., Veit, K., Hombach, V., Dedio, J., & Ivashchenko, Y. (2008). Interleukin-1β stimulates acute phase response and C-reactive protein synthesis by inducing an NFκB- and C/EBPβ-dependent autocrine interleukin-6 loop. *Molecular Immunology*, *45*(9), 2678–2689. https://doi.org/10.1016/j.molimm.2007.12.017

Krawczenko, A., & Klimczak, A. (2022). Adipose Tissue-Derived Mesenchymal Stem/Stromal Cells and Their Contribution to Angiogenic Processes in Tissue Regeneration. *International Journal of Molecular Sciences*, *23*(5), 2425. https://doi.org/10.3390/ijms23052425

Kurata, T., Suzuki, Y., Tateno, S., Miyaki, S., Kondo, R., Bernotiene, E., Mobasheri, A., Giles, W. R., Imaizumi, Y., & Yamamura, H. (2026). Interleukin-1β downregulates K+ currents through Kv1.6 channels and promotes apoptosis by enhancing Ca2+ influx in chondrocytes. *American Journal of Physiology-Cell Physiology*, *330*(4), C909–C925. https://doi.org/10.1152/ajpcell.00381.2025

Lange, C., Bassler, P., Lioznov, M. V., Bruns, H., Kluth, D., Zander, A. R., & Fiegel, H. C. (2005). Hepatocytic gene expression in cultured rat mesenchymal stem cells. *Transplantation Proceedings*, *37*(1), 276–279. https://doi.org/10.1016/j.transproceed.2004.11.087

Le, H., Xu, W., Zhuang, X., Chang, F., Wang, Y., & Ding, J. (2020). Mesenchymal stem cells for cartilage regeneration. *Journal of Tissue Engineering*, *11*, 2041731420943839. https://doi.org/10.1177/2041731420943839

Lebman, D. A., & Edmiston, J. S. (1999). The role of TGF-beta in growth, differentiation, and maturation of B lymphocytes. *Microbes and Infection*, *1*(15), 1297–1304. https://doi.org/10.1016/s1286-4579(99)00254-3

Lee, S. Y., Nakagawa, T., & Reddi, A. H. (2009, November 7). *Mesenchymal Progenitor Cells Derived from Synovium and Infrapatellar Fat Pad as a Source for Superficial Zone Cartilage Tissue Engineering: Analysis of Superficial Zone Protein/Lubricin Expression* [Research-article]. Mary Ann Liebert, Inc. 140 Huguenot Street, 3rd Floor New Rochelle, NY 10801 USA. (140 Huguenot Street, 3rd Floor New

Rochelle, NY 10801 USA). Https://Home.Liebertpub.Com/Tea. https://doi.org/10.1089/ten.tea.2009.0104
Lefer, A. M., Tsao, P., Aoki, N., & Palladino, M. A. (1990). Mediation of cardioprotection by transforming growth factor-beta. *Science (New York, N.Y.)*, *249*(4964), 61–64. https://doi.org/10.1126/science.2164258
Lekshmi, N., Geetha, C. S., & Mohanan, P. V. (2012). Detection of interleukin -1β from isolated human lymphocyte in response to lipopolysaccharide and lipoteichoic acid. *Indian Journal of Pharmacology*, *44*(6), 726. https://doi.org/10.4103/0253-7613.103269
Levitan, E. S., Hemmick, L. M., Birnberg, N. C., & Kaczmarek, L. K. (1991). Dexamethasone Increases Potassium Channel Messenger RNA and Activity in Clonal Pituitary Cells. *Molecular Endocrinology*, *5*(12), 1903–1908. https://doi.org/10.1210/mend-5-12-1903
Li, C., Meng, X., Wang, L., & Dai, X. (2023). Mechanism of action of non-coding RNAs and traditional Chinese medicine in myocardial fibrosis: Focus on the TGF-β/Smad signaling pathway. *Frontiers in Pharmacology*, *14*. https://doi.org/10.3389/fphar.2023.1092148
Li, W., Zhou, Y., Han, L., Wang, L., & Lu, X. L. (2022). Calcium signaling of primary chondrocytes and ATDC5 chondrogenic cells under osmotic stress and mechanical stimulation. *Journal of Biomechanics*, *145*, 111388. https://doi.org/10.1016/j.jbiomech.2022.111388
Li, Y., Chen, W., Deng, H., Li, T., Liu, Z., Liu, X., Zhang, Z., Chen, X., Sheng, J., & Li, K. (2022). TGF-β1 Protects Trauma-injured Murine Cortical Neurons by Upregulating L-type Calcium Channel Cav1.2 via the p38 Pathway. *Neuroscience*, *492*, 47–57. https://doi.org/10.1016/j.neuroscience.2022.04.010
Li, Y., Liu, L., Ding, X., Liu, Y., Yang, Q., & Ren, B. (2020). Interleukin-1β attenuates the proliferation and differentiation of oligodendrocyte precursor cells through regulation of the microRNA-202-3p/β-catenin/Gli1 axis. *International Journal of Molecular Medicine*, *46*(3), 1217–1224. https://doi.org/10.3892/ijmm.2020.4648
Liang, J. J., & Callans, D. J. (2017). Electrophysiologic Testing and Cardiac Mapping. In P. Kowey, J. P. Piccini, G. Naccarelli, & J. A. Reiffel (Eds.), *Cardiac Arrhythmias, Pacing and Sudden Death* (pp. 75–86). Springer International Publishing. https://doi.org/10.1007/978-3-319-58000-5_7
Lin, C., Zhang, Y., Zhang, K., Zheng, Y., Lu, L., Chang, H., Yang, H., Yang, Y., Wan, Y., Wang, S., Yuan, M., Yan, Z., Zhang, R., He, Y., Ge, G., Wu, D., & Chen, J. (2019). Fever Promotes T Lymphocyte Trafficking via a Thermal Sensory Pathway Involving Heat Shock Protein 90 and α4 Integrins. *Immunity*, *50*(1), 137-151.e6. https://doi.org/10.1016/j.immuni.2018.11.013
Lipscombe, D. (2002). L-Type Calcium Channels. *Circulation Research*, *90*(9), 933–935. https://doi.org/10.1161/01.RES.0000019740.52306.92

Lipsky, P. E. (1985). Role of Interleukin-1 in Human B-Cell Activation. In S. Gillis & F. P. Inman (Eds.), *The Interleukins* (pp. 195–217). Springer US. https://doi.org/10.1007/978-1-4684-4838-2_8

Litmanovich, A., Khazim, K., & Cohen, I. (2018). The Role of Interleukin-1 in the Pathogenesis of Cancer and its Potential as a Therapeutic Target in Clinical Practice. *Oncology and Therapy*, *6*(2), 109–127. https://doi.org/10.1007/s40487-018-0089-z

Liu, Q., Cheng, G., Wang, Z., Zhan, S., Xiong, B., & Zhao, X. (2015). Bone marrow-derived mesenchymal stem cells differentiate into nerve-like cells in vitro after transfection with brain-derived neurotrophic factor gene. *In Vitro Cellular & Developmental Biology. Animal*, *51*(3), 319–327. https://doi.org/10.1007/s11626-015-9875-1

Liu, R. R., & Danesh, H. (2023). Adult Mesenchymal Stem Cell Collection and Banking. In C. W. Hunter, T. T. Davis, & M. J. DePalma (Eds.), *Regenerative Medicine: A Complete Guide for Musculoskeletal and Spine Disorders* (pp. 81–88). Springer International Publishing. https://doi.org/10.1007/978-3-030-75517-1_8

Liu, S., & Schreur, K. D. (1995). G protein-mediated suppression of L-type Ca2+ current by interleukin-1 beta in cultured rat ventricular myocytes. *American Journal of Physiology-Cell Physiology*, *268*(2), C339–C349. https://doi.org/10.1152/ajpcell.1995.268.2.C339

Liu, Y., Terata, K., Rusch, N. J., & Gutterman, D. D. (2001). High Glucose Impairs Voltage-Gated K+ Channel Current in Rat Small Coronary Arteries. *Circulation Research*, *89*(2), 146–152. https://doi.org/10.1161/hh1401.093294

Liu, Z., Sheng, J., Peng, G., Yang, J., Chen, W., & Li, K. (2018). TGF-β1 Regulation of P-JNK and L-Type Calcium Channel Cav1.2 in Cortical Neurons. *Journal of Molecular Neuroscience*, *64*(3), 374–384. https://doi.org/10.1007/s12031-018-1033-2

Lopez-Castejon, G., & Brough, D. (2011). Understanding the mechanism of IL-1β secretion. *Cytokine & Growth Factor Reviews*, *22*(4), 189–195. https://doi.org/10.1016/j.cytogfr.2011.10.001

Lu, L., Wang, P., Zou, Y., Zha, Z., Huang, H., Guan, M., Wu, Y., & Liu, G. (2020). IL-1β Promotes Stemness of Tumor Cells by Activating Smad/ID1 Signaling Pathway. *International Journal of Medical Sciences*, *17*(9), 1257–1268. https://doi.org/10.7150/ijms.44285

Lu, Y. T., Wei, L. S., Wang, Z. Y., Li, W., Duan, Y. W., Gao, M., Liu, J., Zhao, Y. H., & Li, S. L. (2018). [TGF-β3 improves bone mesenchymal stem cells toward chondrogenic differentiation under hypoxia environment]. *Zhonghua Yi Xue Za Zhi*, *98*(27), 2198–2202. https://doi.org/10.3760/cma.j.issn.0376-2491.2018.27.015

LUO, L., CRUZ, T., & McCULLOCH, C. (1997). Interleukin 1-induced calcium signalling in chondrocytes requires focal adhesions. *Biochemical Journal*, *324*(2), 653–658. https://doi.org/10.1042/bj3240653

Lv, M., Zhou, Y., Chen, X., Han, L., Wang, L., & Lu, X. L. (2017). Calcium Signaling of in situ Chondrocytes in Articular Cartilage under Compressive Loading: Roles of Calcium Sources and Cell Membrane Ion Channels. *Journal of Orthopaedic Research : Official Publication of the Orthopaedic Research Society*, *36*(2), 730. https://doi.org/10.1002/jor.23768

Lv, M., Zhou, Y., Chen, X., Han, L., Wang, L., & Lu, X. L. (2018). Calcium Signaling of in situ Chondrocytes in Articular Cartilage under Compressive Loading: Roles of Calcium Sources and Cell Membrane Ion Channels. *Journal of Orthopaedic Research : Official Publication of the Orthopaedic Research Society*, *36*(2), 730–738. https://doi.org/10.1002/jor.23768

Lv, M., Zhou, Y., Polson, S. W., Wan, L. Q., Wang, M., Han, L., Wang, L., & Lu, X. L. (2019). Identification of Chondrocyte Genes and Signaling Pathways in Response to Acute Joint Inflammation. *Scientific Reports*, *9*, 93. https://doi.org/10.1038/s41598-018-36500-2

Mahr, S., Neumayer, N., Gerhard, M., Classen, M., & Prinz, C. (2000). IL-1β–Induced apoptosis in rat gastric enterochromaffin-like cells is mediated by iNOS, NF-κB, and Bax protein. *Gastroenterology*, *118*(3), 515–524. https://doi.org/10.1016/S0016-5085(00)70257-5

Mancilla, E. E., Galindo, M., Fertilio, B., Herrera, M., Salas, K., Gatica, H., & Goecke, A. (2007). L-type calcium channels in growth plate chondrocytes participate in endochondral ossification. *Journal of Cellular Biochemistry*, *101*(2), 389–398. https://doi.org/10.1002/jcb.21183

Mardones, R., Giai Via, A., Pipino, G., Jofre, C. M., Muñoz, S., Narvaez, E., & Maffulli, N. (2020). BM-MSCs differentiated to chondrocytes for treatment of full-thickness cartilage defect of the knee. *Journal of Orthopaedic Surgery and Research*, *15*(1), 455. https://doi.org/10.1186/s13018-020-01852-x

Marrero - Berrios, I., Salter, S. E., Hirday, R., Rabolli, C. P., Tan, A., Hung, C. T., Schloss, R. S., & Yarmush, M. L. (2024). In vitro inflammatory multi-cellular model of osteoarthritis. *Osteoarthritis and Cartilage Open*, *6*(1), 100432. https://doi.org/10.1016/j.ocarto.2023.100432

Marstrand, P., Theilade, J., Andersson, C., Bundgaard, H., Weeke, P. E., Tfelt-Hansen, J., Jespersen, C., Gislason, G., Torp-Pedersen, C., Kanters, J. K., & Jørgensen, M. E. (2019). Long QT syndrome is associated with an increased burden of diabetes, psychiatric and neurological comorbidities: A nationwide cohort study. *Open Heart*, *6*(2), e001161. https://doi.org/10.1136/openhrt-2019-001161

Massagué, J., Seoane, J., & Wotton, D. (2005). Smad transcription factors. *Genes & Development*, *19*(23), 2783–2810. https://doi.org/10.1101/gad.1350705

Matsumura, E., Tsuji, K., Komori, K., Koga, H., Sekiya, I., & Muneta, T. (2017). Pretreatment with IL-1β enhances proliferation and chondrogenic

potential of synovium-derived mesenchymal stem cells. *Cytotherapy*, *19*(2), 181–193. https://doi.org/10.1016/j.jcyt.2016.11.004
Matta, C., Fodor, J., Szíjgyártó, Z., Juhász, T., Gergely, P., Csernoch, L., & Zákány, R. (2008). Cytosolic free Ca2+ concentration exhibits a characteristic temporal pattern during in vitro cartilage differentiation: A possible regulatory role of calcineurin in Ca-signalling of chondrogenic cells. *Cell Calcium*, *44*(3), 310–323. https://doi.org/10.1016/j.ceca.2007.12.010
Matta, C., & Zakany, R. (2013). Calcium signalling in chondrogenesis: Implications for cartilage repair. *Frontiers in Bioscience-Scholar*, *5*(1), Article 1. https://doi.org/10.2741/S374
Matta, C., Zákány, R., & Mobasheri, A. (2015). Voltage-Dependent Calcium Channels in Chondrocytes: Roles in Health and Disease. *Current Rheumatology Reports*, *17*(7), 43. https://doi.org/10.1007/s11926-015-0521-4
Mauck, R. L., Yuan, X., & Tuan, R. S. (2006). Chondrogenic differentiation and functional maturation of bovine mesenchymal stem cells in long-term agarose culture. *Osteoarthritis and Cartilage*, *14*(2), 179–189. https://doi.org/10.1016/j.joca.2005.09.002
McGowan, T. A., Madesh, M., Zhu, Y., Wang, L., Russo, M., Deelman, L., Henning, R., Joseph, S., Hajnoczky, G., & Sharma, K. (2002). TGF-β-induced Ca2+ influx involves the type III IP3 receptor and regulates actin cytoskeleton. *American Journal of Physiology-Renal Physiology*, *282*(5), F910–F920. https://doi.org/10.1152/ajprenal.00252.2001
Meesuk, L., Suwanprateeb, J., Thammarakcharoen, F., Tantrawatpan, C., Kheolamai, P., Palang, I., Tantikanlayaporn, D., & Manochantr, S. (2022). Osteogenic differentiation and proliferation potentials of human bone marrow and umbilical cord-derived mesenchymal stem cells on the 3D-printed hydroxyapatite scaffolds. *Scientific Reports*, *12*(1), 19509. https://doi.org/10.1038/s41598-022-24160-2
Mejia-Luna, L., & Avila, G. (2004). Ca2+ channel regulation by transforming growth factor-β1 and bone morphogenetic protein-2 in developing mice myotubes. *The Journal of Physiology*, *559*(Pt 1), 41–54. https://doi.org/10.1113/jphysiol.2004.066852
Melman, Y. F., Domènech, A., De La Luna, S., & McDonald, T. V. (2001). Structural Determinants of KvLQT1 Control by the KCNE Family of Proteins. *Journal of Biological Chemistry*, *276*(9), 6439–6444. https://doi.org/10.1074/jbc.M010713200
Mendiola, A. S., & Cardona, A. E. (2018). The IL-1β phenomena in neuroinflammatory diseases. *Journal of Neural Transmission (Vienna, Austria : 1996)*, *125*(5), 781–795. https://doi.org/10.1007/s00702-017-1732-9
Mestril, S., Kim, R., Hinman, S. S., Gomez, S. M., & Allbritton, N. L. (2021). Stem/Proliferative and Differentiated Cells within Primary Murine Colonic Epithelium Display Distinct Intracellular Free Ca2+

Signal Codes. *Advanced Healthcare Materials*, *10*(22), 2101318. https://doi.org/10.1002/adhm.202101318
Mobasheri, A., Lewis, R., Ferreira-Mendes, A., Rufino, A., Dart, C., & Barrett-Jolley, R. (2012). Potassium channels in articular chondrocytes. *Channels*, *6*(6), 416–425. https://doi.org/10.4161/chan.22340
Mobasheri, A., Matta, C., Uzielienė, I., Budd, E., Martín-Vasallo, P., & Bernotiene, E. (2019). The chondrocyte channelome: A narrative review. *Joint Bone Spine*, *86*(1), 29–35. https://doi.org/10.1016/j.jbspin.2018.01.012
Modi, P., Shah, B. M., & Patel, S. (2023). Interleukin-1β converting enzyme (ICE): A comprehensive review on discovery and development of caspase-1 inhibitors. *European Journal of Medicinal Chemistry*, *261*, 115861. https://doi.org/10.1016/j.ejmech.2023.115861
Moonshi, S. S., Adelnia, H., Wu, Y., & Ta, H. T. (2022). Placenta-Derived Mesenchymal Stem Cells for Treatment of Diseases: A Clinically Relevant Source. *Advanced Therapeutics*, *5*(10), 2200054. https://doi.org/10.1002/adtp.202200054
Morgat, C., Fressart, V., Porretta, A. P., Neyroud, N., Messali, A., Temmar, Y., Algalarrondo, V., Surget, E., Bloch, A., Leenhardt, A., Denjoy, I., & Extramiana, F. (2024). Genetic characterization of KCNQ1 variants improves risk stratification in type 1 long QT syndrome patients. *Europace: European Pacing, Arrhythmias, and Cardiac Electrophysiology: Journal of the Working Groups on Cardiac Pacing, Arrhythmias, and Cardiac Cellular Electrophysiology of the European Society of Cardiology*, *26*(6), euae136. https://doi.org/10.1093/europace/euae136
Moss, A. J. (2003). Long QT Syndrome. *JAMA*, *289*(16), 2041–2044. https://doi.org/10.1001/jama.289.16.2041
Mouw, J. K., Imler, S. M., & Levenston, M. E. (2007). Ion-channel Regulation of Chondrocyte Matrix Synthesis in 3D Culture Under Static and Dynamic Compression. *Biomechanics and Modeling in Mechanobiology*, *6*(1), 33–41. https://doi.org/10.1007/s10237-006-0034-1
Mukherjee, S., Kolb, M. R. J., Duan, F., & Janssen, L. J. (2012). Transforming Growth Factor–β Evokes Ca2+ Waves and Enhances Gene Expression in Human Pulmonary Fibroblasts. *American Journal of Respiratory Cell and Molecular Biology*, *46*(6), 757–764. https://doi.org/10.1165/rcmb.2011-0223OC
Muldoon, L. L., Rodland, K. D., & Magun, B. E. (1988). Transforming growth factor beta and epidermal growth factor alter calcium influx and phosphatidylinositol turnover in rat-1 fibroblasts. *Journal of Biological Chemistry*, *263*(35), 18834–18841. https://doi.org/10.1016/S0021-9258(18)37358-7
Mumme, M., Scotti, C., Papadimitropoulos, A., Todorov, A., Hoffmann, W., Bocelli-Tyndall, C., Jakob, M., Wendt, D., Martin, I., & Barbero, A.

(2012). Interleukin-1β modulates endochondral ossification by human adult bone marrow stromal cells. *European Cells & Materials*, *24*, 224–236. https://doi.org/10.22203/ecm.v024a16

Murakami, S., Lefebvre, V., & Crombrugghe, B. de. (2000). Potent Inhibition of the Master Chondrogenic FactorSox9 Gene by Interleukin-1 and Tumor Necrosis Factor-α *. *Journal of Biological Chemistry*, *275*(5), 3687–3692. https://doi.org/10.1074/jbc.275.5.3687

Nakagawa, Y., Muneta, T., Otabe, K., Ozeki, N., Mizuno, M., Udo, M., Saito, R., Yanagisawa, K., Ichinose, S., Koga, H., Tsuji, K., & Sekiya, I. (2016). Cartilage Derived from Bone Marrow Mesenchymal Stem Cells Expresses Lubricin In Vitro and In Vivo. *PLOS ONE*, *11*(2), e0148777. https://doi.org/10.1371/journal.pone.0148777

Nakajo, K. (2019). Gating modulation of the KCNQ1 channel by KCNE proteins studied by voltage-clamp fluorometry. *Biophysics and Physicobiology*, *16*, 121–126. https://doi.org/10.2142/biophysico.16.0_121

Nakajo, K., & Kubo, Y. (2015). KCNQ1 channel modulation by KCNE proteins via the voltage-sensing domain. *The Journal of Physiology*, *593*(Pt 12), 2617–2625. https://doi.org/10.1113/jphysiol.2014.287672

Nakatani, S., Ueda, H., Kawata, A., Sato, Y., Inomata, K., Mano, H., Wada, M., & Kobata, K. (2025). Calcium-sensing receptor induces the apoptosis of chondrocytes in cooperation with phosphate transporter. *FEBS Open Bio*, *16*(3), 496–502. https://doi.org/10.1002/2211-5463.70142

Nesti, L. J., Caterson, E. j., Li, W.-J., Chang, R., McCann, T. D., Hoek, J. B., & Tuan, R. S. (2007). TGF-β1 calcium signaling in osteoblasts. *Journal of Cellular Biochemistry*, *101*(2), 348–359. https://doi.org/10.1002/jcb.21180

Neybecker, P., Henrionnet, C., Pape, E., Grossin, L., Mainard, D., Galois, L., Loeuille, D., Gillet, P., & Pinzano, A. (2020). Respective stemness and chondrogenic potential of mesenchymal stem cells isolated from human bone marrow, synovial membrane, and synovial fluid. *Stem Cell Research & Therapy*, *11*(1), 316. https://doi.org/10.1186/s13287-020-01786-5

Ooi, A., Wong, A., Esau, L., Lemtiri-Chlieh, F., & Gehring, C. (2016). A Guide to Transient Expression of Membrane Proteins in HEK-293 Cells for Functional Characterization. *Frontiers in Physiology*, *7*, 300. https://doi.org/10.3389/fphys.2016.00300

Park, H.-M., Lee, J.-H., & Lee, Y.-J. (2020). Positive Association of Serum Alkaline Phosphatase Level with Severe Knee Osteoarthritis: A Nationwide Population-Based Study. *Diagnostics*, *10*(12), 1016. https://doi.org/10.3390/diagnostics10121016

Park, S., Bello, A., Arai, Y., Ahn, J., Kim, D., Cha, K.-Y., Baek, I., Park, H., & Lee, S.-H. (2021). Functional Duality of Chondrocyte Hypertrophy and Biomedical Application Trends in Osteoarthritis. *Pharmaceutics*, *13*(8), Article 8. https://doi.org/10.3390/pharmaceutics13081139

Peng, Y., Zhuang, Y., Zhang, Y., Zuo, J., & Ding, J. (2023). Dynamically adaptive scaffolds for cartilage tissue engineering. *MedComm – Biomaterials and Applications*, *2*(3), e49. https://doi.org/10.1002/mba2.49

Pérez-García, M. T., Cidad, P., & López-López, J. R. (2018). The secret life of ion channels: Kv1.3 potassium channels and proliferation. *American Journal of Physiology. Cell Physiology*, *314*(1), C27–C42. https://doi.org/10.1152/ajpcell.00136.2017

Pettipher, E. R., Higgs, G. A., & Henderson, B. (1986). Interleukin 1 induces leukocyte infiltration and cartilage proteoglycan degradation in the synovial joint. *Proceedings of the National Academy of Sciences*, *83*(22), 8749–8753. (world). https://doi.org/10.1073/pnas.83.22.8749

Phan, M. N., Leddy, H. A., Votta, B. J., Kumar, S., Levy, D. S., Lipshutz, D. B., Lee, S. H., Liedtke, W., & Guilak, F. (2009). Functional characterization of TRPV4 as an osmotically sensitive ion channel in porcine articular chondrocytes. *Arthritis & Rheumatism*, *60*(10), 3028–3037. https://doi.org/10.1002/art.24799

Physiology of cardiac conduction and contractility – McMaster Pathophysiology Review. (2013, October 7). https://www.pathophys.org/physiology-of-cardiac-conduction-and-contractility/

Piippo, K., Swan, H., Pasternack, M., Chapman, H., Paavonen, K., Viitasalo, M., Toivonen, L., & Kontula, K. (2001). A founder mutation of the potassium channel KCNQ1 in long QT syndrome: Implications for estimation of disease prevalence and molecular diagnostics. *Journal of the American College of Cardiology*, *37*(2), 562–568. https://doi.org/10.1016/S0735-1097(00)01124-4

Pingguan-Murphy, B., Lee, D. A., Bader, D. L., & Knight, M. M. (2005). Activation of chondrocytes calcium signalling by dynamic compression is independent of number of cycles. *Archives of Biochemistry and Biophysics*, *444*(1), 45–51. https://doi.org/10.1016/j.abb.2005.09.015

Pittenger, M. F., Mackay, A. M., Beck, S. C., Jaiswal, R. K., Douglas, R., Mosca, J. D., Moorman, M. A., Simonetti, D. W., Craig, S., & Marshak, D. R. (1999). Multilineage Potential of Adult Human Mesenchymal Stem Cells. *Science*, *284*(5411), 143–147. https://doi.org/10.1126/science.284.5411.143

Plata-Salamán, C. R., & ffrench-Mullen, J. M. (1993). Interleukin-2 modulates calcium currents in dissociated hippocampal CA1 neurons. *Neuroreport*, *4*(5), 579–581. https://doi.org/10.1097/00001756-199305000-00030

Ponce-Balbuena, D., & Deschênes, I. (2021). Long QT syndrome—Bench to bedside. *Heart Rhythm O2*, *2*(1), 89–106. https://doi.org/10.1016/j.hroo.2021.01.006

Priori, S. G., Blomström-Lundqvist, C., Mazzanti, A., Blom, N., Borggrefe, M., Camm, J., Elliott, P. M., Fitzsimons, D., Hatala, R., Hindricks, G.,

Kirchhof, P., Kjeldsen, K., Kuck, K.-H., Hernandez-Madrid, A., Nikolaou, N., Norekvål, T. M., Spaulding, C., Van Veldhuisen, D. J., & ESC Scientific Document Group. (2015). 2015 ESC Guidelines for the management of patients with ventricular arrhythmias and the prevention of sudden cardiac death: The Task Force for the Management of Patients with Ventricular Arrhythmias and the Prevention of Sudden Cardiac Death of the European Society of Cardiology (ESC)Endorsed by: Association for European Paediatric and Congenital Cardiology (AEPC). *European Heart Journal*, *36*(41), 2793–2867. https://doi.org/10.1093/eurheartj/ehv316

Pritchard, S., & Guilak, F. (2006). Effects of interleukin-1 on calcium signaling and the increase of filamentous actin in isolated and in situ articular chondrocytes. *Arthritis & Rheumatism*, *54*(7), 2164–2174. https://doi.org/10.1002/art.21941

Qi, X., Shao, M., Peng, H., Bi, Z., Su, Z., & Li, H. (2010). In vitro differentiation of bone marrow stromal cells into neurons and glial cells and differential protein expression in a two-compartment bone marrow stromal cell/neuron co-culture system. *Journal of Clinical Neuroscience*, *17*(7), 908–913. https://doi.org/10.1016/j.jocn.2009.10.013

Ramesh, S., Wildey, G. M., & Howe, P. H. (2009). Transforming growth factor β (TGFβ)-induced apoptosis. *Cell Cycle (Georgetown, Tex.)*, *8*(1), 11–17. https://doi.org/10.4161/cc.8.1.7291

Ranganathan, P., Agrawal, A., Bhushan, R., Chavalmane, A. K., Kalathur, R. K. R., Takahashi, T., & Kondaiah, P. (2007). Expression profiling of genes regulated by TGF-beta: Differential regulation in normal and tumour cells. *BMC Genomics*, *8*, 98. https://doi.org/10.1186/1471-2164-8-98

Remst, D. F. G., Blaney Davidson, E. N., Vitters, E. L., Bank, R. A., van den Berg, W. B., & Van der Kraan, P. M. (2014). TGF-ß induces Lysyl hydroxylase 2b in human synovial osteoarthritic fibroblasts through ALK5 signaling. *Cell and Tissue Research*, *355*(1), 163–171. https://doi.org/10.1007/s00441-013-1740-5

Ren, K., & Torres, R. (2009). Role of interleukin-1β during pain and inflammation. *Brain Research Reviews*, *60*(1), 57–64. https://doi.org/10.1016/j.brainresrev.2008.12.020

Rim, Y. A., Nam, Y., & Ju, J. H. (2020). The Role of Chondrocyte Hypertrophy and Senescence in Osteoarthritis Initiation and Progression. *International Journal of Molecular Sciences*, *21*(7), Article 7. https://doi.org/10.3390/ijms21072358

Rinné, S., Oertli, A., Nagel, C., Tomsits, P., Jenewein, T., Kääb, S., Kauferstein, S., Loewe, A., Beckmann, B. M., & Decher, N. (2023). Functional Characterization of a Spectrum of Novel Romano-Ward Syndrome KCNQ1 Variants. *International Journal of Molecular Sciences*, *24*(2), 1350. https://doi.org/10.3390/ijms24021350

Roberts, A. B., Anzano, M. A., Lamb, L. C., Smith, J. M., & Sporn, M. B. (1981). New class of transforming growth factors potentiated by epidermal growth factor: Isolation from non-neoplastic tissues. *Proceedings of the National Academy of Sciences of the United States of America*, *78*(9), 5339–5343. https://doi.org/10.1073/pnas.78.9.5339

Robson, M. C., Phillip, L. G., Cooper, D. M., Lyle, W. G., Robson, L. E., Odom, L., Hill, D. P., Hanham, A. F., & Ksander, G. A. (1995). Safety and effect of transforming growth factor-beta(2) for treatment of venous stasis ulcers. *Wound Repair and Regeneration: Official Publication of the Wound Healing Society [and] the European Tissue Repair Society*, *3*(2), 157–167. https://doi.org/10.1046/j.1524-475X.1995.30207.x

Roden, D. M., Thompson, K. A., Hoffman, B. F., & Woosley, R. L. (1986). Clinical features and basic mechanisms of quinidine-induced arrhythmias. *Journal of the American College of Cardiology*, *8*(1, Supplement 1), 73A-78A. https://doi.org/10.1016/S0735-1097(86)80032-8

Rosenkranz, S., Flesch, M., Amann, K., Haeuseler, C., Kilter, H., Seeland, U., Schlüter, K.-D., & Böhm, M. (2002). Alterations of β-adrenergic signaling and cardiac hypertrophy in transgenic mice overexpressing TGF-β1. *American Journal of Physiology-Heart and Circulatory Physiology*, *283*(3), H1253–H1262. https://doi.org/10.1152/ajpheart.00578.2001

Rudzitis, C. N., Lakk, M., Singh, A., Redmon, S. N., Kirdajová, D., Tseng, Y.-T., De Ieso, M. L., Stamer, W. D., Herberg, S., & Krizaj, D. (2025). TRPV4 activation by TGFβ2 enhances cellular contractility and drives ocular hypertension. *eLife*, *14*, RP104894. https://doi.org/10.7554/eLife.104894

Ruiz, M., Maumus, M., Fonteneau, G., Pers, Y.-M., Ferreira, R., Dagneaux, L., Delfour, C., Houard, X., Berenbaum, F., Rannou, F., Jorgensen, C., & Noël, D. (2019). TGFβi is involved in the chondrogenic differentiation of mesenchymal stem cells and is dysregulated in osteoarthritis. *Osteoarthritis and Cartilage*, *27*(3), 493–503. https://doi.org/10.1016/j.joca.2018.11.005

Saitta, B., Elphingstone, J., Limfat, S., Shkhyan, R., & Evseenko, D. (2019). CaMKII Inhibition in Human Primary and Pluripotent Stem Cell-Derived Chondrocytes Modulates effects of TGFβ and BMP Through SMAD Signaling. *Osteoarthritis and Cartilage*, *27*(1), 158–171. https://doi.org/10.1016/j.joca.2018.08.017

Sanguinetti, M. C., Curran, M. E., Zou, A., Shen, J., Spector, P. S., Atkinson, D. L., & Keating, M. T. (1996). Coassembly of K(V)LQT1 and minK (IsK) proteins to form cardiac I(Ks) potassium channel. *Nature*, *384*(6604), 80–83. https://doi.org/10.1038/384080a0

Santana, L. F., Cheng, E. P., & Lederer, W. J. (2010). How does the shape of the cardiac action potential control calcium signaling and contraction in

the heart? *Journal of Molecular and Cellular Cardiology*, *49*(6), 901–903. https://doi.org/10.1016/j.yjmcc.2010.09.005
Schroeder, B. C., Waldegger, S., Fehr, S., Bleich, M., Warth, R., Greger, R., & Jentsch, T. J. (2000). A constitutively open potassium channel formed by KCNQ1 and KCNE3. *Nature*, *403*(6766), 196–199. https://doi.org/10.1038/35003200
Schwartz, P. J., Moreno, C., Kotta, M.-C., Pedrazzini, M., Crotti, L., Dagradi, F., Castelletti, S., Haugaa, K. H., Denjoy, I., Shkolnikova, M. A., Brink, P. A., Heradien, M. J., Seyen, S. R. M., Spätjens, R. L. H. M. G., Spazzolini, C., & Volders, P. G. A. (2021). Mutation location and IKs regulation in the arrhythmic risk of long QT syndrome type 1: The importance of the KCNQ1 S6 region. *European Heart Journal*, *42*(46), 4743–4755. https://doi.org/10.1093/eurheartj/ehab582
Shakibaei, M., Schulze-Tanzil, G., John, T., & Mobasheri, A. (2005). Curcumin protects human chondrocytes from IL-l1beta-induced inhibition of collagen type II and beta1-integrin expression and activation of caspase-3: An immunomorphological study. *Annals of Anatomy = Anatomischer Anzeiger: Official Organ of the Anatomische Gesellschaft*, *187*(5–6), 487–497. https://doi.org/10.1016/j.aanat.2005.06.007
Shao, Y., Alicknavitch, M., & Farach-Carson, M. C. (2005). Expression of voltage sensitive calcium channel (VSCC) L-type Cav1.2 (alpha1C) and T-type Cav3.2 (alpha1H) subunits during mouse bone development. *Developmental Dynamics: An Official Publication of the American Association of Anatomists*, *234*(1), 54–62. https://doi.org/10.1002/dvdy.20517
Shelest, A., Alaburda, A., Vaiciuleviciute, R., Uzieliene, I., Bialaglovyte, P., & Bernotiene, E. (2025). The Effect of TGF-β3 and IL-1β on L-Type Voltage-Operated Calcium Channels and Calcium Ion Homeostasis in Osteoarthritic Chondrocytes and Human Bone Marrow-Derived Mesenchymal Stem Cells During Chondrogenesis. *Pharmaceutics*, *17*(3), 343. https://doi.org/10.3390/pharmaceutics17030343
Shen, X., Hu, L., Li, Z., Wang, L., Pang, X., Wen, C.-Y., & Tang, B. (2021). Extracellular Calcium Ion Concentration Regulates Chondrocyte Elastic Modulus and Adhesion Behavior. *International Journal of Molecular Sciences*, *22*(18), 10034. https://doi.org/10.3390/ijms221810034
Shi, S., Wu, X., Wang, X., Hao, W., Miao, H., Zhen, L., & Nie, S. (2016). Differentiation of Bone Marrow Mesenchymal Stem Cells to Cardiomyocyte-Like Cells Is Regulated by the Combined Low Dose Treatment of Transforming Growth Factor-β1 and 5-Azacytidine. *Stem Cells International*, *2016*, 3816256. https://doi.org/10.1155/2016/3816256
Simsa-Maziel, S., & Monsonego-Ornan, E. (2012). Interleukin-1β Promotes Proliferation and Inhibits Differentiation of Chondrocytes through a Mechanism Involving Down-Regulation of FGFR-3 and p21. *Endocrinology*, *153*(5), 2296–2310. https://doi.org/10.1210/en.2011-1756

Solchaga, L. A., Penick, K. J., & Welter, J. F. (2011). Chondrogenic Differentiation of Bone Marrow-Derived Mesenchymal Stem Cells: Tips and Tricks. *Methods in Molecular Biology (Clifton, N.J.)*, *698*, 253–278. https://doi.org/10.1007/978-1-60761-999-4_20

Sophia Fox, A. J., Bedi, A., & Rodeo, S. A. (2009). The Basic Science of Articular Cartilage. *Sports Health*, *1*(6), 461–468. https://doi.org/10.1177/1941738109350438

Sorensen, D. W., & van Berlo, J. H. (2020). The Role of TGF - β Signaling in Cardiomyocyte Proliferation. *Current Heart Failure Reports*, *17*(5), 225–233. https://doi.org/10.1007/s11897-020-00470-2

Striessnig, J., Pinggera, A., Kaur, G., Bock, G., & Tuluc, P. (2014). L-type Ca2+ channels in heart and brain. *Wiley Interdisciplinary Reviews. Membrane Transport and Signaling*, *3*(2), 15–38. https://doi.org/10.1002/wmts.102

Surges, R., Taggart, P., Sander, J. W., & Walker, M. C. (2010). Too long or too short? New insights into abnormal cardiac repolarization in people with chronic epilepsy and its potential role in sudden unexpected death. *Epilepsia*, *51*(5), 738–744. https://doi.org/10.1111/j.1528-1167.2010.02571.x

Takamatsu, A., Ohkawara, B., Ito, M., Masuda, A., Sakai, T., Ishiguro, N., & Ohno, K. (2014). Verapamil protects against cartilage degradation in osteoarthritis by inhibiting Wnt/β-catenin signaling. *PloS One*, *9*(3), e92699. https://doi.org/10.1371/journal.pone.0092699

Tester, D. J., & Ackerman, M. J. (2014). GENETICS OF LONG QT SYNDROME. *Methodist DeBakey Cardiovascular Journal*, *10*(1), 29–33. https://doi.org/10.14797/mdcj-10-1-29

Tester, D. J., Will, M. L., Haglund, C. M., & Ackerman, M. J. (2005). Compendium of cardiac channel mutations in 541 consecutive unrelated patients referred for long QT syndrome genetic testing. *Heart Rhythm*, *2*(5), 507–517. https://doi.org/10.1016/j.hrthm.2005.01.020

Thielen, N. G. M., Neefjes, M., Vitters, E. L., van Beuningen, H. M., Blom, A. B., Koenders, M. I., van Lent, P. L. E. M., van de Loo, F. A. J., Blaney Davidson, E. N., van Caam, A. P. M., & Van der Kraan, P. M. (2022). Identification of Transcription Factors Responsible for a Transforming Growth Factor-β-Driven Hypertrophy-like Phenotype in Human Osteoarthritic Chondrocytes. *Cells*, *11*(7), Article 7. https://doi.org/10.3390/cells11071232

Thielen, N. G. M., Van der Kraan, P. M., & van Caam, A. P. M. (2019). TGFβ/BMP Signaling Pathway in Cartilage Homeostasis. *Cells*, *8*(9), Article 9. https://doi.org/10.3390/cells8090969

Thielen, N., Neefjes, M., Wiegertjes, R., van den Akker, G., Vitters, E., van Beuningen, H., Blaney Davidson, E., Koenders, M., van Lent, P., van de Loo, F., van Caam, A., & V

an der Kraan, P. (2021). Osteoarthritis-Related Inflammation Blocks TGF-β's Protective Effect on Chondrocyte Hypertrophy via

(de)Phosphorylation of the SMAD2/3 Linker Region. *International Journal of Molecular Sciences*, *22*(15), 8124. https://doi.org/10.3390/ijms22158124

Thomas, P., & Smart, T. G. (2005). HEK293 cell line: A vehicle for the expression of recombinant proteins. *Journal of Pharmacological and Toxicological Methods*, *51*(3), 187–200. https://doi.org/10.1016/j.vascn.2004.08.014

Thompson, B., & Satin, L. S. (2021). Beta-Cell Ion Channels and Their Role in Regulating Insulin Secretion. *Comprehensive Physiology*, *11*(4), 1–21. https://doi.org/10.1002/cphy.c210004

Thorpe, S. D., Buckley, C. T., Vinardell, T., O'Brien, F. J., Campbell, V. A., & Kelly, D. J. (2010). The Response of Bone Marrow-Derived Mesenchymal Stem Cells to Dynamic Compression Following TGF-β3 Induced Chondrogenic Differentiation. *Annals of Biomedical Engineering*, *38*(9), 2896–2909. https://doi.org/10.1007/s10439-010-0059-6

Timofeeva, Y., & Volynski, K. (2015). Calmodulin as a major calcium buffer shaping vesicular release and short-term synaptic plasticity: Facilitation through buffer dislocation. *Frontiers in Cellular Neuroscience*, *9*. https://doi.org/10.3389/fncel.2015.00239

Tinel, N. (2000). KCNE2 confers background current characteristics to the cardiac KCNQ1 potassium channel. *The EMBO Journal*, *19*(23), 6326–6330. https://doi.org/10.1093/emboj/19.23.6326

Tong, L., Yu, H., Huang, X., Shen, J., Xiao, G., Chen, L., Wang, H., Xing, L., & Chen, D. (2022). Current understanding of osteoarthritis pathogenesis and relevant new approaches. *Bone Research*, *10*, 60. https://doi.org/10.1038/s41413-022-00226-9

Tristani-Firouzi, M., Chen, J., Mitcheson, J. S., & Sanguinetti, M. C. (2001). Molecular biology of K+ channels and their role in cardiac arrhythmias1. *The American Journal of Medicine*, *110*(1), 50–59. https://doi.org/10.1016/S0002-9343(00)00623-9

Tsuji, W., Rubin, J. P., & Marra, K. G. (2014). Adipose-derived stem cells: Implications in tissue regeneration. *World Journal of Stem Cells*, *6*(3), 312–321. https://doi.org/10.4252/wjsc.v6.i3.312

Uzieliene, I., Bagdonas, E., Hoshi, K., Sakamoto, T., Hikita, A., Tachtamisevaite, Z., Rakauskiene, G., Kvederas, G., Mobasheri, A., & Bernotiene, E. (2021). Different phenotypes and chondrogenic responses of human menstrual blood and bone marrow mesenchymal stem cells to activin A and TGF-β3. *Stem Cell Research & Therapy*, *12*, 251. https://doi.org/10.1186/s13287-021-02286-w

Uzieliene, I., Bernotas, P., Mobasheri, A., & Bernotiene, E. (2018). The Role of Physical Stimuli on Calcium Channels in Chondrogenic Differentiation of Mesenchymal Stem Cells. *International Journal of Molecular Sciences*, *19*(10), 2998. https://doi.org/10.3390/ijms19102998

Uzieliene, I., Bernotiene, E., Rakauskiene, G., Denkovskij, J., Bagdonas, E., Mackiewicz, Z., Porvaneckas, N., Kvederas, G., & Mobasheri, A. (2019). The Antihypertensive Drug Nifedipine Modulates the Metabolism of Chondrocytes and Human Bone Marrow-Derived Mesenchymal Stem Cells. *Frontiers in Endocrinology*, *10*, 756. https://doi.org/10.3389/fendo.2019.00756

Uzieliene, I., Bialaglovyte, P., Miksiunas, R., Lebedis, I., Pachaleva, J., Vaiciuleviciute, R., Ramanaviciene, A., Kvederas, G., & Bernotiene, E. (2023). Menstrual Blood-Derived Stem Cell Paracrine Factors Possess Stimulatory Effects on Chondrogenesis In Vitro and Diminish the Degradation of Articular Cartilage during Osteoarthritis. *Bioengineering*, *10*(9), Article 9. https://doi.org/10.3390/bioengineering10091001

Uzieliene, I., Bironaite, D., Bagdonas, E., Pachaleva, J., Sobolev, A., Tsai, W.-B., Kvederas, G., & Bernotiene, E. (2023). The Effects of Mechanical Load on Chondrogenic Responses of Bone Marrow Mesenchymal Stem Cells and Chondrocytes Encapsulated in Chondroitin Sulfate-Based Hydrogel. *International Journal of Molecular Sciences*, *24*(3), Article 3. https://doi.org/10.3390/ijms24032915

Uzieliene, I., Bironaite, D., Miksiunas, R., Bagdonas, E., Vaiciuleviciute, R., Mobasheri, A., & Bernotiene, E. (2023). The Effect of CaV1.2 Inhibitor Nifedipine on Chondrogenic Differentiation of Human Bone Marrow or Menstrual Blood-Derived Mesenchymal Stem Cells and Chondrocytes. *International Journal of Molecular Sciences*, *24*(7), 6730. https://doi.org/10.3390/ijms24076730

Uzieliene, I., Popov, A., Lisyte, V., Kugaudaite, G., Bialaglovyte, P., Vaiciuleviciute, R., Kvederas, G., Bernotiene, E., & Ramanaviciene, A. (2023). Stimulation of Chondrocyte and Bone Marrow Mesenchymal Stem Cell Chondrogenic Response by Polypyrrole and Polypyrrole/Gold Nanoparticles. *Polymers*, *15*(11), 2571. https://doi.org/10.3390/polym15112571

Van der Kraan, P. M., & van den Berg, W. B. (2012). Chondrocyte hypertrophy and osteoarthritis: Role in initiation and progression of cartilage degeneration? *Osteoarthritis and Cartilage*, *20*(3), 223–232. https://doi.org/10.1016/j.joca.2011.12.003

Varró, A., Tomek, J., Nagy, N., Virág, L., Passini, E., Rodriguez, B., & Baczkó, I. (2021). Cardiac transmembrane ion channels and action potentials: Cellular physiology and arrhythmogenic behavior. *Physiological Reviews*, *101*(3), 1083–1176. https://doi.org/10.1152/physrev.00024.2019

Vidal, M. A., Robinson, S. O., Lopez, M. J., Paulsen, D. B., Borkhsenious, O., Johnson, J. R., Moore, R. M., & Gimble, J. M. (2008). Comparison of chondrogenic potential in equine mesenchymal stromal cells derived from adipose tissue and bone marrow. *Veterinary Surgery: VS*, *37*(8), 713–724. https://doi.org/10.1111/j.1532-950X.2008.00462.x

Viskin, S. (2009). The QT interval: Too long, too short or just right. *Heart Rhythm*, *6*(5), 711–715. https://doi.org/10.1016/j.hrthm.2009.02.044

Wang, H.-S., Hung, S.-C., Peng, S.-T., Huang, C.-C., Wei, H.-M., Guo, Y.-J., Fu, Y.-S., Lai, M.-C., & Chen, C.-C. (2004). Mesenchymal stem cells in the Wharton's jelly of the human umbilical cord. *Stem Cells (Dayton, Ohio)*, *22*(7), 1330–1337. https://doi.org/10.1634/stemcells.2004-0013

Wang, L., Wada, Y., Ballan, N., Schmeckpeper, J., Huang, J., Rau, C. D., Wang, Y., Gepstein, L., & Knollmann, B. C. (2021). Triiodothyronine and dexamethasone alter potassium channel expression and promote electrophysiological maturation of human-induced pluripotent stem cell-derived cardiomyocytes. *Journal of Molecular and Cellular Cardiology*, *161*, 130–138. https://doi.org/10.1016/j.yjmcc.2021.08.005

Wang, M.-K., Sun, H.-Q., Xiang, Y.-C., Jiang, F., Su, Y.-P., & Zou, Z.-M. (2012). Different roles of TGF-β in the multi-lineage differentiation of stem cells. *World Journal of Stem Cells*, *4*(5), 28–34. https://doi.org/10.4252/wjsc.v4.i5.28

Wang, X., Fu, S., Wang, Y., Yu, P., Hu, J., Gu, W., Xu, X.-M., & Lu, P. (2007). Interleukin-1beta mediates proliferation and differentiation of multipotent neural precursor cells through the activation of SAPK/JNK pathway. *Molecular and Cellular Neurosciences*, *36*(3), 343–354. https://doi.org/10.1016/j.mcn.2007.07.005

Wee, A.-S., Lim, C.-K., Tan, S.-L., Ahmad, T. S., & Kamarul, T. (2022). TGF-β1 and -β3 for Mesenchymal Stem Cells Chondrogenic Differentiation on Poly (Vinyl Alcohol)-Chitosan-Poly (Ethylene Glycol) Scaffold. *Tissue Engineering Part C: Methods*, *28*(10), 501–510. https://doi.org/10.1089/ten.tec.2022.0112

Wehling, N., Palmer, G. D., Pilapil, C., Liu, F., Wells, J. W., Müller, P. E., Evans, C. H., & Porter, R. M. (2009). Interleukin-1 and tumor necrosis factor-α inhibit chondrogenesis by human mesenchymal stem cells through NF-κB dependent pathways. *Arthritis and Rheumatism*, *60*(3), 801–812. https://doi.org/10.1002/art.24352

Wicks, S. J., Lui, S., Abdel-Wahab, N., Mason, R. M., & Chantry, A. (2000). Inactivation of Smad-Transforming Growth Factor β Signaling by Ca2+-Calmodulin-Dependent Protein Kinase II. *Molecular and Cellular Biology*, *20*(21), 8103–8111.

Wrobel, E., Tapken, D., & Seebohm, G. (2012). The KCNE Tango – How KCNE1 Interacts with Kv7.1. *Frontiers in Pharmacology*, *3*. https://doi.org/10.3389/fphar.2012.00142

Wu, J., Ding, W.-G., & Horie, M. (2016). Molecular pathogenesis of long QT syndrome type 1. *Journal of Arrhythmia*, *32*(5), 381–388. https://doi.org/10.1016/j.joa.2015.12.006

Wu, M. Y., & Hill, C. S. (2009). Tgf-beta superfamily signaling in embryonic development and homeostasis. *Developmental Cell*, *16*(3), 329–343. https://doi.org/10.1016/j.devcel.2009.02.012

Wu, Q., & Chen, Q. (2000). Mechanoregulation of Chondrocyte Proliferation, Maturation, and Hypertrophy: Ion-Channel Dependent Transduction of Matrix Deformation Signals. *Experimental Cell Research*, *256*(2), 383–391. https://doi.org/10.1006/excr.2000.4847

Wu, X., Perez, M. E., Noskov, S. Y., & Larsson, H. P. (2021). A general mechanism of KCNE1 modulation of KCNQ1 channels involving non-canonical VSD-PD coupling. *Communications Biology*, *4*(1), 887. https://doi.org/10.1038/s42003-021-02418-1

Wuttisiriboon, K., Tippayawat, P., Daduang, J., & Limpaiboon, T. (2023). Ca2+/Calmodulin-dependent Protein Kinase II Inhibitor KN-93 Enhances Chondrogenesis of Bone Marrow Mesenchymal Stem Cells and Delays Chondrogenic Hypertrophy. *In Vivo (Athens, Greece)*, *37*(2), 667–678. https://doi.org/10.21873/invivo.13127

Xia, P., Wang, X., Qu, Y., Lin, Q., Cheng, K., Gao, M., Ren, S., Zhang, T., & Li, X. (2017). TGF-β1-induced chondrogenesis of bone marrow mesenchymal stem cells is promoted by low-intensity pulsed ultrasound through the integrin-mTOR signaling pathway. *Stem Cell Research & Therapy*, *8*(1), 281. https://doi.org/10.1186/s13287-017-0733-9

Xu, F., Liu, C., Zhou, D., & Zhang, L. (2016). TGF-β/SMAD Pathway and Its Regulation in Hepatic Fibrosis. *Journal of Histochemistry and Cytochemistry*, *64*(3), 157–167. https://doi.org/10.1369/0022155415627681

Xu, H., & Van Remmen, H. (2021). The SarcoEndoplasmic Reticulum Calcium ATPase (SERCA) pump: A potential target for intervention in aging and skeletal muscle pathologies. *Skeletal Muscle*, *11*(1), 25. https://doi.org/10.1186/s13395-021-00280-7

Xu, W., & Lipscombe, D. (2001). Neuronal CaV1.3α1 L-Type Channels Activate at Relatively Hyperpolarized Membrane Potentials and Are Incompletely Inhibited by Dihydropyridines. *The Journal of Neuroscience*, *21*(16), 5944–5951. https://doi.org/10.1523/JNEUROSCI.21-16-05944.2001

Xue, J., Zeng, W., Han, Y., John, S., Ottolia, M., & Jiang, Y. (2023). Structural mechanisms of the human cardiac sodium-calcium exchanger NCX1. *Nature Communications*, *14*(1), 6181. https://doi.org/10.1038/s41467-023-41885-4

Yamagata, K., Nakayamada, S., & Tanaka, Y. (2018). Use of mesenchymal stem cells seeded on the scaffold in articular cartilage repair. *Inflammation and Regeneration*, *38*, 4. https://doi.org/10.1186/s41232-018-0061-1

Yang, X., Chen, L., Xu, X., Li, C., Huang, C., & Deng, C.-X. (2001). TGF-β/Smad3 Signals Repress Chondrocyte Hypertrophic Differentiation and Are Required for Maintaining Articular Cartilage. *The Journal of Cell Biology*, *153*(1), 35–46.

Yang, Z., Zou, Y., Guo, X. M., Tan, H. S., Denslin, V., Yeow, C. H., Ren, X. F., Liu, T. M., Hui, J. H., & Lee, E. H. (2012). Temporal Activation of

β-Catenin Signaling in the Chondrogenic Process of Mesenchymal Stem Cells Affects the Phenotype of the Cartilage Generated. *Stem Cells and Development*, *21*(11), 1966–1976. https://doi.org/10.1089/scd.2011.0376

Yao, J., Long, H., Zhao, J., Zhong, G., & Li, J. (2020). Nifedipine inhibits oxidative stress and ameliorates osteoarthritis by activating the nuclear factor erythroid-2-related factor 2 pathway. *Life Sciences*, *253*, 117292. https://doi.org/10.1016/j.lfs.2020.117292

Yin, S., Zhang, L., Ding, L., Huang, Z., Xu, B., Li, X., Wang, P., & Mao, J. (2018). Transient receptor potential ankyrin 1 (trpa1) mediates il-1β-induced apoptosis in rat chondrocytes via calcium overload and mitochondrial dysfunction. *Journal of Inflammation*, *15*(1), 27. https://doi.org/10.1186/s12950-018-0204-9

Yoo, S.-A., Park, B.-H., Yoon, H.-J., Lee, J.-Y., Song, J.-H., Kim, H. A., Cho, C.-S., & Kim, W.-U. (2007). Calcineurin modulates the catabolic and anabolic activity of chondrocytes and participates in the progression of experimental osteoarthritis. *Arthritis & Rheumatism*, *56*(7), 2299–2311. https://doi.org/10.1002/art.22731

Yoon, Y., Hwang, S., Tuj Saima, F., Young Kim, M., Koo Baik, S., & Woo Eom, Y. (2023). AKT regulates IL-1β-induced proliferation and activation of hepatic stellate cells. *BIOCELL*, *47*(3), 669–676. https://doi.org/10.32604/biocell.2023.025365

Zhang, H., Gao, J., Tang, Y., Jin, T., & Tao, J. (2023). Inflammasomes cross-talk with lymphocytes to connect the innate and adaptive immune response. *Journal of Advanced Research*, *54*, 181–193. https://doi.org/10.1016/j.jare.2023.01.012

Zhang, X., Zheng, H., Zhu, H.-Y., Hu, S., Wang, S., Jiang, X.-H., & Xu, G.-Y. (2015). Acute effects of TGFβ1 on neuronal excitability and involvement in the pain of rats with chronic pancreatitis. *Journal of Neurogastroenterology and Motility*, *22*. https://doi.org/10.5056/jnm15127

Zhao, Y., Xu, J., Gong, J., & Qian, L. (2009). L-type calcium channel current up-regulation by chronic stress is associated with increased α1c subunit expression in rat ventricular myocytes. *Cell Stress & Chaperones*, *14*(1), 33–41. https://doi.org/10.1007/s12192-008-0052-2

Zheng, Q., Zhou, G., Morello, R., Chen, Y., Garcia-Rojas, X., & Lee, B. (2003). Type X collagen gene regulation by Runx2 contributes directly to its hypertrophic chondrocyte–specific expression in vivo. *The Journal of Cell Biology*, *162*(5), 833–842. https://doi.org/10.1083/jcb.200211089

Zhou, C., Qi, C., Zhao, J., Wang, F., Zhang, W., Li, C., Jing, J., Kang, X., & Chai, Z. (2011). Interleukin-1β Inhibits Voltage-Gated Sodium Currents in a Time- and Dose-Dependent Manner in Cortical Neurons. *Neurochemical Research*, *36*(6), 1116–1123. https://doi.org/10.1007/s11064-011-0456-8

Zuk, P. A., Zhu, M., Ashjian, P., De Ugarte, D. A., Huang, J. I., Mizuno, H., Alfonso, Z. C., Fraser, J. K., Benhaim, P., & Hedrick, M. H. (2002).

Human adipose tissue is a source of multipotent stem cells. *Molecular Biology of the Cell*, *13*(12), 4279–4295. https://doi.org/10.1091/mbc.e02-02-0105

LIST OF PUBLICATIONS

Publications on the topic of the thesis:

1. Shelest, A., Alaburda, A., Vaiciuleviciute, R., Uzieliene, I., Bialaglovyte, P., & Bernotiene, E. (2025). The Effect of TGF-β3 and IL-1β on L-Type Voltage-Operated Calcium Channels and Calcium Ion Homeostasis in Osteoarthritic Chondrocytes and Human Bone Marrow-Derived Mesenchymal Stem Cells During Chondrogenesis. Pharmaceutics, 17(3), 343, 2025. https://doi.org/10.3390/pharmaceutics17030343
2. Bileisiene, N., Shelest, A., Petraityte, G., Alaburda, A., Sasnauskiene, A., Jasinevicius, A., Kairys, V., Dapkunas, J., Mikstiene, V., Zitkute, V., Maldziene, Z., Barysiene, J., & Preiksaitiene, E. Long QT syndrome type 1: Clinical and functional characterization of *KCNQ1* variant c.1111G > C. BMC Cardiovascular Disorders, 25(1), 841, 2025. https://doi.org/10.1186/s12872-025-05335-x

Conferences on the thesis topic:

- (Presentation) Anastasiia Shelest, Aidas Alaburda. Functionality of L-type calcium channels in differentiating mesenchymal stem cells. VI International scientific conference for students and young scientists "Current problems of biology and ecology". October, 21-22th, 2020, Vinnitsia, Ukraine.
- (Poster) Anastasiia Shelest, Raminta Vaičiulevičiūtė, Eiva Bernotienė, Aidas Alaburda. Functionality of L-type Ca2+ channels in human mesenchymal stem cells during chondrogenic differentiation. The COINS 2022. February 28th, 2022, Vilnius, Lithuania.
- (Presentation) Anastasiia Shelest, Aidas Alaburda. Investigation of functional activity of Ca^{2+} channel in human mesenchymal stem cells during chondrogenic differentiation. 15th Jonas Pranas Aleksa International Scientific Interdisciplinary Conference “Development Of The State Role In The XX Century: National And International Context”. September 23rd, 2022, Šiauliai, Lithuania.
- (Poster) Anastasiia Shelest, Raminta Vaičiulevičiūtė, Eiva Bernotienė, Aidas Alaburda. Functional activity of L-type Ca2+ channels in bone marrow-derived human mesenchymal stem cells during chondrogenic differentiation and in chondrocytes.

International 3rd Baltic Biophysics Conference. October 6-7th, 2022, Vilnius, Lithuania.

- (Presentation) Anastasiia Shelest, Andrius Jasinevičius, Aušra Sasnauskienė, Gunda Petraitytė, Aidas Alaburda. Impact of the p.Ala371Pro Mutation on the Function of the KCNQ1 Potassium Channel. The 19th All-Ukrainian Conference of Young Scientists of the Institute of Molecular Biology and Genetics of the NAS of Ukraine. May 20-21th, 2025, Kyiv, Ukraine.
- (Poster) Anastasiia Shelest, Gunda Petraityte, Ausra Sasnauskiene, Aidas Alaburda. Effect of the *KCNQ1* p.(Ala371Pro) variant on $Kv_{7.1}$ Channel Function. LSC scientific conference 2026. May 7–8th, 2026, Vilnius, Lithuania.

Other conferences:

- (Poster) Anastasiia Shelest, Raminta Vaičiulevičiūtė, Eiva Bernotienė, Aidas Alaburda. Maturity Assessment Of Human-Induced Pluripotent Stem Cells Derived Cardiomyocytes. The COINS 2023. April 24-26th, 2023, Vilnius, Lithuanian.

ACKNOWLEDGEMENTS

I would like to express my deepest gratitude to my supervisor, Aidas Alaburda, for his invaluable guidance, unwavering support, and endless patience throughout this journey. I am sincerely thankful for every discussion, every piece of advice, and every moment of understanding during both the challenging and rewarding stages of my PhD.

I am also deeply grateful to everyone who stood by me along this path – my colleagues, friends, and family – for their support, belief, and presence. Each of you contributed to this journey in your own way, whether through scientific collaboration, emotional support, or simply being there when it mattered most.

This achievement would not have been possible without all of you.

ABOUT THE AUTHOR

Anastasiia Shelest — Curriculum vitae

Contact information:

PhD student
Life Sciences Center
Vilnius University
Saulėtekio ave 7,
LT-10257
Vilnius, Lithuania

Phone:
+370 662 27 823
Email:
anastasiia.shelest@gmc.vu.lt,

Education:

- *PhD student in Biophysics*, Vilnius University, Lithuania — present
- *MSc Life Sciences*, Vytautas Magnus University, Lithuania — 2020
- *MSc Biology*, Vasyl' Stus Donetsk National University, Ukraine — 2019
- *BSc Biology*, Vasyl' Stus Donetsk National University, Ukraine — 2018

Work experience:

Junior researcher — 2021-2022
Centre for Innovative Medicine
*Biologist researche*r — 2024-2026
Vilnius University
Laboratory assistant
Vilnius University — 2025-present
Junior Researcher
Vilnius University — 2025-present

Participation in projects:

Electrophysiological recording, data acquisition and analysis
(project: LMT-DOT4 (Nr.DOTSUT-215 (09.3.3-LMT-K-712-01-0157)) — 2021-2022

SANTRAUKA

ĮVADAS

Joniniai kanalai yra esminiai ląstelinės signalizacijos komponentai ir atlieka kritinį vaidmenį reguliuojant ląstelių funkcijas įvairiuose ląstelių tipuose. Elektriškai aktyviose ląstelėse, tokiose kaip neuronai ir raumenų ląstelės, joniniai kanalai yra būtini elektrinių signalų generavimui (Kawai, 2024; Varró et al., 2021). Tačiau daugelis joninių kanalų taip pat yra ekspresuojami elektriškai neaktyviose ląstelėse, kur jie dalyvauja įvairiuose ląstelių signalizacijos procesuose ir prisideda prie homeostazės palaikymo, proliferacijos ir diferenciacijos reguliavimo, hormonų sekrecijos kontrolės bei ląstelės tūrio reguliavimo (Bijlenga et al., 2000; Jahn et al., 2021; Pérez-García et al., 2018; Thompson & Satin, 2021). Todėl tinkama joninių kanalų funkcija yra būtina fiziologinėms funkcijoms palaikyti tiek elektriškai aktyviose, tiek elektriškai neaktyviose ląstelėse.

Chondrocitai priskiriami ląstelėms, kurios nėra elektriškai aktyvios, tačiau šiose specializuotose ląstelėse jonų kanalų medijuojama signalizacija atlieka svarbų reguliacinį vaidmenį (Matta et al., 2015). Ca^{2+} signalizacija laikoma pagrindiniu chondrocitų biologinių funkcijų reguliatoriumi, įskaitant apoptozę (Nakatani et al., 2025), migraciją (Shen et al., 2021), proliferaciją (Mancilla et al., 2007) ir chondrogeninę diferenciaciją (Atsuta et al., 2019; Wu & Chen, 2000).

Viduląstelinio Ca^{2+} lygio (iCa^{2+}) pokyčiai laikomi vienais ankstyviausių chondrocitų ląstelinių atsakų į fizinius stimulus, įskaitant suspaudimą (Pingguan-Murphy et al., 2005), mechaninę apkrovą (Lv et al., 2017), skysčio tekėjimą (Degala et al., 2012), hidrostatinį slėgį (Browning et al., 2004) ir osmosinį stresą (W. Li et al., 2022). iCa^{2+} svyravimai veikia kaip viduląsteliniai antriniai signalai, aktyvinantys daugelį tolimesnių signalinių kelių kuriuose dalyvauja nuo Ca^{2+} priklausomi mediatoriai, įskaitant Ca^{2+}/kalmodulino priklausomą kinazę II (CaMKII) (Wei et al., 2018), kalcineuriną ir transkripcijos faktorių NFAT (Yoo et al., 2007), taip reguliuodami genų ekspresiją (Park et al., 2020).

iCa^{2+} reguliacija chondrocituose priklauso nuo Ca^{2+} patekimo per plazminėje membranoje esančius kanalus arba Ca^{2+} išsiskyrimo iš vidinių saugyklų (Mobasheri et al., 2019). Ankstesni tyrimai parodė didelę Ca^{2+} kanalų ekspresijos įvairovę chondrocituose, įskaitant įtampai jautrius Ca^{2+} kanalus (VGCC) (Shao et al., 2005), laikino receptoriaus potencialo (TRP)

kanalus (Gavenis et al., 2009; Phan et al., 2009) bei Ca^{2+} iš vidinių saugyklų valdomus Ca^{2+} kanalus (SOC) (Inayama et al., 2015).

Manoma, iCa^{2+} reguliacijai chondrocituose L tipo potencialo valdomi kalcio kanalai (L-VOCCs) vaidina svarbų vaidmenį. Šie kanalai buvo identifikuoti tiek besivystančiuose (Shao et al., 2005), tiek subrendusiuose chondrocituose (Atsuta et al., 2019; Matta et al., 2015b; Uzieliene, Bironaite, Miksiunas, et al., 2023). Nustatyta, kad L-VGCCs yra svarbūs chondrocitų proliferacijos ir augimo reguliatoriai, nes farmakologinis šių kanalų slopinimas reikšmingai sumažino proliferaciją (Uzieliene et al., 2019; Q. Wu & Chen, 2000) ir sutrikdė augimą (Mancilla et al., 2007). Be to, L-VGCCs prisideda prie biomechaninių savybių palaikymo, nes šių kanalų slopinimas sumažino sGAG sintezę mechaniškai stimuliuotuose chondrocituose (Mouw et al., 2007).

Žinoma, kad Ca^{2+} patekimas per L-VGCCs yra būtinas kremzlės formavimuisi, nes šių kanalų slopinimas mažina pagrindinių chondrogeninių žymenų, įskaitant *Sox9*, *Col2a1* ir *Agc*, ekspresiją, taip sutrikdydamas normalią kremzlės raidą (Atsuta et al., 2019). Tačiau yra ir prieštaringų rezultatų: kai kurie tyrimai rodo, kad L-VGCCs slopinimas didina chondrogeninių žymenų, tokių kaip *Col2a1* ir *Agc*, ekspresiją (Takamatsu et al., 2014; Uzieliene et al., 2019), kartu mažindamas su osteoartritu susijusių genų, įskaitant *AXIN2* ir *MMP3*, ekspresiją chondrocituose (Takamatsu et al., 2014; Yao et al., 2020).

Visi šie duomenys pabrėžia svarbų L-VGCCs vaidmenį chondrocitų funkcijos reguliavime, tačiau vis dar neaišku, ar stebėti efektai yra tiesioginis L-VGCCs slopinimo rezultatas, ar susiję su papildomais farmakologiniais inhibitorių poveikiais. Reikalingi tiesioginiai L-VGCC aktyvumo tyrimai siekiant išsiaiškinti jų vaidmenį kremzlės fiziologijoje ir patologijoje.

Osteoartrito (OA) metu chondrocitai susiduria su reikšmingu interleukino-1β (IL-1β) gamybos padidėjimu (Daheshia & Yao, 2008; Jenei-Lanzl et al., 2019). Padidėjęs IL-1β dar labiau sustiprina uždegiminius atsakus ir skatina azoto oksido (NO) bei matriksą ardančių fermentų, įskaitant MMP-1 ir MMP-3, sintezę chondrocituose (Yoo et al., 2007). Šie kataboliniai veiksniai skatina ekstraląstelinio matrikso degradaciją ir prisideda prie kremzlės irimo. Todėl IL-1β taip pat plačiai naudojamas OA eksperimentiniuose modeliuose. (Marrero-Berrios et al., 2024; Choi et al., 2013; Henderson & Pettipher, 1988; Pettipher et al., 1986; Kurata et al., 2026).

Nustatyta, kad IL-1β didina iCa^{2+} lygį kiaulių (Pritchard & Guilak, 2006) ir pelių (Kurata et al., 2026) chondrocituose. Pelių chondrocituose šis poveikis vyksta per L-VGCCs. Be to, IL-1β sukeltas Ca^{2+} patekimas per šiuos

kanalus gali sukelti pelių chondrocitų apoptozę, sutrikdydamas mitochondrijų funkciją (Kurata et al., 2026). Taip pat buvo parodyta, kad IL-1β reikšmingai padidina L-VGCCs ekspresiją galvijų chondrocituose (Lv et al., 2019). IL-1β taip pat reikšmingai padidina plazminėje membranoje lokalizuotų L-VGCCs ekspresiją pelių chondrocituose (Kurata et al., 2026). Tačiau kaip IL-1β veikia Ca^{2+} homeostazę žmogaus chondrocituose, vis dar nėra žinoma.

Iš kaulų čiulpų kilusios mezenchiminės kamieninės ląstelės (BM-MSCs) gali diferencijuotis į kelis ląstelių tipus, įskaitant chondrocitus, osteoblastus ir adipocitus (L. Hu et al., 2018; Mardones et al., 2020). In vitro transformuojantis augimo faktorius beta (TGF-β), ypač TGF-β3, dažnai naudojamas chondrogeninei diferenciacijai skatinti aktyvuojant kremzlei specifinių genų ekspresiją (Xia et al., 2017; Y. T. Lu et al., 2018; Uzieliene et al., 2019; Wee et al., 2022; Uzieliene, Bironaite, Miksiunas, et al., 2023). Todėl BM-MSCs, kultivuojamos su TGF-β3, dėl savo chondrogeninio potencialo yra plačiai naudojamos ląstelių pagrindu sukurtose OA gydymo strategijų modeliuose (Le et al., 2020; Xia et al., 2017; Lu et al., 2018; Uzieliene et al., 2019; Wee et al., 2022; Uzieliene et al., 2023).

TGF-β3 geba keisti iCa^{2+} dinamiką daugelyje ląstelių tipų per įvairius signalinius kelius, taip veikdamas ląstelių funkciją (Alevizopoulos et al., 1997; Cailotto et al., 2011; Ishiyama et al., 1996; Luo et al., 1997; McGowan et al., 2002; Mukherjee et al., 2012; Yin et al., 2018). Pavyzdžiui, fibroblastuose TGF-β sukelia iCa^{2+} padidėjimą skatindamas tiek Ca^{2+} patekimą į ląstelę, tiek Ca^{2+} išsiskyrimą iš endoplazminio tinklo (ER) (Alevizopoulos et al., 1997; Mukherjee et al., 2012).

TGF-β sukeltas iCa^{2+} padidėjimas gali priklausyti nuo Ca^{2+} patekimo per L-VGCCs, kaip parodyta insulinomos ląstelėse (Ishiyama et al., 1996; Lv et al., 2019b). Žiurkių chondrocituose TGF-β stimuliacija reikšmingai padidino iCa^{2+} per T- ir L-VGCCs (Cailotto et al., 2011). Taip pat parodyta, kad TGF-β3 didino L-VGCCs ekspresiją genų lygmenyje MenSCs, BM-MSCs ir chondrocituose (Uzieliene, Bironaite, Miksiunas, et al., 2023). Nepaisant to, tikslūs mechanizmai, kaip TGF-β veikia Ca^{2+} signalizaciją žmogaus BM-MSC chondrogenezės metu, išlieka neaiškūs. Šios žinių spragos užpildymas gali prisidėti prie pažangesnių regeneracinės medicinos strategijų kremzlės atkūrimui.

Išoriniai reguliaciniai poveikiai jonų kanalams dažnai yra laikini ir grįžtami, išnykstantys pašalinus išorinį stimulą (Plata-Salamán & ffrench-Mullen, 1993). Priešingai, jonų kanalų struktūros ir funkcijos pokyčiai, nulemti pokyčių genetiniame lygmenyje, paprastai turi ilgalaikį poveikį kanalų aktyvumui. Elektriškai aktyviuose audiniuose, tokiuose kaip širdis,

KCNQ1 koduoja potencialui jautrų kalio kanalą $Kv_{7.1}$, kuris lemia širdies I_{Ks} srovę, o genetinės mutacijos šiame gene gali sukeltisunkias patologines būkles. *KCNQ1* mutacijos gali tiek padidinti, tiek sumažinti jonines sroves (Brewer et al., 2025), kas gali sutrikdyti tiksliai subalansuotą normalią širdies elektrofiziologiją. Viena geriausiai apibūdintų klinikinių būklių, atsirandančių dėl tokios jonų kanalų disfunkcijos, yra ilgo QT sindromas (LQTS). Šiam širdies sutrikimui būdinga uždelsta miokardo repoliarizacija, QT intervalo pailgėjimas elektrokardiogramoje ir padidėjusi sinkopės bei staigios širdinės mirties rizika dėl polimorfinės skilvelinės tachikardijos, vadinamos Torsades de Pointes (Liang & Callans, 2017).

Patogeniniai *KCNQ1*, *KCNH2* ir *SCN5A* variantai yra dažniausios genetinės LQTS priežastys. Tarp nustatytų genetinių priežasčių su *KCNQ1* susijęs LQTS sudaro apie 45 % visų atvejų ir yra dažniausias genetinis šio sutrikimo pogrupis (Morgat et al., 2024). Neseniai keliuose nesusijusiuose Lietuvos šeimose buvo nustatytas retas *KCNQ1* variantas c.1111G>C [p.(Ala371Pro)]. Tačiau nežinoma, kaip šis patogeninis variantas keičia kanalo funkciją. Elektrofiziologinis joninių kanalų funkcijos pokyčių charakterizavimas yra vienas iš svarbiausių metodų nustatant DNR variantų patogeniškumą, nes jis leidžia tiesiogiai susieti genetinius pokyčius su jų funkciniu poveikiu kanalų aktyvumui ir klinikine reikšme.

Tyrimo tikslas ir uždaviniai

Šio tyrimo tikslas buvo įvertinti citokinų poveikį Ca^{2+} homeostazei ir L tipo potencialo valdomiems kalcio kanalams (L-VGCCs), bei nustatyti retojo *KCNQ1* varianto c.1111G>C [p.(Ala371Pro)] funkcinį poveikį $Kv_{7.1}$ kanalo biofizinėms savybėms.

Tyrimo uždaviniai:

• Įvertinti TGF-β3 ir IL-1β poveikį Ca^{2+} homeostazei žmogaus kaulų čiulpų kilmės mezenchiminėse kamieninėse ląstelėse (hBM-MSCs).
• Įvertinti TGF-β3 ir IL-1β poveikį Ca^{2+} homeostazei osteoartritiniuose chondrocituose.
• Išanalizuoti *KCNQ1* p.(Ala371Pro) varianto poveikį vėlyvajai repoliarizacijos kalio srovei (I_{Ks}).

Mokslinis naujumas

Šiame tyrime pirmą kartą:

• Tiesioginiais elektrofiziologiniais matavimais parodyta, kad TGF-β3 funkciškai padidina L-VGCCs aktyvumą hBM-MSCs.
• Parodyta, kad TGF-β3 didina iCa^{2+} osteoartritiniuose chondrocituose be L-VGCCs aktyvacijos.
• Parodyta, kad TGF-β3 sukeltas iCa^{2+} padidėjimas BM-MSCs ir osteoartritiniuose chondrocituose vyksta skirtingais mechanizmais.
• Tiesioginiais elektrofiziologiniais matavimais parodyta, kad *KCNQ1* p.(Ala371Pro) variantas lemia reikšmingą I_{Ks} sumažėjimą dėl sumažėjusio kanalo laidumo.

Praktinė reikšmė

• Įžvalgos apie citokinų priklausomą L-VGCCs reguliaciją BM-MSCs gali prisidėti prie chondrogeninės diferenciacijos protokolų optimizavimo kremzlės audinių inžinerijoje.
• Nustatyti ląstelių tipui specifiniai Ca^{2+} kanalų reguliacijos skirtumai gali padėti kurti tikslingesnes osteoartrito gydymo strategijas.
• Funkcinis *KCNQ1* p.(Ala371Pro) varianto įvertinimas susieja joninio kanalo funkcijos pokyčius su klinikiniais LQTS požymiais.

Disertacijos teiginiai

• TGF-β3 sukelia funkcinį L-VGCCs aktyvumo padidėjimą hBM-MSCs, dėl kurio padidėja Ca^{2+} įtekėjimas, tačiau osteoartritiniuose chondrocituose šis poveikis nepasireiškia.
• Chondrocituose TGF-β3 sukeltas viduląsteliniоCa^{2+} padidėjimas vyksta nepriklausomai nuo L-VGCCs aktyvacijos, kas rodo kitus Ca^{2+} patekimo kelius.
• IL-1β nepaveikia L-VGCCs aktyvumo nei hBM-MSCs, nei osteoartritiniuose chondrocituose.
• *KCNQ1* p.(Ala371Pro) variantas lemia LQTS dėl kanalo laidumo sumažėjimo.

Tyrimo struktūra

Disertaciją paremta dviejų tyrimų rezultatais, publikuotais dviejuose recenzuojamuose moksliniuose žurnaluose. Pirmajame tyrime buvo tirtas TGF-β3 ir IL-1β poveikis L-VGCCs bei Ca^{2+} homeostazei osteoartritiniuose chondrocituose ir hBM-MSCs chondrogenezės metu. Atsižvelgiant į žinomą Ca^{2+} signalizacijos vaidmenį chondrogenezėje ir osteoartrito patofiziologijoje, buvo iškelta hipotezė, kad TGF-β3 ir IL-1β sukelta L-VGCCs moduliacija prisideda prie iCa^{2+} homeostazės pokyčių ir taip reguliuoja chondrogeninius

bei uždegiminius atsakus. Antrajame tyrime buvo nagrinėjamos su LQTS susijusio *KCNQ1* c.1111G>C [p.(Ala371Pro)] varianto funkcinės pasekmės. Buvo iškelta hipotezė, kad šis patogeninis variantas pakeičia $Kv_{7.1}$ kanalo funkciją ir sutrikdo širdies elektrofiziologines savybes, taip didindamas aritmogeninę riziką.

METODAI

1.1 Joninių kanalų aktyvumo analizė naudojant „whole-cell patch-clamp“ metodą

Šiame tyrime joninių kanalų aktyvumui tiesiogiai įvertinti buvo naudojama „patch-clamp“ technika „whole-cell“ konfigūracijoje.

Ląstelės buvo išsėtos ant 12 mm dengiamųjų stiklelių, perkeltos į 33 mm Petri lėkštelę su tirpalu, optimizuotu $I_{Ca,L}$ arba I_{Ks} matavimams atitinkamai. Registruota ląsteles vizualizuojant Nikon FN-S2N mikroskopu. „Patch“ pipetės buvo formuojamos iš borosilikatinio stiklo kapiliarų naudojant elektrodų ištraukėją (Model P-1000; Sutter Instrument, JAV), užpildytų pipetės tirpalu jų varža siekė 2–8 MΩ.

„Whole-cell patch-clamp“ registracijos buvo atliekamos kambario temperatūroje (21 ± 1 °C). Pirmiausia buvo suformuojama „cell-attached“ konfigūracija, sukuriant didelės varžos („gigaseal“) kontaktą tarp pipetės ir ląstelės membranos, naudojant švelnų siurbimą (Pav. 1A). Vėliau „whole-cell“ konfigūracija buvo pasiekta papildomu siurbimu, suardant membranos fragmentą po pipetės galu (Pav. 1B).

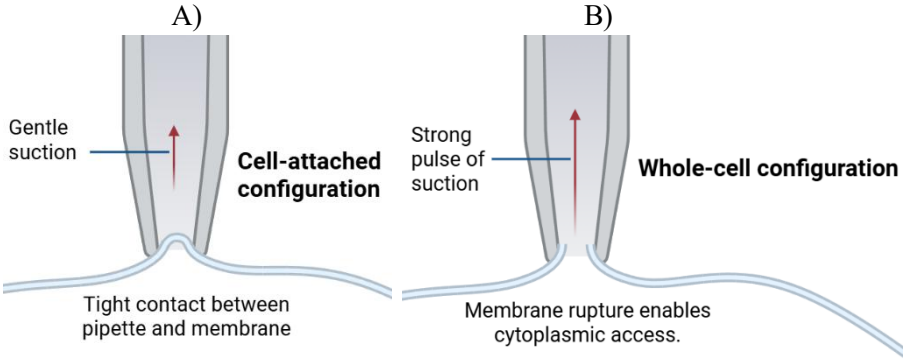

Pav. 1. Patch-clamp konfigūracijos.
A) „Cell-attached“ konfigūracija su „gigaseal“ formavimu.
B) „Whole-cell“ konfigūracija po membranos suardymo ir kontakto su citoplazma susidarymo. Paveikslas sukurtas naudojant BioRender.com (www.biorender.com, žiūrėta 2025 m. vasario 26 d.).

Registracijos buvo atliekamos naudojant viduląstelinės registracijos stiprintuvą Multiclamp 700B (Molecular Devices), valdomą pCLAMP 10.5 programinės įrangos.

$I_{Ca,L}$ arba I_{Ks} buvo registruojamos naudojant atitinkamus potencialo fiksavimo protokolus, derinant palaikymo potencialą ir depoliarizuojančius potencialo žingsnius. Nusistovėjusios būsenos srovė buvo matuojama

kiekvieno depoliarizuojančio žingsnio pabaigoje, kai srovė pasiekdavo stabilų lygį ir trumpalaikiai svyravimai buvo minimalūs (Gray & Santin, 2023). Šios vertės buvo naudojamos visos ląstelės srovės įvertinimui.

1.2 TGF-β3 ir IL-1β poveikis L-VGCCs ir Ca^{2+} homeostazei osteoartritinėse chondrocituose ir hBM-MSCs chondrogenezės metu

Tyrimas buvo atliktas bendradarbiaujant su Inovatyvios medicinos centru (IMC). Ši tyrimo dalis buvo dalinai finansuota pagal EU HORIZON-WIDERA-2021-ACCESS-03-01 projektą „Twinning for Promoting Excellence, Ability and Knowledge to develop novel approaches for targeting inflammatory and degenerative age-related joint diseases“ (Grant No. 101079489 – TWINFLAG).

hBM-MSCs ir pirminiai chondrocitai buvo gauti iš savanorių suaugusių donorų, kurie pateikė rašytinį informuotą sutikimą. Visos procedūros, susijusios su hBM-MSCs ir chondrocitais, buvo atliktos laikantis institucinės Bioetikos komiteto reglamentų pagal leidimą Nr. 158200-14-741-257, patvirtintą 2014 m. birželio 9 d.

1.2.1 hBM-MSCs ir chondrocitų izoliacija ir kultivavimas

Žmogaus audinių mėginiai buvo gauti iš Vilniaus universiteto ligoninės Santaros klinikų. Sąnarinės kremzlės mėginiai buvo paimti kaip audiniai, pašalinti artroskopinių operacijų metu iš 4 OA sergančių pacientų (amžius 64 ± 14 metų), neturinčių sisteminių, ūmių ar lėtinių gretutinių ligų.

Chondrocitai buvo izoliuoti ir kultivuoti pagal anksčiau aprašytus standartizuotus protokolus (Uzieliene et al., 2019). Trumpai, kremzlės mėginiai buvo plaunami PBS su 1% penicilino-streptomicino tirpalu (PS) (Gibco, Life Technologies, Waltham, MA, USA), susmulkinti į mažus gabalėlius ir inkubuoti mažo gliukozės kiekio (1 g/L) DMEM terpėje (Capricorn Scientific, Ebsdorfergrund, Germany) su 1% PS, 37 °C temperatūroje ir 5% CO2 aplinkoje. Po to mėginiai buvo nuplauti ir fermentiškai apdoroti: pirmiausia pronazės tirpalu1 valandą, po to II tipo kolagenazės tirpalu 10 mL/g audinio santykiu 4 valandas, abiem atvejais 37 °C temperatūroje ir 5% CO2 aplinkoje. Izoliuoti chondrocitai buvo kultivuojami visavertėje terpėje, sudarytoje iš mažo gliukozės kiekio DMEM terpės, 1% PS ir 10% galvijų vaisiaus serumo (FBS), 37 °C inkubatoriuje su 5% CO_2, keičiant terpę du kartus per savaitę.

hBM-MSCs buvo izoliuotos iš 3 OA sergančių donorų (amžius 52 ± 10 metų) pagal standartinius IMC protokolus po sąnario keitimo chirurginių procedūrų. hBM-MSCs buvo inkubuojamos tokiomis pačiomis sąlygomis

kaip chondrocitai, papildomai pridedant 1 ng/mL fibroblastų augimo faktoriaus 2 (Sigma Aldrich, Burlington, MA, USA), siekiant išlaikyti jų kamieninių ląstelių potencialą ir išvengti spontaninės diferenciacijos. Izoliuotos hBM-MSCs buvo kultivuojamos visavertėje terpėje37 °C inkubatoriuje su 5% CO2, keičiant terpę du kartus per savaitę.

Visiems eksperimentams buvo naudojamos 2–3 pasažų (P2–P3) hBM-MSCs ir chondrocitai.

1.2.2 Chondrogeninė diferenciacija

Proliferacijos terpę sudarė DMEM su 1 g/L gliukozės, papildyta 10% FBS ir 1% PS.

Chondrogeninės diferenciacijos terpė, taikyta tiek hBM-MSCs, tiek chondrocitams, buvo sudaryta iš didelio gliukozės kiekio DMEM terpės (4.5 g/L), 1% PS, 1% insulino-transferino-seleno papildo (Gibco, Life Technologies, Waltham, MA, USA), 350 nM L-proline (Carl Roth, Karlsruhe, Germany), 100 nM deksametazono (Sigma Aldrich, Burlington, MA, USA) ir 170 nM askorbo rūgšties-2-fosfato (Sigma Aldrich, Burlington, MA, USA).

Ląstelės, kultivuotos chondrogeninėje terpėje, buvo 24 valandas veikiamos arba 10 ng/mL TGF-β3 (Gibco, Life Technologies), arba 10 ng/mL IL-1β (ProSpec, Ness-Ziona, Israel). 10 ng/mL TGF-β3 koncentracija buvo pasirinkta visiems eksperimentams, nes tai yra dažnai naudojama dozė chondrogeninei diferenciacijai skatinti (Uzieliene et al., 2021). Atitinkamai, IL-1β buvo taikytas 10 ng/mL koncentracijos, remiantis ankstesniais tyrimais, parodžiusiais, kad ši koncentracija efektyviai sukelia ankstyvus degeneracinius pokyčius žmogaus chondrocituose (Shakibaei et al., 2005). Visose sąlygose buvo nuosekliai taikoma 24 valandų inkubacija, siekiant užfiksuoti pirminius ląstelinius atsakus.

1.2.3 Viduląstelinio kalcio lygio iCa^{2+} matavimas

iCa^{2+} vertinimas buvo atliktas išsėjant hBM-MSCs ir chondrocitus į 6-šulinėlių plokšteles po 200 000 ląstelių/šulinėlyje. Kai ląstelės pasiekė 95% konfluenciją, po tolimesnės inkubacijos su IL-1β arba TGF-β3, hBM-MSCs ir chondrocitai buvo atskirti naudojant 0.25% trypsino EDTA, suskaičiuoti ir perkelti į naujus 1.5 mL mėgintuvėlius 100 000 ląstelių/mėgintuvėlyje tankiu. Šios ląstelės buvo dažytos Cal-520 dažikliu (1 μM) (Interchim, Montlucon, France) 30 min., nuplautos PBS ir matuotos naudojant Luminex Guava Flow citometrą (Luminex Corporation, Austin, TX, USA). Duomenys buvo analizuoti naudojant FlowJo programinę įrangą, 10 versiją (FlowJo Corp., Ashland, OR, USA).

1.2.4 hBM-MSCs ir chondrocitų elektrofiziologinė registracija

$I_{Ca,L}$ tyrimui buvo naudojamas modifikuotas Krebso–Ringerio tirpalas ne kalcio, kurio sudėtis (mM): 150 NaCl, 5.4 KCl, 10 $BaCl_2$, 2 $MgCl_2$, 11 ggliukozė ir 10 HEPES, pH sureguliuotas iki 7.4 naudojant NaOH. Šiame tirpale Ca^{2+} buvo pakeistas Ba^{2+}, siekiant padidinti L-VGCC sukeliamos srovės amplitudę, nes Ba^{2+} efektyviau praeina per L-tipo kanalus ir sumažina Ca^{2+}-priklausomą inaktyvaciją, taip palengvindamas srovės aptikimą (Hess & Tsien, 1984; Heubach et al., 2004).

Pipetės tirpalą sudarė šie komponentai (mM): 130 KCl, 10 Na aspartatas, 3 MgATP, 0.2 $CaCl_2$, 2 etilenglikolio tetraacto rūgštis (EGTA) ir 5 (HEPES), pH sureguliuotas iki 7.3 naudojant KOH (Fabiato and Fabiato, 1979; Heubach et al., 2004).
Nifedipinas (10 μM) ir Bay-K8644 (10 μM), naudoti atitinkamai kaip L-VGCC blokatorius ir aktyvatorius, prieš matavimus buvo pridėti į išorinį tirpalą. Abu junginiai įsigyti iš Sigma Aldrich (Burlington, MA, USA).

Siekiant izoliuoti $I_{Ca,L}$, membraninės srovės buvo registruojamos naudojant potencialo fiksavimo protokolą, kuriame nuo laikymo potencialo ties -40 mV sekė depoliarizuojantys 100 ms trukmės 10 mV didėjančios amplitudės žingsniai iki aukščiausios +10 mV vertės (Heubach et al., 1999) (Pav. 2A).
Kadangi stebimas maksimalus Ca^{2+} jonų įtekėjimas per L-VGCCs vyksta ties membranos potencialais 0 ir +10 mV (Heubach et al., 2004; Zhao et al., 2009), nuotėkio laidumoįvertinimui buvo naudoti trys ikislenkstiniai potencialai (−30, −20, −10 mV), kurie buvo tiesiškai ekstrapoliuoti ties 0 ir +10 mV (Pav. 2B) ir vėliau atimti iš eksperimentinių duomenų. Nuotėkio srovės korekcija leido izoliuoti tik nuo įtampos priklausomą srovės komponentą.

A

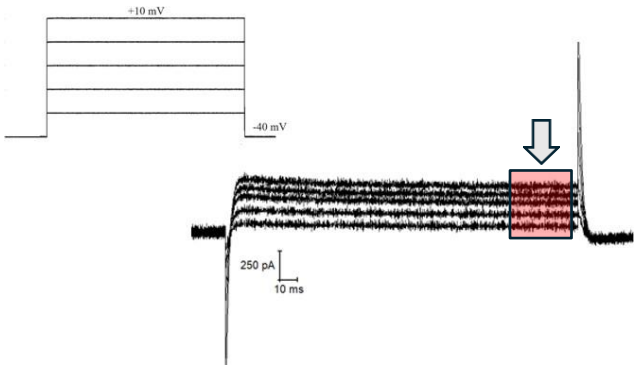

B

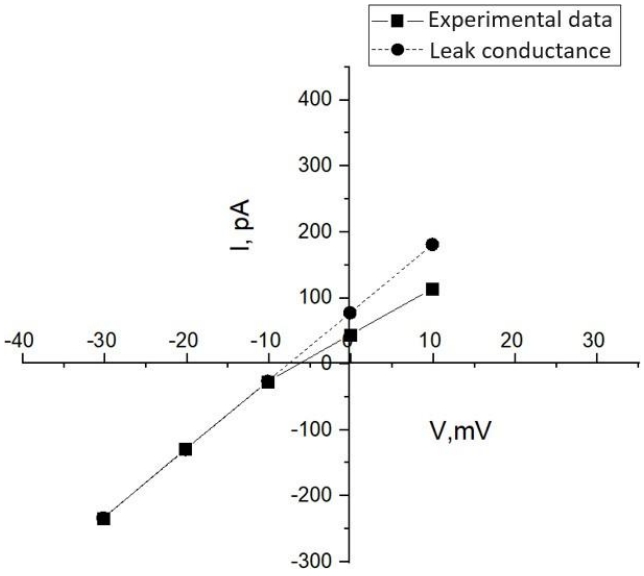

Pav. 2. Įtekanti srovė, užregistruota „patch-clamp“ metodu „whole-cell“ konfigūracijoje.

A) Potencialo fiksavimo protokolas ir reprezentatyvūs „whole-cell“ srovės įrašų pavyzdžiai, užregistruoti hBM-MSCs. Rodyklė nurodo 30 ms intervalą įtampos žingsnių pabaigoje, naudotą nusistovėjusios srovės matavimui B) Vienos hBM-MSC gautos srovės priklausomybės nuo potencialo pavyzdys.

Srovė, koreguota atimant nuotėkio srovę ir normalizuota pagal nuotėkio srovę (I_{LSN}), ties +10 mV buvo naudojama L-VGCC funkciniam

aktyvumui įvertinti hBM-MSC ir chondrocituose. Neigiama I_{LSN} reikšmė rodo įtekančią nuo potencialo priklausomą srovę, tuo tarpu teigiama I_{LSN} – ištekančią nuo potencialo priklausomą srovę.

Mūsų nuotėkio laidumo nustatymo metodas buvo pagrįstas trimis duomenų taškais (−30, −20, −10 mV), kuriuose galima nedidelė $I_{Ca,L}$ srovė (Heubach et al., 2004; Zhao et al., 2009). Tai gali sumažinti gautas I_{LSN} vertes ties +10 mV.

1.2.5 Pagrindinių Ca^{2+} reguliatorių genų ekspresijos analizė

hBM-MSCs ir chondrocitai buvo pasėti į 6-šulinėlių plokšteles 200 000 ląstelių/duobutėje tankiu. Kai ląstelės pasiekė 95% konfluenciją, jos buvo veikiamos IL-1β arba TGF-β3. Po to ląstelės buvo lizuotos naudojant LTR lizavimo buferį (Qiagen, 74104, Hilden, Germany), o RNA buvo išskirta pagal gamintojo instrukcijas. Visų mėginių RNA koncentracija ir grynumas buvo išmatuoti naudojant SpectraMax i3 (Molecular Devices, San Jose, CA, USA). RNA buvo atvirkščiai transkribuota naudojant „Maxima cDNA synthesis kit“ rinkinį su dsDNase apdorojimu (Thermo Fisher Scientific, Waltham, MA, USA). RT-qPCR reakcijos mišiniai buvo paruošti naudojant „Maxima Probe qPCR Master Mix“ rinkinį (Thermo Fisher Scientific, Waltham, MA, USA) ir „TaqMan Gene expression Assays“ rinkinį (*RPS9*–Hs02339424_g1, *B2M*–Hs00984230_m1, *CACNA1C*–Hs00167681_m1, *ATP2A2*–Hs00544877_m1 (Thermo Fisher Scientific, Waltham, MA, USA)). Reakcijos buvo atliktos naudojant „Agilent AriaMx“ sistemą (Agilent Technologies, Santa Clara, CA, JAV) trimis techniniais pakartojimais. Programa pradėta pradine denatūracija 95 °C temperatūroje 10 min., po kurios atlikta 40 ciklų: denatūracija 95 °C temperatūroje 15 s ir pradmenų prisijungimas bei grandinės ilginimas 60 °C temperatūroje 60 s.

Santykiniai genų transkriptų lygiai buvo apskaičiuoti atimant normalizavimo Ct reikšmę (dviejų *RPS9* ir *B2M* geometrinį vidurkį) iš tiriamo geno Ct, taip gaunant dCt reikšmes, kurios vėliau buvo transformuotos į 2-dCt reikšmes ir padaugintos iš 1000 geresniam grafiniam atvaizdavimui.

1.3 LQT1: *KCNQ1* varianto c.1111G > C klinikinė ir funkcinė charakterizacija

Tyrimas buvo atliktas bendradarbiaujant su Vilniaus universiteto ligoninės Santaros klinikomis. Dalis tyrimų buvo finansuota Lietuvos mokslo tarybos (S-MIP-21-15; PI: EP). Tyrimas buvo vykdomas gavus Vilniaus regioninio biomedicininių tyrimų etikos komiteto patvirtinimą (protokolo kodas 2020/1-1182-669, patvirtinta 2020 m. sausio 28 d.; ir protokolo kodas 2021/9-1373-849, patvirtinta 2021 m. rugsėjo 21 d.).

Visos procedūros, susijusios su žmonėmis, buvo vykdomos laikantis Helsinkio deklaracijoje nustatytų etinių principų. Visi tiriamieji prieš dalyvavimą pateikė rašytinį informuotą sutikimą, o visi biologiniai mėginiai prieš laboratorinį apdorojimą buvo nuasmeninti ir koduoti, siekiant užtikrinti konfidencialumą ir atitiktį etiniams standartams.

1.3.1 Heterozigotinio *KCNQ1* c.1111G>C varianto klinikinis vertinimas

Vilniaus universiteto ligoninėje Santaros klinikose buvo identifikuotos penkios Lietuvos šeimos su retu patogeniniu *KCNQ1* variantu NM_000218.3:c.1111G>C. Devynių suaugusiųjų klinikinis vertinimas buvo atliktas nuo 2022 m. gruodžio iki 2023 m. gruodžio pagal tyrimo protokolą jų stebėjimo metu. Klinikinis vertinimas apėmė su liga susijusių simptomų anamnezę, šeimos istorijos surinkimą ir 12 derivacijų EKGatliekant fizinio krūvio testą.

1.3.2 HEK293 ląstelių transfekcija

Žmogaus embrioninės inkstų ląstelės (HEK293) buvo pasėtos į 24-šulinėlių plokšteles (Thermo Scientific Biolite 24-well Multidish) 80 000 ląstelių/ml tankiu vieną dieną prieš transfekciją. Pagal gamintojo protokolą transfekcijai buvo naudojamas „Lipofectamine® 3000 Transfection Reagent“ rinkinys (Thermo Fisher Scientific). *KCNE1* koduojanti plazmidė buvo pIRES_EGFP_GA_KCNE1, kuri buvo gauta iš Al George (Addgene plasmid #173160; http://n2t.net/addgene:173160; RRID: Addgene_173160). Ląstelės buvo transfekuotos skirtingomis plazmidžių kombinacijomis (*KCNQ1_wt+KCNE1, KCNQ1_mut+KCNE1*), išlaikant gamintojo rekomenduotą plazmidinės DNR kiekį. Po transfekcijos ląstelės buvo grąžintos į inkubatorių (37 °C, 5 % CO_2).

1.3.3 Transfekuotų HEK293 ląstelių elektrofiziologinėregistracija

„Whole-cell“ potencialo fiksacijos registracijos buvo atliekamos HEK293 ląstelėse praėjus 2–3 dienoms po transfekcijos arba laukinio tipo*KCNQ1* (WT), arba *KCNQ1* p.(Ala371Pro) variantu, kartu ekspresuojant *KCNE1* subvienetą, siekiant įvertinti $Kv_{7.1}$ kanalo funkciją.

HEK293 ląstelių linija buvo pasirinkta dėl jos pastovios morfologijos (Ooi et al., 2016), adhezijos savybių (Inada et al., 2016) ir plataus naudojimo jonų kanalų tyrimuose (Thomas & Smart, 2005).

Plazmidės, koduojančios *KCNQ1* kartu su oranžine spalva fluorescuojančiu baltymu 1 (CyOFP1)) ir *KCNE1* (kartu su sustiprintu žaliai fluorescuojančiu baltymu (EGFP)), buvo naudojamos transfekuotų ląstelių identifikavimui (Pav. 3).

Fluorescencinė mikroskopija buvo naudojama sėkmingai transfekuotų ląstelių identifikavimui. CyOFP1 fluorescencija buvo vizualizuojama naudojant G-2A filtrų rinkinį (žadinmas 510–560 nm, emisija 590 nm), o EGFP fluorescencija buvo nustatoma naudojant B-2A filtrų rinkinį (žadinimas 450–490 nm, emisija 520 nm). Vaizdai buvo fiksuojami naudojant 2 s ekspozicijos laiką. Elektrofiziologiniams įrašams buvo pasirinktos ląstelės, turinčios abu fluorescencinius žymenis (CyOFP1 ir EGFP), kas rodė sėkmingą transfekciją (Pav. 3).

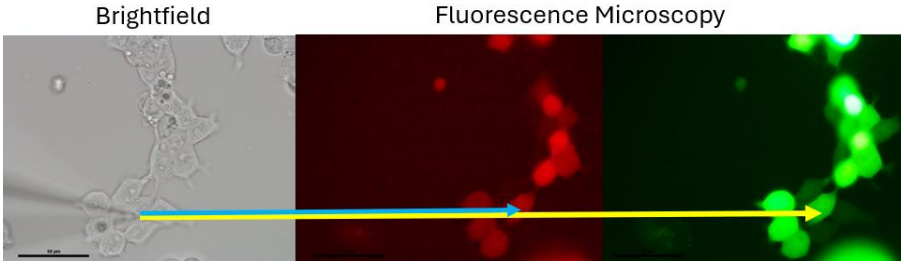

Pav. 3. Kairėje: šviesinės mikroskopijos vaizdas, rodantis ląstelę, prijungtą prie „patch“ pipetės. Dešinėje: fluorescencinės mikroskopijos to paties matymo lauko vaizdas, kur mėlyna rodyklė nurodo CyOFP1-teigiamą ląstelę (su *KCNQ1*), o geltona rodyklė – EGFP teigiamą ląstelę (su *KCNE1*), naudotą „patch-clamp“ registracijai.

Pipetės tirpalą sudarė (mM): 140 KCl, 1 Na2-ATP, 2 EGTA, 10 HEPES, 0.1 $CaCl_2$, 1 $MgCl_2$ ir 10 gliukozė, pH sureguliuotas iki 7.4 naudojant KOH.

Registracijai naudoto Tyrodo tirpalo sudėtis (mM): 140 NaCl, 4 KCl, 2 $CaCl_2$, 1 $MgCl_2$, 10 HEPES ir 10 gliukozė, pH sureguliuotas iki 7.4 naudojant NaOH.

Chromanolis 293B, ištirpintas dimetilsulfokside galutinėje 10 µM koncentracijoje, buvo naudojamas kaip specifinis $Kv_{7.1}$ kanalų inhibitorius.

Membraninės srovės buvo registruojamos naudojant fiksuoto potencialo protokolą, kuriame nuo laikymo potencialo ties -90 mV sekė depoliarizuojantys 2 s trukmės kas 20 mV didėjantys žingsniai iki galutinės potencialo vertės ties +70 mV (Pav. 4A).

$Kv_{7.1}$ sukeltos srovės aktyvacijos slenkstis yra apie -40 mV (Aidery et al., 2012). Nuotėkio laidumo įvertinimui buvo naudojamos srovės ties trimis ikislenkstiniais potencialais (-90, -70 ir -50 mV), iš jų gauta nuotekio srovė buvo tiesiškai ekstrapoliuojama diapazone nuo -30 iki +70 mV (Pav. 4B). Nuotėkio srovės korekcija leido izoliuoti nuo potencialo priklausomą srovės komponentą. Analizei buvo naudoti srovės tankiai (pA/pF), gauti nuo potencialo priklausomos srovės komponentą normalizavus pagal ląstelės membranos talpą.

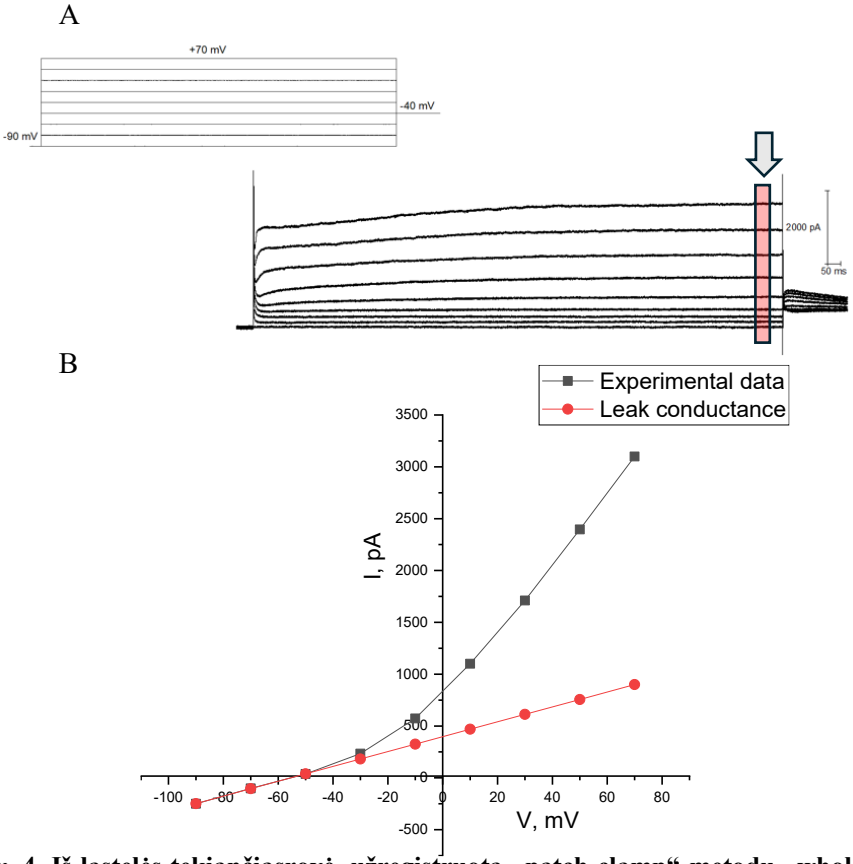

Pav. 4. Iš ląstelės tekiančiasrovė, užregistruota „patch-clamp“ metodu „whole-cell“ konfigūracijoje.A) Potencialo fiksavimo protokolas ir reprezentatyvūs srovės įrašų pavyzdžiai, užregistruoti HEK293 ląstelėse, transfekuotose laukinio tipo

KCNQ1 kartu ekspresuojant *KCNE1* subvienetą. Rodyklė nurodo 50 ms intervalą įtampos žingsnių pabaigoje, kuriame buvo matuojama nusistovėjusi srovė.
B) HEK293 ląstelės srovės priklausomybės nuo potencialo pavyzdys, rodantis iš ląstelės ištekančią srovę.

Srovės tankiai taip pat buvo naudojami laidumo–potencialo (G-V) kreivėms sudaryti, siekiant nustatyti kanalo aktyvacijos priklausomybę nuo potencialo. Laidumas (G) gautas srovės pokytį (ΔI) padalinus iš membranos potencialo pokyčio (ΔV) kiekviename įtampos žingsnyje.

G_{max} ir $V_{1/2}$ buvo gauti pritaikius G/G_{max} kreivei Boltzmann‘o lygtį.

$$G(V) = G_{min} + \frac{(\mathrm{G_{max}} - \mathrm{G_{min}})}{1 + \exp(\frac{V - V_{1/2}}{s})}$$

G_{min} yra minimali laidumo reikšmė, G_{max} – maksimali laidumo reikšmė, $V_{1/2}$ – nuo įtampos priklausomos aktyvacijos vidurio taškas, o s – nuolydžio faktorius.

1.4 Statistinė analizė

Normalumo įvertinimui buvo naudojamas „Shapiro-Wilk“ testas (Origin Pro). Pirmajame tyrime duomenys atitiko normalųjį pasiskirstymą. Statistiniai skirtumai tarp grupių buvo vertinami naudojant vienfaktorinę dispersinę analizę (one-way ANOVA) su OriginPro programine įranga, versija 9.5 (OriginLab Corporation, Northampton, MA, USA), o skirtumai tarp dviejų grupių buvo vertinami naudojant neporinį dvipusį Studento t-testą (Microsoft Excel). Tekste duomenys pateikiami kaip vidurkis ± standartinis nuokrypis (SD).

Antrajame projekte duomenys neatitiko normalaus pasiskirstymo. Todėl statistinė analizė buvo atlikta naudojant neparametrinį „Kruskal-Wallis“ testą (Origin Pro), skirtą skirtumams tarp kelių grupių įvertinti, o palyginimams tarp dviejų grupių buvo naudojamas „Mann-Whitney U“ testas (Origin Pro). Statistinis reikšmingumas buvo nustatytas kaip $*p \leq 0.05$. Paveiksluose reikšmingumo lygiai nurodomi atitinkamose legendose. Rezultatai pateikiami kaip vidurkis ± standartinė vidurkio paklaida, „n“ reiškia ląstelių skaičių.

1.5 Autorių indėlis

hBM-MSCs ir chondrocitų izoliaciją bei kultivavimą, iCa^{2+} įvertinimą ir genų ekspresijos analizę hBM-MSCs ir chondrocituose atliko IMC kolegos.

KCNQ1 p.(Ala371Pro) varianto klinikinis vertinimas buvo atliktas Vilniaus universiteto ligoninėje Santaros klinikose. Ląstelių transfekciją atliko Vilniaus universiteto Gyvybės mokslų centro Biomokslų instituto Biochemijos ir molekulinės biologijos katedros kolegos. Visus elektrofiziologinius įrašus, įskaitant duomenų surinkimą ir analizę, atliko disertacijos autorė.

REZULTATAI

Šios disertacijos rezultatai pagrįsti dviem publikuotais recenzuojamuose moksliniuose žurnaluose straipsniais.

Pirmajame tyrime buvo tirtas transformuojančio augimo faktoriaus beta 3 (TGF-β3) ir interleukino-1β (IL-1β) poveikis L tipo potencialo valdomiems kalcio kanalams (L-VGCCs) bei Ca^{2+} homeostazei osteoartritiniuose chondrocituose ir žmogaus kaulų čiulpų mezenchiminėse kamieninėse ląstelėse (hBM-MSCs) chondrogenezės metu. Ca^{2+} homeostazė buvo vertinama trimis aspektais: viduląsteline Ca^{2+} koncentracija (iCa^{2+}), L tipo kalcio srovėmis ($I_{Ca,L}$) bei *CACNA1C* ir *ATP2A2* genų raiška.

Antrasis tyrimas buvo skirtas LQT1 sindromui: *KCNQ1* geno varianto c.1111G > C klinikinei ir funkcinei charakteristikai. Šioje dalyje buvo apjungti klinikiniai duomenys ir tiesioginiai elektrofiziologiniai mutantinio $Kv_{7.1}$ kanalo, turinčio *KCNQ1* variantą, sukeltų srovių tyrimai.

2.1. TGF-β3 ir IL-1β poveikis L-VGCCs bei Ca^{2+} homeostazei osteoartritiniuose chondrocituose ir hBM-MSCs chondrogenezės metu

2.1.1. TGF-β3 sukelia viduląstelinės Ca^{2+} koncentracijos padidėjimą

Manoma, kad Ca^{2+} kanalai atlieka esminį vaidmenį chondrogeninėje diferenciacijoje (Uzieliene ir kt., 2018). Taip pat žinoma, kad šio proceso metu kinta viduląstelinė Ca^{2+} koncentracija (iCa^{2+}), rodanti aktyvią Ca^{2+} homeostazės reguliaciją chondrogenezės metu (Fodor ir kt., 2013; Matta ir Zakany, 2013). Kadangi TGF-β3 yra plačiai naudojamas chondrogenezei sukelti (Uzieliene ir kt., 2019; Wee ir kt., 2022; Xia ir kt., 2017), o IL-1β yra svarbus uždegiminis mediatorius, susijęs su osteoartritinėmis būklėmis (Kobayashi ir kt., 2005), pirmiausia buvo tirta, kaip šie citokinai veikia iCa^{2+} hBM-MSCs ir chondrocituose chondrogeninės diferenciacijos metu.

TGF-β3 reikšmingai padidino iCa^{2+} tiek hBM-MSCs, tiek chondrocituose, tuo tarpu IL-1β, reikšmingų pokyčių nesukėlė (Pav. 5).

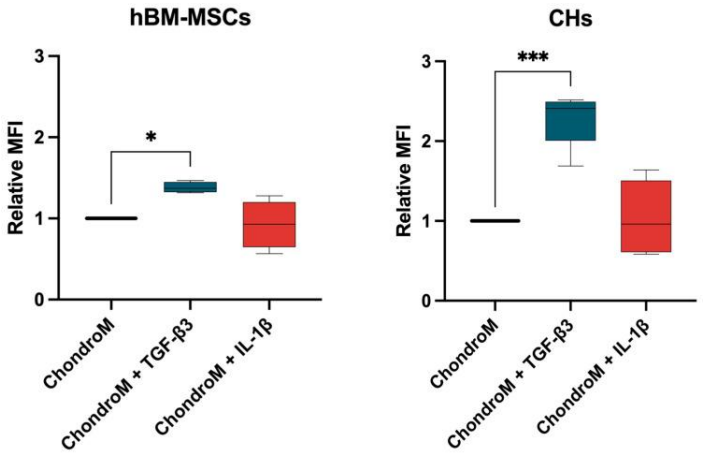

Pav. 5. iCa^{2+} lygiai hBM-MSCs ir chondrocituose (CHs). Medianinis fluorescencijos intensyvumas (MFI) pateikiamas kaip santykis su nedažyta kontrole. Duomenys pateikiami kaip vidurkis ± standartinis nuokrypis (SD). * $p < 0.05$, *** $p < 0.001$.

2.1.2 TGF-β3 sukelia nifedipinui jautrią $I_{Ca,L}$ hBM-MSCs

Insulinomos ląstelėse TGF-β3 sukeltas iCa^{2+} padidėjimas priklausė nuo Ca^{2+} patekimo per L-VGCCs (Ishiyama et al., 1996). Be to, ankstesni tyrimai parodė, kad tik nedidelėje dalyje nediferencijuotų hBM-MSCs stebėta maža $I_{Ca,L}$ (Heubach et al., 2004; Kawano et al., 2002). Funkcinis L-VGCCs vaidmuo Ca^{2+} hBM-MSCs homeostazėje šiuo metu pilnai neaiškus. Siekiant ištirti, kaip TGF-β3 gali sukelti iCa^{2+} padidėjimą hBM-MSCs, buvo tirtas jo poveikis L-VGCCs funkciniam aktyvumui chondrogeninėje terpėje. Papildomai buvo įvertintas ir IL-1β poveikis L-VGCCs funkciniam aktyvumui hBM-MSCs.

hBM-MSCs, kultivuotos proliferacijos terpėje, neparodė reikšmingo I_{LSN} (0.006 ± 0.04, n = 22) (Pav. 6).

Kadangi chondrogeninė terpė yra papildyta didelio gliukozės kiekio DMEM, 1 % PS, insulino–transferino–seleno priedu, L-prolinu, deksametazonu ir kitais bioaktyviais junginiais, kurių kiekvienas potencialiai gali paveikti joninių kanalų funkciją (Levitan et al., 1991; Y. Liu et al., 2001; L. Wang et al., 2021), buvo įvertintas vien tik chondrogeninės terpės poveikis L-VGCCs funkciniam aktyvumui.

Kultivavimas chondrogeninėje terpėje nesukėlė reikšmingų I_{LSN} pokyčių hBM-MSCs (−0.01 ± 0.03, n = 12), lyginant su proliferacijos terpe (Pav. 6).

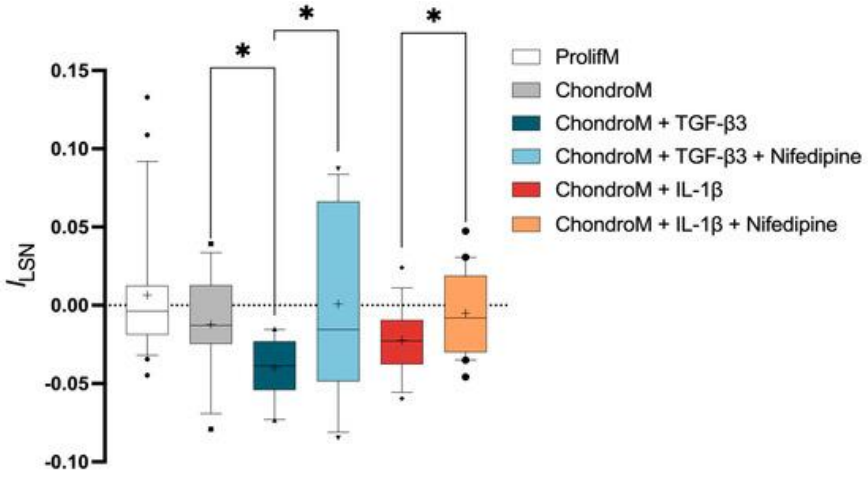

Pav. 6. I_{LSN} hBM-MSCs. Srovė buvo matuojama ląstelėse, kultivuotose proliferacijos terpėje (ProlifM) ir Chondrogeninėje terpėje (ChondroM) su TGF-β3 (10 ng/mL) arba IL-1β (10 ng/mL), su nifedipinu arba be jo. Duomenys pateikiami nurodant medianą, viršutinį (90) ir apatinį (10) procentilius. Išskirtys pavaizduoti kaip atskiri taškai už ūsų ribų. *$p < 0.05$. Ląstelių skaičius kiekvienoje sąlygoje nurodytas tekste.

TGF-β3 poveikis hBM-MSCs sukėlė reikšmingai neigiamą I_{LSN} (−0.04 ± 0.02; n = 14), lyginant su vien tik chondrogenine terpe (Pav. 6). TGF-β3 sukeltas neigiamas I_{LSN} buvo jautrus nifedipinui, L-VGCC blokatoriui (0.0007 ± 0.06, n = 12) (Pav. 6).

hBM-MSCs IL-1β poveikyje buvo stebima tendenciją sukelti neigiamą, tačiau statistiškai nereikšmingą I_{LSN}, lyginant su chondrogenine terpe (−0.02 ± 0.02, n = 16) (Pav. 6). Nifedipinas sukėlė reikšmingą šios I_{LSN} sumažėjimą (−0.005 ± 0.03; n = 20) (Pav. 6).

2.1.3 L-VGCCs neprisideda prie TGF-β3 sukelto iCa^{2+}padidėjimo chondrocituose

Siekiant ištirti, kaip TGF-β3 gali sukelti iCa^{2+} padidėjimą chondrocituose, buvo tiriamas jo poveikis L-VGCCs funkciniam aktyvumui. Papildomai buvo tirtas IL-1β poveikis L-VGCCs funkciniam aktyvumui chondrocituose.

Chondrocitai, kultivuoti proliferacijos terpėje, neparodė reikšmingo I_{LSN} (−0.007 ± 0.02, n = 42) (Pav. 7A). Bay-K8644, L-VGCC aktyvatoriaus, pridėjimas į proliferacijos terpę nesukėlė reikšmingo I_{LSN} pokyčio (−0.01 ± 0.01, n = 16) (Pav. 7B).

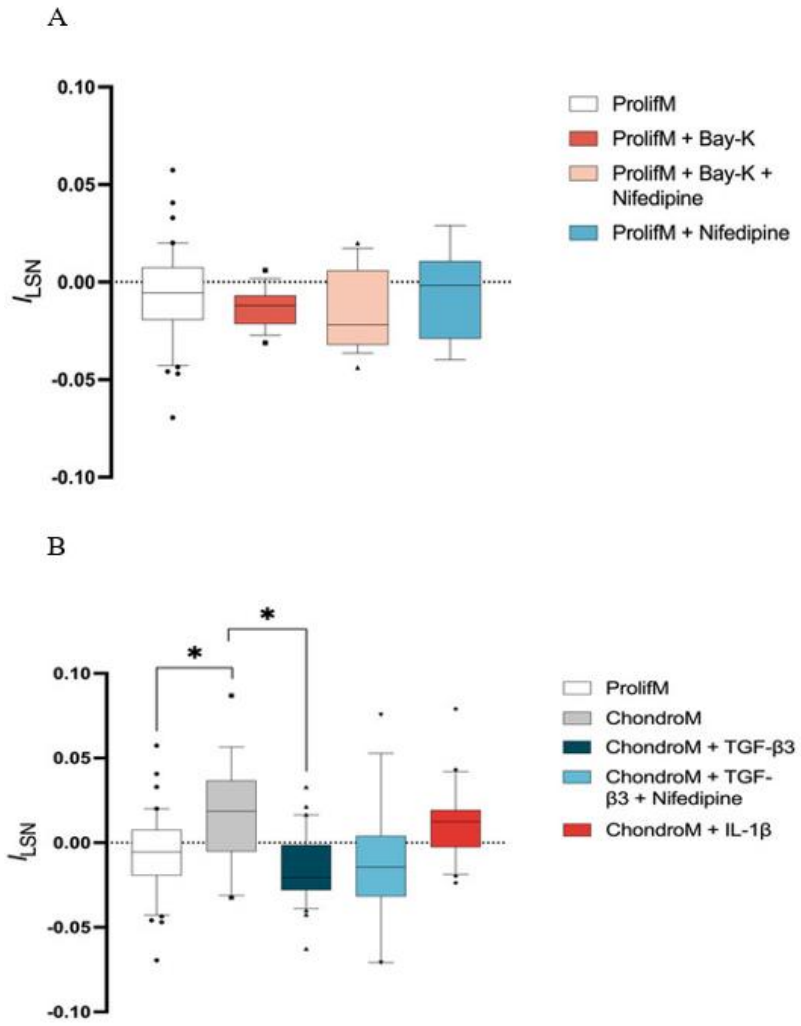

Pav. 7. I_{LSN} chondrocituose. Srovė buvo matuojama ląstelėse, kultivuotose: A) proliferacijos terpėje (ProlifM) kartu su Bay-K8644, nifedipinu arba abiemvienu metu ; B) proliferacijos terpėje ir chondrogeninėje terpėje (ChondroM) su TGF-β3 (10 ng/mL) arba IL-1β (10 ng/mL), su nifedipinu arba be jo. Duomenys pateikiami nurodant medianą, viršutinį (90) ir apatinį (10) procentilius. Išskirtys pavaizduotos kaip atskiri taškai už ūsų ribų. * $p < 0.05$. Ląstelių skaičius kiekvienoje sąlygoje nurodytas tekste.

Į ląstelę įtekanti srovė galėjo būti kompensuojama nuo potencialo priklausomomis (Mobasheri et al., 2012). Be to, I_{LSN} pokyčių nebuvimas po Bay-K8644 pridėjimo rodyti, kad dauguma L-VGCCs jau buvo aktyvuoti. Ši hipotezė buvo patikrinta pridėjus nifedipino. Nifedipinas arba Bay-K8644

kartu su nifedipinu nesukėlė reikšmingų I_{LSN} pokyčių (atitinkamai −0.006 ± 0.02, n = 9 ir −0.01 ± 0.02, n = 18) (Pav. 7A).

Chondrocitų inkubacija chondrogeninėje terpėje sukėlė reikšmingai teigiamą I_{LSN} (0.02 ± 0.03; n = 18), rodantį nuo potencialo priklausomos ištekančios srovės aktyvaciją (Pav. 7B).

TGF-β3 pridėjimas į chondrogeninę terpę sukėlė reikšmingai neigiamą I_{LSN} (−0.02 ± 0.01, n = 31), lyginant su chondrocitais, kultivuotais tik chondrogeninėje terpėje (Pav. 7B). TGF-β3 sukeltas neigiamas I_{LSN} nebuvo jautrus nifedipinui (−0.01 ± 0.04, n = 16) (Pav. 7B).

IL-1β pridėjimas nepakeitė I_{LSN} (0.01 ± 0.02, n = 20), lyginant su vien tik chondrogenine terpe (Pav. 7B).

2.1.4 TGF-β3 ir IL-1β skirtingai reguliuoja *CACNA1C* ir *ATP2A2* ekspresiją

Yra duomenų, kad tiek TGF-β3, tiek padidėję iCa^{2+} lygiai gali moduliuoti Ca^{2+} homeostazę genų ekspresijos lygmenyje (C. M. Johnson et al., 1997; Y. Liu et al., 2001; Ranganathan et al., 2007). Siekiant tai išsiaiškinti buvo tirta, kaip šie veiksniai veikia pagrindinių Ca^{2+} reguliatorių ekspresiją. Konkrečiai buvo analizuota *CACNA1C* ir *ATP2A2* ekspresija. *CACNA1C* koduoja L-VGCC subvienetą $Cav_{1.2}$, kuris yra vienas pagrindinių Ca^{2+} patekimo į ląstelę kelių, tuo tarpu *ATP2A2* koduoja SERCA pompą, atsakingą už Ca^{2+} grąžinimą į ER ir bazinio iCa^{2+} atkūrimą. Papildomai buvo įvertintas IL-1β poveikis *CACNA1C* ir *ATP2A2* ekspresijai.

CACNA1C ekspresija reikšmingai sumažėjo chondrocituose veikiant tiek TGF-β3, tiek IL-1β, tuo tarpu hBM-MSCs šie citokinai pokyčių nesukėlė (Pav. 8A).

ATP2A2 ekspresija reikšmingai padidėjo hBM-MSCs veikiant tiek TGF-β3, tiek IL-1β. Chondrocituose *ATP2A2* ekspresija reikšmingai padidėjo tik po TGF-β3 poveikio (Pav. 8B).

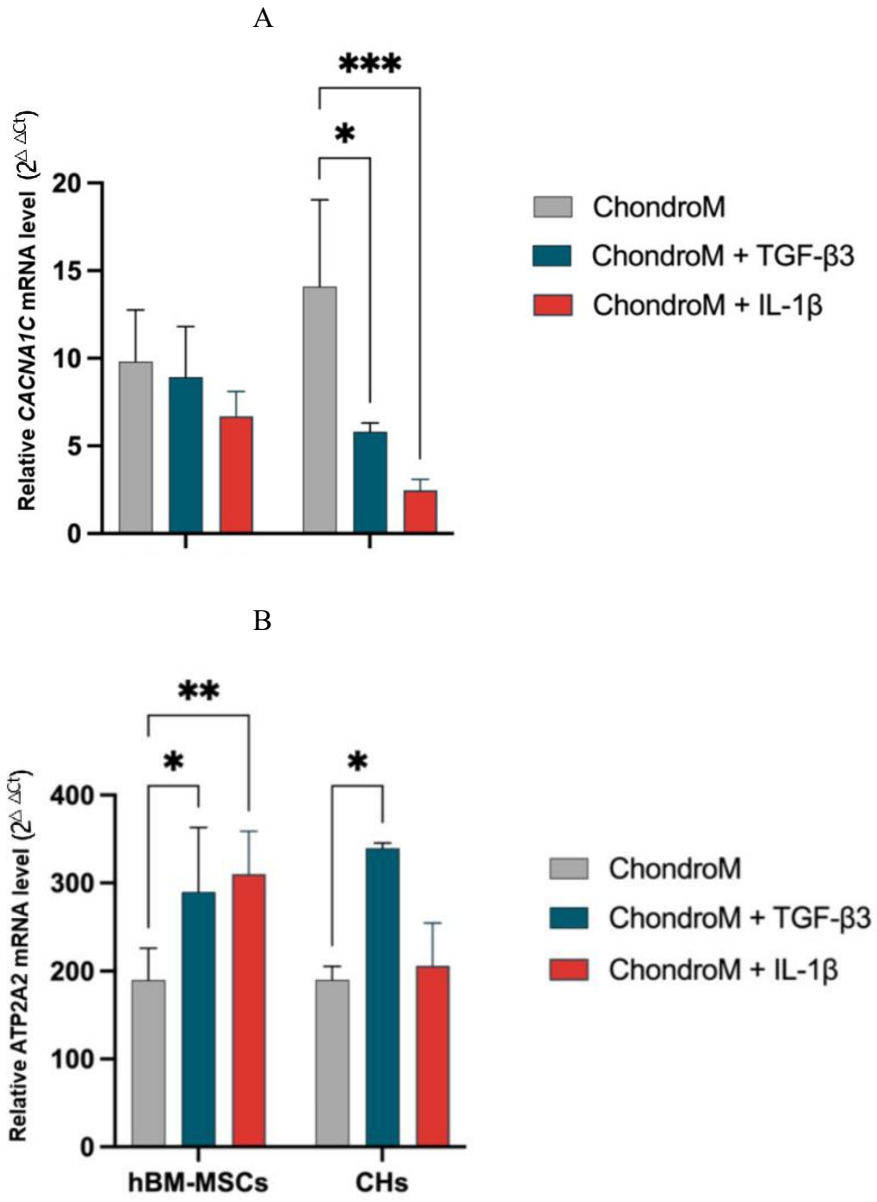

Pav. 8. IL-1β (10 ng/mL) ir TGF-β3 (10 ng/mL) poveikis hBM-MSCs ir chondrocitų (CHs) $Cav_{1.2}$ (*CACNA1C*) ir SERCA2 pompos (*ATP2A2*) genų ekspresijai. A) *CACNA1C* ir B) *ATP2A2* ekspresijos santykis buvo analizuotas chondrogeninėje terpėje (ChondroM) su TGF-β3 (10 ng/mL) ir IL-1β (10 ng/mL). Pateikiami santykiniai transkriptų lygiai po normalizavimo pagal referentinių genų B2M ir RPS9 geometrinį vidurkį. Duomenys pateikiami kaip vidurkis ± standartinis nuokrypis (SD). * $p < 0.05$, ** $p < 0.01$, *** $p < 0.001$.

2.2 LQT1: *KCNQ1* varianto c.1111G > C klinikinė ir funkcinė charakterizacija

2.2.1 Heterozigotinio *KCNQ1* c.1111G>C varianto nešiotojų klinikinė charakterizacija

Ilgo QT intervalo sindromas yra reta paveldima širdies liga, kurios galutinės diagnozės nustatymas gali būti sudėtingas ir užtrukti ilgą laiką dėl genetinio heterogeniškumo. Klinikinėje praktikoje genetinis testavimas dažniausiai orientuojamas į tris pagrindinius genus – *KCNQ1*, *KCNH2* ir *SCN5A* (Kapa et al., 2009). Šiame tyrime pacientai buvo nukreipti genetiniam tyrimui remiantis ilgo QT intervalo sindromo požymiais, nustatytais kardiologinio įvertinimo metu. Tai leido identifikuoti devynis heterozigotinius *KCNQ1* varianto c.1111G>C [p.(Ala371Pro)] nešiotojus, koduojančius $Kv_{7.1}$ kanalo α-subvienetą, penkiose nesusijusiose Lietuvos šeimose, įskaitant penkis vyrus (56%) ir keturias moteris (44%), kurių amžius klinikinio įvertinimo metu buvo 18–47 metai. Keturi asmenys (44%) buvo simptominiai: vienas nurodė daugybinius sinkopės epizodus fizinio aktyvumo metu (konkurencinis sportas), o trys patyrė fizinio krūvio sukeltą aritminę presinkopę. Simptomų pradžia pasireiškė vaikystėje arba paauglystėje (10–16 metų). Be to, trijose šeimose buvo registruoti staigios širdies sutrikomo nulemtos mirties atvejai (viena moteris 34 metų ir du vyrai 53 ir 59 metų amžiaus), kas pabrėžia klinikinį fenotipo reikšmingumą. Didžiausio fizinio krūvio metu atliekant 12 derivacijų EKG tyrimą dauguma tiriamųjų (89%) buvo būdingas QTc pailgėjimas >480 ms. Apibendrinant, šie duomenys patvirtina ryšį tarp *KCNQ1* varianto c.1111G>C, koduojančio $Kv_{7.1}$ kanalo α-subvienetą, ir ilgo QT intervalo sindromo fenotipo, kuriam būdingi su fiziniu krūviu susiję simptomai, fizinio krūvio sukeltas QTc pailgėjimas ir šeimyninis staigios mirties pasireiškimas.

Bendras klinikinis įvertinimas atskleidė nuoseklų, nuo fizinio krūvio priklausomą QTc pailgėjimą, rodantį sutrikusią skilvelių repoliarizaciją. Kadangi skilvelių repoliarizacija yra kritiškai priklausoma nuo I_{Ks}, šie rezultatai paskatino tolesnį tiesioginį identifikuoto *KCNQ1* varianto poveikio $Kv_{7.1}$ kanalo funkcijai elektrofiziologinį tyrimą naudojant „patch-clamp“ metodus.

2.2.2 *KCNQ1* variantas sumažina $Kv_{7.1}$ kanalų srovės tankį

Širdyje funkciniai $Kv_{7.1}$ kanalai yra sudaryti kartu su *KCNE1* subvienetais, kurie reikšmingai keičia kanalo funkciją ir biofizikines savybes. *KCNE1* ypač padidina $Kv_{7.1}$ kanalų srovės amplitudę (Barhanin et al., 1996; Nakajo & Kubo, 2015; Sanguinetti et al., 1996). Atsižvelgiant į tai, buvo tirta, kaip *KCNQ1* p.(Ala371Pro) variantas veikia $Kv_{7.1}$ kanalų elektrofiziologines savybes, lyginant ląsteles, ekspresuojančias laukinio tipo arba *KCNQ1* p.(Ala371Pro) variantą kartu su *KCNE1*.

Reikšmingi srovės tankio skirtumai tarp tiriamų grupių buvo stebimi jau ties +10 mV ir progresyviai didėjo didėjant depoliarizacijos žingsniams (Pav. 9B). Ties +30 mV $Kv_{7.1}$ sukeltos srovės tankis buvo reikšmingai didesnis ląstelėse, ekspresuojančiose laukinio tipo *KCNQ1* kartu su *KCNE1* (15.80 ± 1.09 pA/pF, n = 11), lyginant su ląstelėmis, ekspresuojančiomis *KCNQ1* p.(Ala371Pro) variantą kartu su *KCNE1* (10.84 ± 0.48 pA/pF, n = 24) (Pav. 9B).

Ties +70 mV šis skirtumas buvo dar didesnis: 33.92 ± 2.44 pA/pF, n = 11 laukinio tipo grupėje ir 19.87 ± 0.86 pA/pF, n = 24 *KCNQ1* p.(Ala371Pro) varianto grupėje (Pav. 9B). Šie rezultatai rodo, kad *KCNQ1* p.(Ala371Pro) variantas sukėlė dalinį $Kv_{7.1}$ kanalų funkcijos praradimą (LOF).

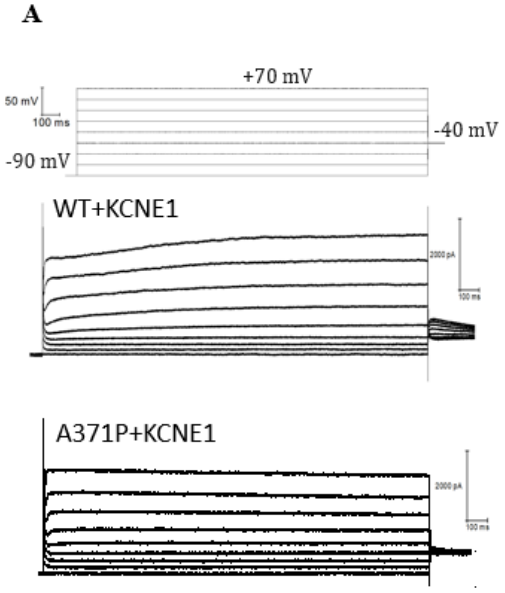

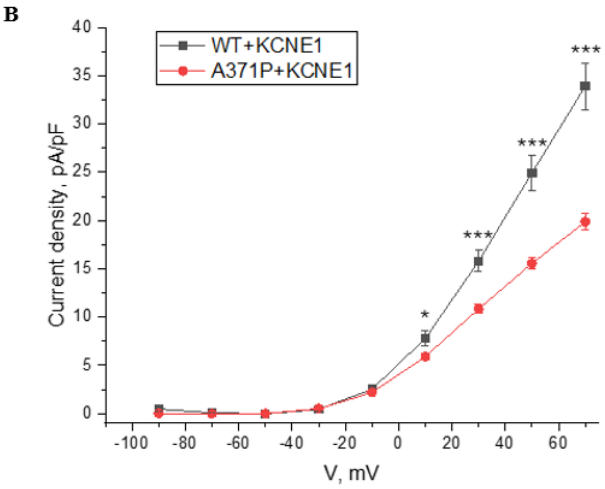

Pav. 9. I_{Ks} HEK293 ląstelėse, transfekuotose laukinio tipo *KCNQ1* (WT) arba *KCNQ1* p.(Ala371Pro) variantu (A371P), kartu su *KCNE1*. A) *Viršuje*: potencialo fiksacijos protokolas, prasidedantis nuo laikymo potencialo ties -90 mV ir taikant 2 s trukmės depoliarizacijos žingsnius kas 20 mV iki +70 mV. *Apačioje:* reprezentatyvūs registruotų srovių įrašai. B) Srovės tankio priklausomybė nuo membranos potencialo (I–V) nurodytose grupėse. Ląstelių skaičius kiekvienoje sąlygoje nurodytas tekste. Duomenys pateikiami kaip vidurkis ± standartinė vidurkio paklaida (SEM).. * $p \leq 0.05$, *** $p \leq 0.005$.

2.2.3 Pakitusių $Kv_{7.1}$ kanalų Jautrumas Chromanoliui

Siekiant patvirtinti stebimų ištekančių srovių kilmę, buvo tirtas šių srovių jautrumas chromanoliui 293B, selektyviam $Kv_{7.1}$ blokatoriui. Srovės tankis, stebėtas ląstelėse, kartu ekspresuojančiose laukinio tipo *KCNQ1* su *KCNE1*, buvo reikšmingai sumažintas chromanoliu iki 10.70 ± 3.98 pA/pF (n = 6; Pav. 10) ties +70 mV, patvirtinant $Kv_{7.1}$ kanalų indėlį nagrinėtoms srovėms.

KCNQ1 p.(Ala371Pro) variantas, kartu ekspresuotas su *KCNE1*, taip pat buvo jautrus chromanoliui: srovės tankis reikšmingai sumažėjo iki 10.86 ± 1.45 pA/pF ties +70 mV (n = 7; Pav. 10). Šie rezultatai rodo, kad nors *KCNQ1* p.(Ala371Pro) variantas sumažina $Kv_{7.1}$ tarpininkaujamą srovę, kanalas išlieka jautrus chromanoliui.

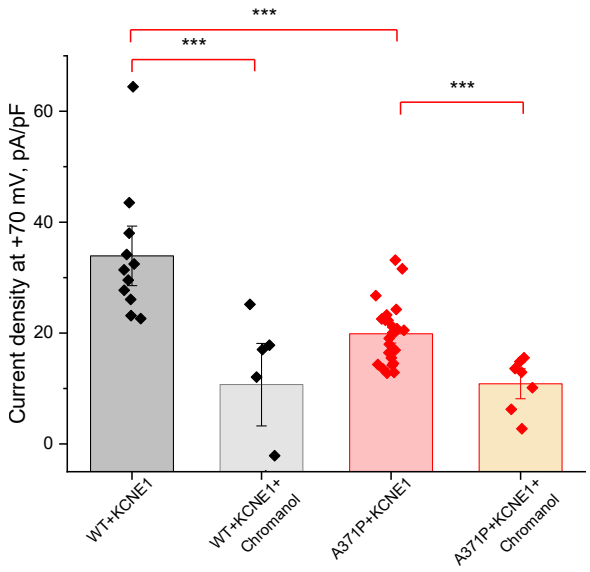

Pav. 10. Srovės tankiai (pA/pF) ties +70 mV HEK293 ląstelėse, transfekuotose laukinio tipo *KCNQ1* (WT) arba *KCNQ1* p.(Ala371Pro) variantu (A371P), kartu ekspresuojant *KCNE1*, su ir be chromanolio 293B (10 µM). Chromanolis 293B buvo taikytas $Kv_{7.1}$ srovės blokavimui. Rezultatai pateikti kaip vidurkis ± standartinė vidurkio paklaida (SEM); ; kiekvienas rombas atitinka atskirą ląstelę. *** $p \leq 0.005$.

2.2.4 A371P sumažina $Kv_{7.1}$ kanalų laidumą nekeisdamas aktyvacijos priklausomybės nuo potencialo

Sumažėjęs srovės tankis ląstelėse, ekspresuojančiose *KCNQ1* p.(Ala371Pro) variantą kartu su *KCNE1*, gali būti susijęs su sumažėjusiu $Kv_{7.1}$ kanalų laidumu arba pakitusia aktyvacijos priklausomybe nuo potencialo. *KCNQ1* p.(Ala371Pro) variantas nepakeitė $Kv_{7.1}$ kanalų aktyvacijos priklausomybės nuo įtampos, lyginant su laukinio tipo ($V_{1/2}$: -21.16 ± 1.57 mV, n = 24 A371P+KCNE1 grupei ir -15.49 ± 2.10 mV, n = 11 WT+KCNE1 grupei; Pav. 11C).

Maksimalus $Kv_{7.1}$ kanalo laidumas (G_{max}) buvo reikšmingai sumažintas dėl šio varianto (0.27 ± 0.01 nS/pF, n = 24), lyginant su laukiniu tipu (0.51 ± 0.04 nS/pF, n = 11) (Pav. 11A, B).

Šie rezultatai rodo, kad *KCNQ1* p.(Ala371Pro) variantas sutrikdo normalią $Kv_{7.1}$ kanalų vartų funkciją sumažindamas kanalų laidumą.

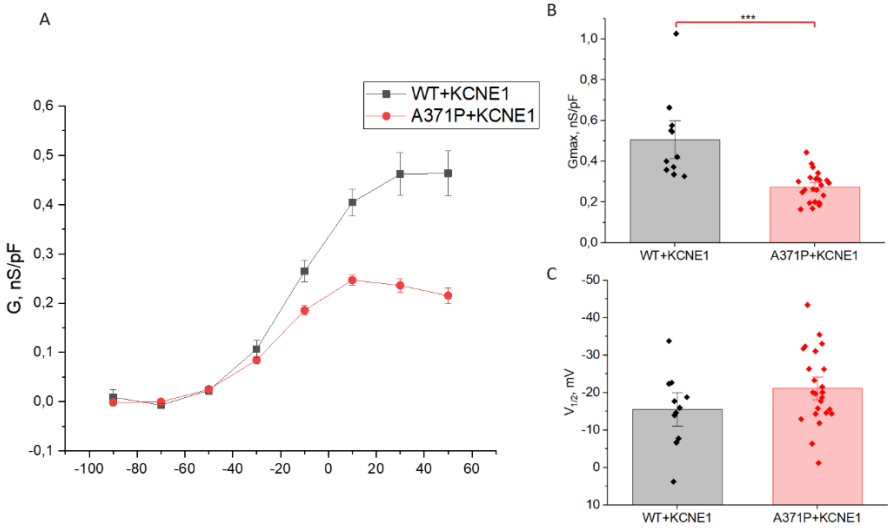

Pav. 11. Srovių aktyvacija HEK293 ląstelėse, transfekuotose laukinio tipo *KCNQ1* (WT) arba *KCNQ1* p.(Ala371Pro) variantu (A371P), kartu ekspresuojant *KCNE1*. A) Laidumo priklausomybė nuo potencialo. Simboliai su paklaidų ūsais rodo vidurkį ± standartinę vidurkio paklaidą (SEM). B) Maksimalus laidumas (G_{max}). C) Aktyvacijos vidurio taškas ($V_{1/2}$). Stulpeliai rodo vidurkį ± standartinę vidurkio paklaidą (SEM); kiekvienas rombas atitinka atskirą ląstelę. *** $p \leq 0.005$.

DISKUSIJA

Šiame tyrime buvo nagrinėti du skirtingi mechanizmai, reguliuojantys įtampa valdomų jonų kanalų funkcionalumąą: moduliacija išoriniais veiksniais ir pokyčiai dėl genetinių variantų. Konkrečiai buvo vertinamas citokinų poveikis Ca^{2+} homeostazei, daugiausia dėmesio skiriant L-VGCCs, koduojamiems *CACNA1C*, bei įvertintos retos *KCNQ1* varianto c.1111G>C [p.(Ala371Pro)] funkcinės pasekmės $Kv_{7.1}$ kanalo funkcijai.

Siekiant nustatyti L-VGCCs funkcionalumo pokyčius po 24 val. poveikio 10 ng/mL TGF-β3 ir 10 ng/mL IL-1β tiek hBM-MSCs, tiek chondrocituose buvo įvertinti trys Ca^{2+} homeostazės aspektai:

1. iCa^{2+}lygis;
2. $I_{Ca,L}$, suteikiantis informacijos, ar Ca^{2+} patenka į ląsteles per L-VGCCs;
3. *CACNA1C* ir *ATP2A2* genų ekspresija, atspindinti ląstelių atsaką į pakitusius iCa^{2+}lygius siekiant atkurti homeostazę.

Citokinų moduliacija jonų kanalų funkcijai priklauso nuo dozės ir poveikio laiko, todel skirtingi ląstelių atsakai stebimi priklausomai nuo stimuliacijos intensyvumo ir trukmės (Almuraikhi et al., 2025; Rudzitis et al., 2025; Zhou et al., 2011). Šiame tyrime visiems eksperimentams buvo naudojama 10 ng/mL TGF-β3 koncentracija, nes tai standartinė koncentracija chondrogeninei diferenciacijai indukuoti (Uzieliene et al., 2021). Panašiai 10 ng/mL IL-1β buvo pasirinkta remiantis literatūros šaltiniais, nes parodyta, kad ji sukelia ankstyvus degeneracinius pokyčius žmogaus chondrocituose (Shakibaei et al., 2005). 24 val. inkubacijos laikotarpis buvo pasirinktas ankstyviems ląsteliniams pokyčiams tirti.

Po TGF-β3 poveikio buvo stebėtas iCa^{2+} padidėjimas tiek hBM-MSCs, tiek chondrocituose. TGF-β3 padidino $I_{Ca,L}$ BM-hMSCs, tačiau ne chondrocituose. *CACNA1C* geno ekspresija buvo reikšmingai sumažinta chondrocituose tiek TGF-β3, tiek IL-1β poveikyje, tuo tarpu hBM-MSCs buvo stebima tik mažėjimo tendencija. *ATP2A2* geno ekspresija padidėjo dėl TGF-β3 ir IL-1β poveikio hBM-MSCs, o chondrocituose – tik dėl TGF-β3.

Iš trijų TGF-β izoformų, aptinkamų žinduoliuose, TGF-β1 ir TGF-β3 dažniausiai naudojami chondrogenezės indukcijai (Uzieliene et al., 2019; Wee et al., 2022; Xia et al., 2017). Šiame tyrime buvo pasirinktas TGF-β3, nes parodyta, kad jis turi didesnį potencialą skatinti chondrogeninę diferenciaciją nei TGF-β1 (Barry et al., 2001).

TGF-β3 reikšmingai padidino iCa^{2+} tiek hBM-MSCs, tiek chondrocituose (Shelest et al., 2025). Ankstesni tyrimai parodė, kad iCa^{2+}

padidėjimas gali įvykti jau per pirmą minutę po TGF-β1 poveikio chondrocituose (Cailotto et al., 2011). Be to, TGF-β sukeltas iCa^{2+} padidėjimas buvo stebėtas ir kituose ląstelių tipuose, įskaitant neuronus (Y. Li et al., 2022; X. Zhang et al., 2015), osteoblastus (Nesti et al., 2007) ir fibroblastus (Alevizopoulos et al., 1997; Muldoon et al., 1988).

Buvo parodyta, kad IL-1β didina viduląstelinį Ca^{2+} žiurkių chondrocituose vikdamas per TRPA1 (Yin et al., 2018). Tačiau mūsų tyrimas parodė, kad 24 val. poveikis 10 ng/mL IL-1β nesukelia iCa^{2+} pokyčių nei hBM-MSCs, nei chondrocituose, kas atitinka ankstesnius tyrimus šio tipo ląstelėse (Uzieliene et al., 2019).

iCa^{2+} reguliacijai ląstelėse svarbus Ca^{2+} patekimas per plazminėje membranoje esančius kanalus, tarp jų ir L-VGCCs. Chondrocituose L-VGCC aktyvacija siejama su OA patogeneze, todėl šie kanalai laikomi potencialiais terapiniais taikiniais OA gydymui. TGF-β3 sukeltas iCa^{2+} padidėjimas gali būti susijęs su L-VGCCs funkcinio aktyvumo pokyčiais. Todėl buvo tirtas L-VGCCs funkcinis aktyvumas vertinant I_{LSN} ties +10 mV, kuris atitinka $I_{Ca,L}$ piką (Zhao et al., 2009). Nuotėkio srovės korekcija leido izoliuoti $I_{Ca,L}$ nuo kitų, potencialui nejautrių (daugiausia kalio) srovių hBM-MSCs (Heubach et al., 2004) ir chondrocituose (Clark et al., 2011), o normalizavimas sumažino ląstelės dydžio įtaką.

hBM-MSCs inkubacija su TGF-β3 sukėlė padidėjusią nifedipinui jautrią į ląstelę įtekančią srovę, kas patvirtina L-VGCCs aktyvaciją. Ši aktyvacija gali būti sudėtingos signalinės kaskados rezultatas, sukeliamas TGF-β3. Pavyzdžiui, parodyta, kad TGF-β didina β-adrenerginę signalizaciją (Rosenkranz et al., 2002), o β-adrenerginių receptorių aktyvinimas žinomas kaip $I_{Ca,L}$ aktyvatorius (Ganesan et al., 2006).

hBM-MSCs inkubacija su IL-1β parodė tendenciją didinti į ląstelę tekančia nifedipinui jautrią srovę, tačiau šis pokytis nebuvo statistiškai reikšmingas.

Buvo parodyta, kad L-VGCCs inhibicija nifedipinu mažina chondrocitų proliferaciją (Uzieliene et al., 2019), kas rodo šių kanalų funkcinį vaidmenį. Tačiau mūsų tyrime L-VGCCs aktyvumo chondrocituose proliferacijos terpėje neaptikta. Pastebėtas reikšmingas iš ląstelės ištekančių srovių padidėjimas chondrocitus inkubuojant chondrogeninėje terpėje. Galimai chondrogeninės terpės komponentai, tokie kaip deksametazonas (Levitan et al., 1991; L. Wang et al., 2021), didelė gliukozės koncentracija (Chu et al., 2009) ar streptomicinas (Iscla et al., 2014), galėjo sustiprinti iš ląstelės ištekančias kalio sroves, kas paaiškintų mūsų gautus.

Chondrocitų inkubacija su TGF-β3 sukėlė į ląstelę įtekančias sroves, kurios nebuvo jautrios nifedipinui. Viena iš galimų priežasčių gali būti TGF-β sukeltas kalio kanalų ekspresijos sumažėjimas (Kaur et al., 2013). Bendroji membranos srovė yra į ir iš ląstelės tekačių srovių suma, todėl iš ląstelės tekančios kalio srovės sumažėjimas gali sąlygoti bendros į ląstelę tekančios membraninės srovės padidėjimą.

Mūsų duomenys parodė, kad nei proliferacijos terpė, nei chondrogeninė terpė, nei TGF-β3 ar IL-1β stimuliacija nepakeitė L-VGCCs aktyvumo chondrocituose.

Apibendrinant, mūsų rezultatai hBM-MSCs rodo, kad TGF-β3 poveikis didina iCa^{2+}, bent iš dalies dėl sustiprėjusio $I_{Ca,L}$ (Pav. 12, kairėje). Nors *CACNA1C*, koduojančio L-VGCCs subvienetą, ekspresija nepakito, manome, kad TGF-β3 padidina jau esančių L-VGCCs funkcinį aktyvumą. Be to, TGF-β3 padidina *ATP2A2* ekspresiją (Pav. 12, kairėje). *ATP2A2* padidėjimas gali būti pradinis ląstelės atsakas, skirtas sumažinti padidėjusį iCa^{2+}.

Chondrocituose TGF-β3 taip pat padidina iCa^{2+}, tačiau be $I_{Ca,L}$ pokyčių (Pav. 12, dešinėje), kas rodo skirtingus iCa^{2+} padidėjimo mechanizmus nei hBM-MSCs. Be to, TGF-β3 mažina *CACNA1C* ekspresiją ir didina *ATP2A2* ekspresiją (Pav. 12, dešinėje). Tai rodo dviejų mechanizmų dalyvavimą mažinant padidėjusį iCa^{2+} chondrocituose: stiprinant iCa^{2+} grąžinimą iš citozolio į ER per *ATP2A2* padidėjimą ir mažinant *CACNA1C* ekspresiją.

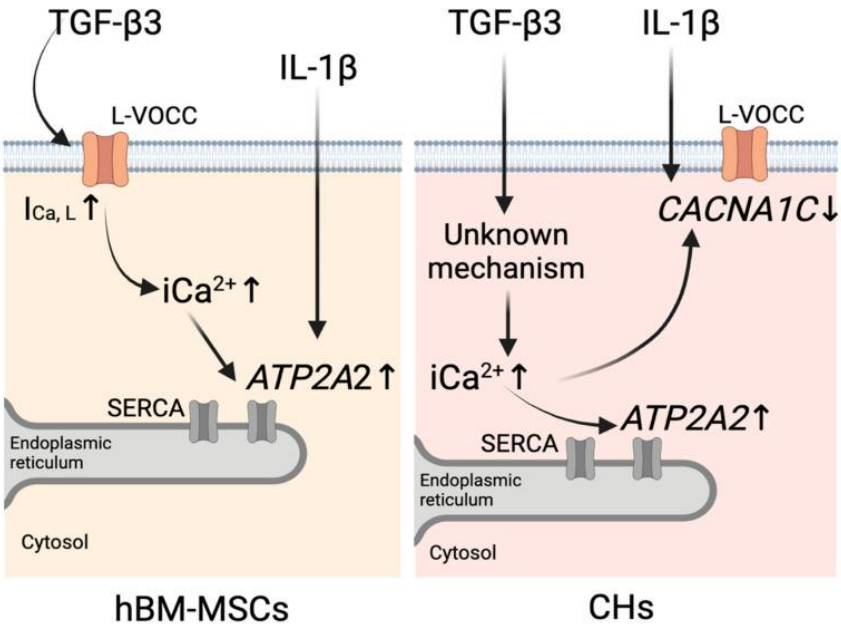

Pav. 12. Siūlomų Ca^{2+} homeostazės reguliacijos mechanizmų schema po TGF-β3 ir IL-1β poveikio hBM-MSCs (kairėje) ir chondrocituose (CHs) (dešinėje). hBM-MSCs TGF-β3 didina viduląstelinio kalcio (iCa^{2+}) lygį sustiprindamas L-tipo kalcio srovę ($I_{Ca,L}$), kas taip pat lemia ir *ATP2A2* ekspresijos padidėjimą. IL-1β didina tik *ATP2A2* ekspresiją. Chondrocituose TGF-β3 didina iCa^{2+} dar nežinomu keliu, kas lemia *ATP2A2* ekspresijos padidėjimą ir *CACNA1C* ekspresijos sumažėjimą. IL-1β mažina *CACNA1C* ekspresiją. Paveikslas sukurtas naudojant BioRender.com (www.biorender.com, žiūrėta 2025 m. vasario 26 d.).

Priešingai nei išoriniai veiksniai, genetiniai jonų kanalų pokyčiai atspindi iš esmės kitokį reguliacijos lygmenį, pasižymintį nuolatiniais, struktūriškai nulemtais poveikiais kanalo aktyvumui. Šis skirtumas ypač svarbus elektriškai aktyviuose audiniuose, kur genetiškai nulemti jonų kanalų funkcijos pokyčiai tiesiogiai formuoja membranos sužadinamumą ir elektrinį stabilumą (Enkvetchakul, 2010). Pavyzdžiui, širdyje $Kv_{7.1}$ kanalai, susijungę su pagalbiniu β-subvienetu KCNE1, generuoja I_{Ks}, kuris atlieka svarbų vaidmenį skilvelių repoliarizacijoje ir širdies veikimo potencialo formavime (Jespersen et al., 2005). Mutacijos *KCNQ1* gene, kuris koduoja $Kv_{7.1}$ kanalo α-subvienetą, keičia I_{Ks}, sukeldamos uždelstą skilvelių repoliarizaciją ir QT intervalo pailgėjimą, taip padidindamos aritmijų riziką (Tristani-Firouzi et al., 2001).

p.Ala371Pro variantas yra lokalizuotas *KCNQ1* HA helix srityje – regione, kuriame anksčiau buvo parodyti konformaciniai pokyčiai, būtini

normaliai kanalo funkcijai ir sąveikai su kalmodulinu (Bileisiene et al., 2025; Brewer et al., 2025). Prognozuojama, kad ši mutacija sutrikdo baltymo struktūrą. Todėl jo funkcinis poveikis buvo įvertintas tiesioginiais elektrofiziologiniais srovių matavimais.

Mūsų rezultatai parodė, kad *KCNQ1* p.(Ala371Pro) variantas, ekspresuojamas kartu su *KCNE1*, sumažino $Kv_{7.1}$ kanalo srovės tankį ties +70 mV maždaug 40 %. Išlikęs jautrumas chromanoliui rodo, kad mutantiniai kanalai išlieka funkcionalūs, o kartu su sumažėjusiu srovės tankiu tai rodo dalinį funkcijos praradimą.

Srovės tankio sumažėjimas, stebėtas *KCNQ1* p.(Ala371Pro) variantui kartu ekspresuojant su *KCNE1*, atitinka ankstesnius tyrimus, kurie parodė, kad įvairūs *KCNQ1* variantai mažina $Kv_{7.1}$ srovę. Pavyzdžiui, mutacijos *KCNQ1* C-terminalinėje srityje, tokios kaip p.(Arg555Cys), ne tik sumažina kanalo srovės tankį, bet ir sukelia ryškų kanalo aktyvacijos priklausomybės nuo potencialo poslinkį į dešinę (Chouabe et al., 1997). Panašiai ir kiti C-terminaliniai mutantai, tokie kaip p.(Arg555His), p.(Ala590Thr) ir p.(Gly589Asp), mažina $Kv_{7.1}$ kanalo srovę ir paslenka aktyvacijos priklausomybę į labiau teigiamus potencialus (Aromolaran et al., 2014; Kinoshita et al., 2014; Piippo et al., 2001).

Priešingai, kai kurios mutacijos, pavyzdžiui p.(Pro535Thr), nekeičia kanalo priklausomybės nuo potencialo, tačiau sumažina maksimalų laidumą (González-Garrido et al., 2021). Šiame tyrime *KCNQ1* p.(Ala371Pro) variantas nepakeitė aktyvacijos priklausomybės nuo potencialo, tačiau sumažino maksimalų kanalo laidumą 42.9 %. Ši mutacija sukelia dalinį $Kv_{7.1}$ kanalų funkcijos praradimą, kas atitinka stebėtus LQT1 fenotipinius požymius (Pav. 13).

Mūsų elektrofiziologiniuose eksperimentuose buvo tiriama homozigotinė p.(Ala371Pro) varianto forma, tačiau klinikinėje praktikoje stebimi tiek homozigotiniai, tiek heterozigotiniai nešiotojai. Šis skirtumas yra kliniškai svarbus, nes zigotiškumo skirtumai gali lemti fenotipo sunkumą ir gali būti susiję su tokiais mechanizmais kaip dominantinio neigiamio poveikio mechanizmai .

Šiame tyrime daugiausia dėmesio buvo skirta tiesioginiam p.(Ala371Pro) varianto poveikiui kalio srovėms. Ar p.(Ala371Pro) variantas sukelia dominantinį neigiamą poveikį, šiuo metu nėra žinoma. Heterozigotiniai pacientai dažnai pasižymi labai lengvu fenotipu, tuo tarpu homozigotiniai individai turi sunkesnius simptomus (Kinoshita et al., 2014). Vis dėlto dominantinį neigiamą poveikį atmesti negalima, kaip parodė ΔF275 mutacija, kuri stipriai slopina $Kv_{7.1}$ srovę ir sukelia LQT1 fenotipą (Aizawa et

al., 2007). Todėl šiame tyrime buvo nagrinėtos tiesioginės funkcinės varianto pasekmės, o galimos heterozigotiškumo ir dominantinio neigiamo poveikio sąveikos išlieka svarbia ateities tyrimų kryptimi.

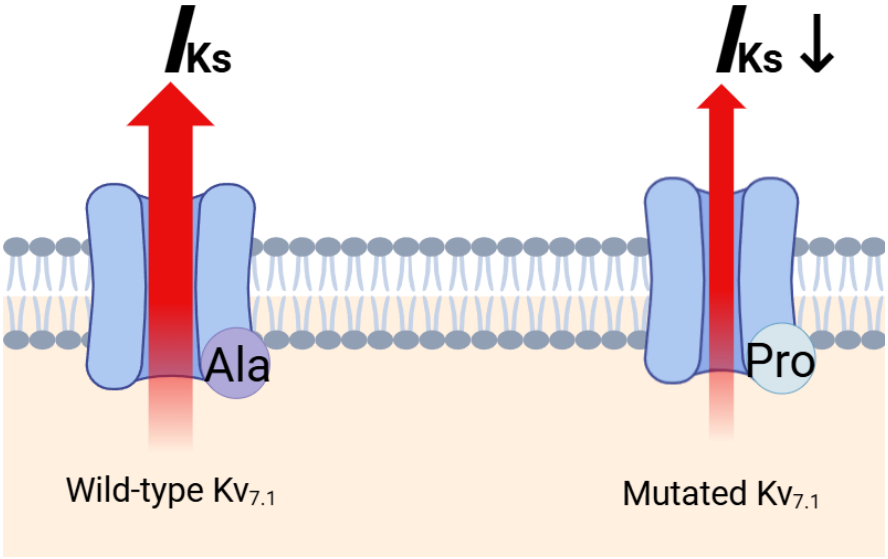

Pav. 13. *KCNQ1* p.(Ala371Pro) varianto įtakos kanalo funkcionalumui schema. Palyginti su laukinio tipo $Kv_{7.1}$ kanalais, kanalai, turintys p.(Ala371Pro) variantą, pasižymi sumažėjusia srove, kas rodo sumažėjusį kanalo laidumą. Alanino pakeitimas prolinu 371 pozicijoje tikėtina keičia kanalo struktūrą ir sutrikdo jonų pralaidumą, kas atitinka funkcijos praradimo efektą. Paveikslas sukurtas naudojant BioRender.com (www.biorender.com, žiūrėta 2026 m. balandžio 1 d.).

IŠVADOS

• TGF-β3 didina viduląstelinio Ca^{2+} kiekį priklausomai nuo ląstelės tipo: hBM-MSCs atveju per L-VGCCs aktyvaciją, o chondrocituose – per nuo L-VGCCs nepriklausomus mechanizmus. IL-1β reikšmingai neveikia nei Ca^{2+} lygio, nei L-VGCCs aktyvumo abiejuose ląstelių tipuose.

• TGF-β3 ir IL-1β paveikia genų, koduojančių Ca^{2+} homeostazę reguliuojančius baltymus ekspresiją priklausomai nuo ląstelės tipo: *CACNA1C*, koduojančio L-VGCCs porą formuojantį α1C subvienetą $Cav_{1.2}$, ekspresijos hBM-MSCs abu citokinai nepaveikia, tačiau sumažina chondrocituose; *ATP2A2*, koduojančio SERCA2, ekspresija padidėja hBM-MSCs abiejų citokinų poveikyje, o chondrocituose –tik po TGF-β3.

• *KCNQ1* p.(Ala371Pro) variantas sukelia $Kv_{7.1}$ kanalo funkcijos praradimą, sumažindamas I_{Ks} laidumą, tačiau nekeisdamas nuo potencialo priklausomos aktyvacijos.

NOTES

NOTES

NOTES

Vilnius University Press
9 Saulėtekio Ave., Building III, LT-10222 Vilnius
Email: info@leidykla.vu.lt, www.leidykla.vu.lt
Print run copies 15